DISSERTATION

Aspects of General Relativity with Negative Cosmological Constant

Ausgeführt zum Zwecke der Erlangung des akademischen Grades eines Doktors der Naturwissenschaften unter der Leitung von

Ass.-Prof. Priv.-Doz. Dr. Daniel Grumiller
Institut für Theoretische Physik (E136)

eingereicht an der Technischen Universität Wien
Fakultät für Physik

von

Dipl.-Ing. Raphaela Wutte
Matrikelnummer: 1126042

Wien, am 24.6.2022

Thesis submitted in partial fulfillment of the requirements for the degree of Doctor of Technical Sciences (Dr. techn.) to the faculty of physics at Technische Universität Wien.

Abstract

Solutions to general relativity with negative cosmological constant are ubiquitous in contemporary physics. They have received a surge of attention due to the Anti-de Sitter/conformal field theory correspondence — a conjecture which asserts that quantum gravity on asymptotically Anti-de Sitter spacetimes is equivalent to a quantum field theory with conformal invariance in one dimension lower. In this thesis, we discuss the causal structure and energy of solutions to Einstein gravity with negative cosmological constant in three and four spacetime dimensions. We show that projection diagrams can be used to visualize the causal structure of BTZ black holes and so-called warped flat spacetimes. The latter correspond to solutions to topologically massive gravity with positive cosmological constant in $(2+1)$ dimensions. It is shown that warped flat spacetimes do not describe black hole solutions. Next, we discuss the energy of solutions to Einstein gravity with negative cosmological constant. To this day, the question of boundedness of energy from below for general relativity with negative cosmological constant remains wide open. For time-symmetric initial data sets, this is the question of whether the energy of asymptotically locally hyperbolic spaces is bounded from below. We show that three-dimensional asymptotically locally hyperbolic spaces with constant negative scalar curvature, arbitrary high genus, and negative total mass exist and explain how this result relates to positive energy theorems in general relativity.

Kurzfassung

Lösungen der Allgemeinen Relativitätstheorie mit negativer kosmologischer Konstante sind in der zeitgenössischen Physik allgegenwärtig. Sie haben aufgrund der vermuteten Anti-de-Sitter/konformen Feldtheorie Korrespondenz viel Aufmerksamkeit erhalten. Diese Hypothese besagt, dass Quantengravitation auf asymptotisch Anti-de-Sitter-Raumzeiten äquivalent zu einer Quantenfeldtheorie mit konformer Invarianz in einer Dimension niedriger ist. In dieser Arbeit untersuchen wir die kausale Struktur und Energie von Lösungen der Allgemeinen Relativitätstheorie mit negativer kosmologischer Konstante in drei und vier Raumzeitdimensionen. Wir zeigen, wie Projektionsdiagramme verwendet werden können, um die kausale Struktur von BTZ-Schwarzen Löchern und sogenannten verzerrt flachen Raumzeiten zu visualisieren. Letztere entsprechen Lösungen topologisch massiver Gravitation mit positiver kosmologischer Konstante in $(2+1)$ Dimensionen. Es wird gezeigt, dass verzerrt flache Raumzeiten keine Schwarzen Löcher sind. Als nächstes untersuchen wir die Energie von Lösungen der Einstein-Gravitation mit negativer kosmologischer Konstante. Bis heute ist die Frage, ob die Energie in der Allgemeinen Relativitätstheorie mit negativer kosmologischer Konstante von unten beschränkt ist, unbeantwortet. Für zeit-symmetrischen Anfangsdaten ist dies die Frage, ob die Energie von asymptotisch lokal hyperbolischen Räumen von unten begrenzt ist. Wir zeigen, dass dreidimensionale asymptotisch lokal hyperbolische Räume mit konstanter negativer skalarer Krümmung, beliebig hohem Genus und negativer Masse existieren und erklären den Zusammenhang mit Positiven Energietheoremen in der Allgemeinen Relativitätstheorie.

Contents

Acknowledgments

First, I would like to thank my supervisor Daniel Grumiller for his continuous support throughout the years. I am deeply grateful to Daniel for the opportunity to complete a PhD in his research group, for giving me the opportunity to work with him and for allowing me the freedom to pursue my own research questions at the same time. Thank you very much for your advice, support and help!

Second, I am grateful to Ricardo Troncoso and Glenn Barnich for doing me the honor of becoming my referees and taking the time to read this manuscript.

I would like to thank all my collaborators from past and current projects for sharing their ideas, time and excitement about physics with me. During my PhD, I had the great pleasure of working with Piotr Chruściel and Erwann Delay and I take this opportunity to thank them for giving me insights into a fascinating area of research. I am especially grateful to Piotr for the many discussions over the last year, his patience in answering my questions and his dedication to science which is truly inspiring. In particular, I would also like to thank Stéphane Detournay for the many discussions and projects we shared over the last four years, his contagious enthusiasm and his continuous encouragement. I am also very grateful to Alejandra Castro for inviting me to visit her group in Amsterdam to work with her and for our ongoing collaboration.

I thank all past and current members of the Fundamental Interaction's Group at TU Wien for sharing their workspace with me and for entertaining discussions over lunch and during group meetings. I am grateful to all members of the Physique théorique et mathématique group in Bruxelles, the String Theory group in Amsterdam and the Centro de Estudios Científicos in Valdivia for their hospitality during my visits and for their warm welcome. I thank everyone who gave me comments regarding my thesis: Florian Ecker, Stefan Prohazka, Martin Sasieta, Georg Stettinger, Piotr, Friedrich and especially Daniel.

Thanks to Georg, Martin and Mateusz Piorkowski for the many interesting discussions about life, physics, math and everything in between and for always encouraging me to follow my passion. Thanks to Susi and Clemens for moral support during the write-up of the thesis. Thank you, Friedrich, for your love and support, your encouragement and for your just criticism – you make me a better person. Thanks to all my friends and family for their unconditional support and for making sure that I have a life outside academia.

I apologize to the many people that I am not mentioning in this list but that had an impact on the success of my PhD: Thank you!

Note to the Reader

This thesis is based on the author's doctoral studies and includes (partially verbatim) the contents of the following papers:

[1] S. Detournay, W. Merbis, G. S. Ng, and R. Wutte, "Warped Flatland," *J*HEP **11** (2020) 061, 2001.00020 ,

[2] P. T. Chruściel, E. Delay, and R. Wutte "Hyperbolic energy and Maskit gluings", 2112.00095 .

In addition to the topics covered here, the author worked on near horizon symmetries in three and four dimensions and published

[3] D. Grumiller, M. Sheikh-Jabbari, C. Troessaert, and R. Wutte, "Interpolating Between Asymptotic and Near Horizon Symmetries," *JHEP* **0**3 (2020) 035, 1911.04503 ,

[4] H. Gonzalez, D. Grumiller, W. Merbis, and R. Wutte, "New entropy formula for Kerr black holes," *EPJ Web Conf.* **1**68 (2018) 01009, 1709.09667 ,

[5] M. Ammon, D. Grumiller, S. Prohazka, M. Riegler, and R. Wutte, "Higher-Spin Flat Space Cosmologies with Soft Hair," *JHEP* **0**5 (2017) 031, 1703.02594 .

0. Conventions

In this thesis we use the metric signature $(-1, ..., 1, 1)$. The Riemann tensor tensor is defined as

$$\nabla_\mu \nabla_\nu \omega_\rho - \nabla_\nu \nabla_\mu \omega_\rho = R_{\mu\nu\rho}{}^\sigma \omega_\sigma \tag{0.1}$$

and the Ricci tensor is defined as

$$R_{\mu\nu} = R_{\mu\rho\nu}{}^\rho \,, \tag{0.2}$$

which is in accordance with the sign conventions used by Wald [6] and Misner, Thorne, Wheeler [7]. Greek letters $(\mu, \nu, \sigma, ...)$ are used as spacetime indices and run from 1 to $d = n + 1$, small Latin letters $(a, b, c, ..., i, j, k, ...)$ are used for spatial indices and run from $1, ...n$. An exception occurs when we discuss the embedding of AdS_3 into $\mathbb{R}^{2,2}$ in section 3.2. Big Latin letters from the beginning of the alphabet $(A, B, C, ...)$ are used as spatial indices for the boundary metric, denoted by either h, h_k or $\mathring{h}$, and run from $1, ...n - 1$. Big latin letters from the middle of the alphabet $(I, J, ...)$ run from $1, ...n - 2$.

Symmetrization and anti-symmetrization of tensors is defined such that already symmetric and antisymmetric tensors stay unchanged:

$$t_{(\mu\nu)} = \frac{1}{2}(t_{\mu\nu} + t_{\nu\mu}) \,, \tag{0.3}$$

$$t_{[\mu\nu]} = \frac{1}{2}(t_{\mu\nu} - t_{\nu\mu}) \,. \tag{0.4}$$

We choose units in which Newton's constant G, the AdS radius ℓ, the speed of light c, Planck's constant $\hbar$ and Boltzmann's constant k_B are all set to 1. We restore Newton's constant G and the AdS radius ℓ only in subsection 3.6.

$d = n + 1$	spacetime dimension
n	spatial dimension
$n - 1$	dimension of the boundary manifold
∇	spacetime covariant derivative
D	covariant derivative of the spatial metric
$\mathscr{D}$	covariant derivative of the boundary metric

1. Introduction

On May 12th, 2022 the Event Horizon Telescope announced the first image of the supermassive black hole at the center of our galaxy. In the Saggitarius A* constellation, a bright ring of gas surrounds the black hole, bent by extremely strong gravitational forces. A black shadow sits in the center of the glowing ring. This shadow contains the so-called event horizon, where gravitational forces are so intense that not even light can escape the gravitational pull anymore.

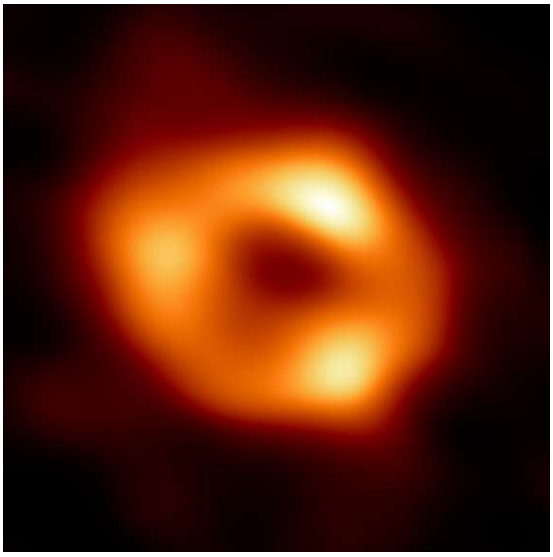

Figure 1.1.: First Image of Saggitarius A* – Credit: Event Horizon Telescope Collaboration

For decades scientists have observed stars orbiting an invisible, gigantic object of 4 million solar masses in the very center of the Milky Way. Observations started in 1918 when Harlow Shapley noticed stars congregating towards the middle of our galaxy and later powerful radio emissions were detected coming from the Saggitarius A* constellation. Following tremendous experimental efforts and results, the 2020 Nobel Prize in Physics was granted for the discovery of black holes. One half was awarded to Roger Penrose *"for the discovery that black hole formation is a robust prediction of the general theory of relativity"*, while the other half was awarded to Reinhard Genzel and Andrea Ghez *"for the discovery of a supermassive compact object at the centre of our galaxy"* [8]. Over 100 years after the theoretical discovery of the first black hole solution in general relativity by Karl Schwarzschild, we may say with utmost conviction that black holes do exist in nature.

These experimental results come mere years after the LIGO and VIRGO collaboration recorded gravitational waves sent out by the merger of two black holes in September 2015. This observation not only provided the first direct detection of gravitational waves, but also showed that binary stellar black hole systems — pairs of black holes formed by the gravitational collapse of massive stars — exist. Subsequently, the 2017 Nobel Prize in Physics was awarded for the discovery of gravitational waves — over a century after their theoretical prediction. General relativity has surpassed all our expectations, it has passed every experimental check, the images of black holes and the detection of gravitational waves being only the latest results in a very long list.

While the classical theory of general relativity has celebrated many successes in recent years, the problem of combining general relativity with quantum mechanics into a theory of quantum gravity is unsolved, as experimental guidance towards a solution is currently out of reach. Not knowing which features the theory of quantum gravity, which describes our universe, exhibits, one is forced to appeal to purely theoretical guidelines such as consistency with the semiclassical approximation and internal mathematical consistency. A guiding principle, in the search for such theories, is the existence of properties that are preserved in the quantum theory. Amongst these properties are (often) conservation laws and associated conserved quantities. A quantity, which will be of particular importance in the fourth chapter of this thesis, is the energy of the gravitational field. In general relativity, unlike in other field theories, there does not exist a meaningful local energy expression of the gravitational field as the effects of gravity can always be suppressed locally due to the equivalence principle. The energy-momentum tensor $T_{\mu\nu}$ appearing on the right side of the Einstein equations[1]

$$R_{\mu\nu} - \frac{1}{2} g_{\mu\nu} R + \Lambda g_{\mu\nu} = 8\pi T_{\mu\nu} \,, \tag{1.1}$$

describes the energy densities arising from non-gravitational fields ("matter") only. The condition that the energy-momentum tensor $T_{\mu\nu}$ be conserved does not suffice to define an associated conserved quantity as a vector is needed to do so. Technically speaking, such a vector is given by $j^\mu = T^\mu_{\ \nu} \xi^\nu$, where ξ^μ is a timelike Killing vector of spacetime. The total energy can then be defined as an integral over a spacelike Cauchy surface Σ

$$E = \int_\Sigma j^\mu n_\mu \,, \tag{1.2}$$

where n_μ is the unit normal to Σ. However, a generic spacetime does not admit any Killing vectors and thus the energy has to be defined in a different way. From a physics perspective, this might be unsurprising, as $T_{\mu\nu}$ only represents the energy content of matter and one would expect the gravitational energy to make a contribution as well. The resolution to this problem lies in the study of isolated systems — systems far away from the influence of gravitational sources. In the case of vanishing cosmological constant,

[1] The Einstein equations intimately tie the curvature of spacetime, encoded in the Ricci tensor $R_{\mu\nu}$ and the Ricci scalar R, to the energy-momentum tensor $T_{\mu\nu}$. The geometry of spacetime is encoded in the metric $g_{\mu\nu}$, the fundamental field of general relativity, and Λ is a fundamental constant of nature, called the cosmological constant.

this is the study of asymptotically flat spacetimes — spacetimes which approach the Minkowski metric at large distances. When the cosmological constant is negative one considers asymptotically Anti-de Sitter (AdS) spacetimes — spacetimes which approach AdS spacetime, the maximally symmetric geometry for negative cosmological constant, at large distances.

While the cosmological constant of our universe is very small and positive, asymptotically AdS spacetimes are ubiquitous in nowadays theoretical high-energy physics. They have received a surge of attention due to the so-called Anti-de Sitter/conformal field theory (AdS/CFT) correspondence, which asserts that quantum gravity on d–dimensional asymptotically AdS spacetimes is equivalent to a $(d-1)$–dimensional quantum field theory with conformal invariance. The AdS/CFT correspondence was formulated by Juan Maldacena in 1997 [9] who conjectured a duality between a type IIB superstring theory on $\mathrm{AdS}_5 \times \mathrm{S}_5$ and an $N = 4$ supersymmetric Yang-Mills theory. The idea that quantum gravity has an effective description in terms of a lower-dimensional quantum field theory without gravity is actually due to 't Hooft [10]. This idea was subsequently named the holographic principle by Leonard Susskind who also suggested a realization might be possible in string theory [11].

In the last two decades, the ideas by 't Hooft, Susskind and Maldacena have been applied to various different setups, e.g. for different values of the cosmological constant, different spacetime dimensions and even different theories of gravity. One reason why scientists are so excited about the AdS/CFT correspondence is that it is a strong-weak duality, meaning that it maps a strongly coupled theory of general relativity to a weakly coupled non-gravitational quantum field theory (and vice versa). Therefore, the correspondence can be used to infer information about regimes otherwise inaccessible.

In the field of AdS/CFT, a particular focus has been the theoretical study of black holes, as for these objects both classical as well as quantum effects play a role. In the early seventies, Bardeen, Bekenstein, Carter and Hawking showed that black holes are thermal objects and obey laws which share close similarities to the laws of thermodynamics. Using quantum field theory on curved backgrounds, Hawking showed in 1975 that quantum mechanical black holes emit elementary particles with the spectrum of a black body at temperature

$$T = \frac{\kappa}{2\pi}\,, \tag{1.3}$$

where κ is the surface gravity. Black holes are objects of non-zero Bekenstein–Hawking entropy

$$S_{BH} = \frac{A}{4}\,, \tag{1.4}$$

which is proportional to the event horizon area A of the black hole. The unusual fact that entropy is proportional to the area of the horizon and not to its volume, inspired the formulation of the holographic principle.

It is puzzling from a thermodynamic perspective, that quantum black holes have a large entropy, as their classical description involves only a few parameters. This is encompassed in the *no hair theorem* which states that classical black holes are fully characterized by three parameters: mass, electric charge and angular momentum. Therefore, if one

interprets the expression (1.4) as a thermodynamic entropy, the question arises what the huge number of microstates associated with the black hole entropy are and whether the entropy of a black hole can be obtained by calculating the number of microstates. Strominger and Vafa [12] made progress in this direction by supplying a microscopic derivation for certain black holes in string theory. Shortly after, this computation was generalized by Strominger [13] to black holes in three-dimensional Einstein gravity with negative cosmological constant and subsequently many papers along these lines followed, amongst them being [14–19]. Almost all these papers rest on the assumption that energy in the gravitational theory is bounded from below, as this assumption is needed in the putative dual field theory to explicitly calculate the number of microstates.

In the semiclassical regime and for negative cosmological constant, this becomes the question of whether energy in general relativity for negatively curved spacetimes is bounded from below. As we will see in this thesis, this question remains wide open to this day. Indeed, in many situations of interest, it is not clear whether a lower bound exists and if there exists a unique geometry that saturates this bound.

Positivity of energy of the gravitational field is of course of enormous interest in its own right — independently from any holographic correspondence. It has played a key role in many investigations in mathematical general relativity, amongst them being the stability of solutions of the Einstein equations and the classification of black hole solutions in general relativity. To the long list of potential applications of positive energy theorems in general relativity, we would thus like to add that they can be used to provide proofs or falsifications of assumptions commonly made in the AdS/CFT literature regarding the spectrum of asymptotically Anti-de Sitter spacetimes. One famous example of this is the Horowitz–Myers conjecture [20], which asserts that the energy of asymptotically locally Anti-de Sitter spacetimes with toroidal conformal infinity, is bounded from below, with the unique lower bound provided by the Horowitz–Myers metric. This conjecture was formed by considering a potential non-supersymmetric AdS/CFT correspondence and showing that the ground state energy in the conformal field theory matched the energy of the Horowitz–Myers metric. The conjecture can thus be regarded as "a highly nontrivial prediction of the AdS/CFT correspondence" [20]. Over the years, it has now become a topic of active research in the mathematical general relativity community. If proven to be true, the conjecture would provide strong evidence in favor of the AdS/CFT correspondence.

1.1. Outline

This thesis discusses the causal structure and energy of solutions to Einstein gravity with negative cosmological constant. Implications on the AdS/CFT correspondence are examined when applicable.

In chapter 2, we review methods to analyze the causal and asymptotic structure of spacetime which are then applied in chapters 3 and 4. The method of conformal completion is discussed in section 2.1, where we also discuss the behavior of selected geometric quantities under conformal transformations. In section 2.2, we introduce a class

of two-dimensional causal diagrams, so-called projection diagrams and compare them to Carter-Penrose diagrams. A short review of the initial data formulation of general relativity is given in section 2.3 which serves as background material for chapter 4.

In chapter 3, the peculiarities of general relativity in $(2+1)$ spacetime dimensions with a negative cosmological constant are discussed. After a brief review of general features, we introduce asymptotically AdS_3 spacetimes in section 3.3. The seminal paper by Brown and Henneaux [21], who studied the asymptotic symmetry group of such spacetimes, is reviewed and vacuum solutions of the Einstein equations which asymptote to the AdS_3 metric at large distances are discussed. The standard interpretation of these results with regard to the AdS_3/CFT_2 correspondence is given. An important vacuum solution to three-dimensional Einstein gravity, the so-called BTZ black hole, is discussed in detail in section 3.4. Particular attention is given to the maximal causal extension of the BTZ black hole and its visualization using projection diagrams. Next, a modification of three-dimensional Einstein gravity, topologically massive gravity (TMG), is reviewed in section 3.5. Selected vacuum solutions to TMG are discussed with a focus on so-called warped flat spacetimes and quotients thereof, which are the subject of my publication [1] (co-authored with Stéphane Detournay, Wout Merbis and Gim Seng Ng). Contrary to claims in [22], we show that these spacetimes do not possess a black hole region and visualize their causal properties with projection diagrams. The chapter ends with section 3.6, where it is reviewed how asymptotic symmetries are used in Strominger's work [13] to perform a microstate counting of three-dimensional BTZ black holes. We focus on the underlying assumptions of this derivation and the necessary conditions on the spectrum of asymptotically AdS_3 spacetimes.

In chapter 4, the contents of my work [2] (co-authored with Piotr Chruściel and Erwann Delay) and their connection to positive energy theorems in general relativity with negative cosmological constant are discussed. We start by introducing two classes of metrics in section 4.1 that are of importance in this context: the Birmingham–Kottler and the Horowitz–Myers spacetimes. Positive mass theorems in general relativity with negative cosmological constant are reviewed in section 4.2. Particular attention is given to the Horowitz–Myers conjecture and its relation to the AdS/CFT correspondence. Sections 4.3 to 4.8 are taken from [2] with only minimal modifications. After giving an introduction and summary of the main results in section 4.3, we review the gluing construction of [23] in section 4.4 by which two asymptotically locally hyperbolic (ALH) manifolds (or time-symmetric general relativistic initial data sets), may be glued together to obtain a new ALH manifold. The definition of energy used in this context is introduced in section 4.6. There, it is also shown how the energy changes upon gluing two ALH manifolds. In section 4.7, we show that there exist three-dimensional conformally compact ALH manifolds without interior boundary, with connected conformal infinity of genus two, with constant negative scalar curvature and with negative mass. We comment on how this construction generalizes to arbitrarily high genus.

2. Preliminaries

In this chapter, we discuss different methods to analyze the causal and asymptotic structure of spacetime that will be used throughout this thesis. Section 2.1 deals with conformal transformations and how they may be used to perform a conformal completion of spacetime. The consequences of the Einstein equations on the nature of the conformal boundary are discussed. Section 2.2 introduces a class of two-dimensional causal diagrams, so-called projection diagrams [24], which can be used to visualize the causal structure of spacetime. After motivating their introduction, projection diagrams are contrasted with the famous Carter-Penrose diagrams. We end by discussing projection diagrams of Minkowski spacetime. In section 2.3 we briefly introduce the initial data formulation of general relativity and the concept of Killing Initial Data.

2.1. Conformal Completion

In this section we follow closely [6] and [25] in the presentation of conformal transformations and conformal completion.

2.1.1. Conformal Transformations

Let M be a d-dimensional Lorentzian manifold with metric $g_{\mu\nu}$. If Ω is a smooth, strictly positive function, then the metric

$$\bar{g}_{\mu\nu} = \Omega^2 g_{\mu\nu} \tag{2.1}$$

is said to result from a conformal transformation.

Now, if some vector v^μ is timelike, null or spacelike with respect to the metric $g_{\mu\nu}$, then it must satisfy the same property with respect to $\bar{g}_{\mu\nu}$. Conversely, if the light cones of two metrics $g_{\mu\nu}$, $\bar{g}_{\mu\nu}$ coincide at a point p in M, then at p the metric $\bar{g}_{\mu\nu}$ must be related to $g_{\mu\nu}$ as $\bar{g}_{\mu\nu} = \Omega^2 g_{\mu\nu}$. Therefore, if two spacetimes $(M, g_{\mu\nu})$, $(M, \bar{g}_{\mu\nu})$ have the same causal structure, then there exists a conformal transformation relating $g_{\mu\nu}$ to $\bar{g}_{\mu\nu}$ [6, appendix D]. In general, a conformal transformation is not associated with a diffeomorphism, but changes the geometry of spacetime in a way that preserves the causal structure. A diffeomorphism $\psi : M \to M$ for which $(\psi^* g)_{\mu\nu} = \Omega^2 g_{\mu\nu}$ is called a conformal isometry. To exemplify how conformal transformations change the geometry, consider geodesics. While under conformal transformations timelike (spacelike) paths are mapped into timelike (spacelike) paths, timelike (spacelike) geodesics are typically mapped into paths that are not geodesics.

In this thesis, the transformation behavior of distinguished geometric quantities under conformal transformations will be of importance – which is discussed next. The

transformation behavior of the Riemann tensor, Ricci tensor and the Ricci scalar under conformal transformations reads [6]

$$\bar{R}_{\mu\nu\rho}{}^{\sigma} = R_{\mu\nu\rho}{}^{\sigma} + 2\delta^{\sigma}_{[\mu}\nabla_{\nu]}\nabla_{\rho}\log\Omega - 2g^{\sigma\eta}g_{\rho[\mu}\nabla_{\nu]}\nabla_{\eta}\log\Omega + 2\Big(\nabla_{[\mu}\log\Omega\Big)\delta^{\sigma}_{\nu]}\nabla_{\rho}\log\Omega - 2\Big(\nabla_{[\mu}\log\Omega\Big)g_{\nu]\rho}g^{\sigma\eta}\nabla_{\eta}\log\Omega - 2g_{\rho[\mu}\delta^{\sigma}_{\nu]}g^{\eta\omega}(\nabla_{\eta}\log\Omega)(\nabla_{\omega}\log\Omega)\,, \tag{2.2}$$

$$\bar{R}_{\mu\nu} = R_{\mu\nu} - (d-2)\nabla_{\mu}\nabla_{\nu}\log\Omega - g_{\mu\nu}g^{\rho\sigma}\nabla_{\rho}\nabla_{\sigma}\log\Omega + (d-2)(\nabla_{\mu}\log\Omega)(\nabla_{\nu}\log\Omega) - (d-2)g_{\mu\nu}g^{\rho\sigma}(\nabla_{\rho}\log\Omega)(\nabla_{\sigma}\log\Omega) \tag{2.3}$$

and

$$\bar{R} = \Omega^{-2}(R - 2(d-1)g^{\mu\nu}\nabla_{\mu}\nabla_{\nu}\log\Omega - (d-2)(d-1)g^{\mu\nu}(\nabla_{\mu}\log\Omega)(\nabla_{\nu}\log\Omega))\,. \tag{2.4}$$

Next, we consider the Weyl tensor $C_{\mu\nu\rho\sigma}$, defined for manifolds with spacetime dimension $d \geq 3$ through the decomposition

$$R_{\mu\nu\rho\sigma} = C_{\mu\nu\rho\sigma} + \frac{2}{d-2}\Big(g_{\mu[\rho}R_{\sigma]\nu} - g_{\nu[\rho}R_{\sigma]\mu}\Big) - \frac{2}{(d-1)(d-2)}R\,g_{\mu[\rho}g_{\sigma]\nu}\,. \tag{2.5}$$

The Weyl tensor is invariant under conformal transformations

$$\bar{C}_{\mu\nu\rho}{}^{\sigma} = C_{\mu\nu\rho}{}^{\sigma}\,. \tag{2.6}$$

For spacetime dimension $d \geq 4$ the vanishing of the Weyl tensor is a necessary and sufficient condition for the manifold to be conformally flat, meaning that locally there exists a conformal factor such that (2.1) with $\bar{g} = \eta$. In spacetime dimension three the Weyl tensor identically vanishes but there exists an obstruction to local conformal flatness: the Cotton tensor. This tensor was discovered by Émile Cotton in 1899 and is defined as

$$C_{\mu\nu\rho} = \nabla_{\rho}R_{\mu\nu} - \nabla_{\nu}R_{\mu\rho} + \frac{1}{2(d-1)}(\nabla_{\nu}R\,g_{\mu\rho} - \nabla_{\rho}R\,g_{\mu\nu})\,. \tag{2.7}$$

Similar to the Weyl tensor in higher dimensions, in spacetime dimension $d = 3$ the Cotton tensor is conformally invariant and vanishes iff the manifold is conformally flat. In $d = 3$, applying the Hodge star operator to (2.7) yields

$$C_{\mu\nu} = \nabla_{\rho}\Big(R_{\mu\sigma} - \frac{1}{4}Rg_{\mu\sigma}\Big)\,\epsilon^{\rho\sigma}{}_{\nu} = C_{\nu\mu}\,, \tag{2.8}$$

which is sometimes referred to as Cotton-York tensor or also Cotton tensor. In the following we refer to (2.8) as Cotton tensor.

2.1.2. Conformal Completion

After having discussed conformal transformations in the previous section, we now discuss conformal completion of a physical spacetime $(M, g_{\mu\nu})$. In this method, the manifold M with metric $g_{\mu\nu}$ is embedded into a bigger manifold $\bar{M}$ which has a boundary. The

manifold $\bar{M}$ is referred to as the unphysical spacetime. The boundary of $\bar{M}$ is typically referred to as $\mathscr{I}$, which is also the nomenclature that we use throughout this thesis. The boundary $\mathscr{I}$ is often also referred to as conformal infinity. The unphysical spacetime $\bar{M}$ is required to admit a smooth metric $\bar{g}_{\mu\nu}$. It is possible to relax smoothness of the unphysical metric at $\mathscr{I}$ but this is not necessary for the purpose of this thesis. In the interior of spacetime the physical metric $g_{\mu\nu}$ is related to the unphysical metric $\bar{g}_{\mu\nu}$ by a conformal transformation, i.e. (2.1), where Ω vanishes at $\mathscr{I}$ and is strictly positive everywhere else. While the unphysical metric $\bar{g}_{\mu\nu}$ is regular on the entire manifold $\bar{M}$, the physical metric $g_{\mu\nu}$ diverges as $\mathscr{I}$ is approached. This is simply the mathematical description of the fact that $\mathscr{I}$ is infinitely far away. Additionally, it is demanded that the normal vector

$$\bar{n}^\mu = \bar{g}^{\mu\nu}\nabla_\nu\Omega \tag{2.9}$$

vanishes nowhere on $\mathscr{I}$, which fixes the rate at which the function Ω goes to zero at $\mathscr{I}$. The transformation behavior of the Ricci scalar under conformal transformations (2.4) can be expressed using the normal vector (2.9) yielding

$$\bar{R} = \Omega^{-2}R - 2(d-1)\,\Omega^{-1}\bar{\nabla}_\mu\bar{n}^\mu + d(d-1)\,\Omega^{-2}\bar{n}_\mu\bar{n}^\mu\,. \tag{2.10}$$

Since the conformal factor Ω vanishes at $\mathscr{I}$ it holds that

$$R \mathrel{\hat{=}} -d(d-1)\bar{n}^\mu\bar{n}_\mu\,, \tag{2.11}$$

where "$\hat{=}$" denotes equality in the limit as $\mathscr{I}$ is approached. It follows from (2.11) that R has a smooth limit to $\mathscr{I}$, if a conformal completion exists as defined above. We now consider spacetimes for which Einstein equations hold

$$R_{\mu\nu} - \frac{1}{2}Rg_{\mu\nu} + \Lambda g_{\mu\nu} = \kappa T_{\mu\nu}\,. \tag{2.12}$$

Now, if the trace of the energy-momentum tensor vanishes at $\mathscr{I}$, i.e. $T_{\mu\nu}g^{\mu\nu} \mathrel{\hat{=}} 0$, then

$$\bar{n}^\mu\bar{n}_\mu \mathrel{\hat{=}} -\frac{2}{(d-1)(d-2)}\Lambda\,. \tag{2.13}$$

Hence, the existence of a conformal completion restricts the nature of the conformal boundary at infinity: In particular, if the Ricci scalar vanishes in the limit as $\mathscr{I}$ is approached, then the boundary must be null. Similarly, if the Ricci scalar approaches a positive (negative) constant, then the boundary must be spacelike (timelike).

Having introduced all the concepts necessary, let us fix the terminology for the rest of this thesis. We say that a metric g on a manifold without boundary M has a *conformal completion* $(\bar{M}, \bar{g})$ if $\bar{M}$ is a manifold with boundary such that $\bar{M} = M \cup \partial\bar{M}$, and if there exists a function $\Omega \geq 0$ on $\bar{M}$ which vanishes precisely on $\partial\bar{M}$, with $d\Omega$ nowhere vanishing on $\partial\bar{M}$, and with $g = \Omega^{-2}\bar{g}$ on M. This definition generalizes to manifolds M with boundary, in which case $\partial\bar{M}$ will be the union of the original boundaries of ∂M, where Ω is strictly positive, and the new ones where Ω vanishes; the new ones are referred to as *boundaries at conformal infinity*. We say that (M, g) is *conformally compactifiable* when $\bar{M}$ is compact.

2.2. Projection Diagrams

In this section, we introduce a class of two-dimensional diagrams which were defined in [24] and contrast them with the well-known Carter-Penrose diagrams. We follow closely [24] and [26]. Conformal Carter-Penrose diagrams are a useful tool to visualize the geometry of two-dimensional Lorentzian spacetimes. They have been successfully used to visualize the geometry of slices of many higher-dimensional spacetimes such as Schwarzschild. To obtain a Carter-Penrose diagram, the first step is to conformally complete the physical spacetime, as described in subsection 2.1.2. In the case of two-dimensional Lorentzian spacetimes this suffices to draw a Carter-Penrose diagram, which is a spacetime diagram where the horizontal axis is space and the vertical axis is time. Light rays move at an angle of 45 degrees.

In the case of higher-dimensional spacetimes, one must find a two-dimensional slice, which provides useful information about the higher-dimensional spacetime. For the Schwarzschild black hole

$$ds^2 = -\left(1 - \frac{2m_c}{r}\right)dt^2 + \frac{dr^2}{1 - \frac{2m_c}{r}} + r^2\left(d\theta^2 + \sin^2\theta d\varphi^2\right) \tag{2.14}$$

the diagram found in literature is obtained by holding θ and φ fixed. *All* causal curves (timelike or null) in the original spacetime are depicted as causal curves in the diagram. Many spacelike curves are displayed as causal curves. Importantly, *all* spacelike curves that appear spacelike in the diagram, are spacelike in spacetime. These properties ensure that causal relations in the diagram properly represent causal relations in spacetime. This is achieved by effectively omitting a strictly positive term in the metric (by taking a slice). The case of the Kerr black hole is more complicated. Consider the Kerr metric in Boyer-Lindquist coordinates

$$\begin{aligned} ds^2 = & -\frac{\Delta_r - a^2\sin^2(\theta)}{\Sigma}dt^2 - \frac{2a\sin^2(\theta)(r^2 + a^2 - \Delta_r)}{\Sigma}dtd\varphi \\ & + \frac{\sin^2(\theta)\left(\left(r^2 + a^2\right)^2 - a^2\sin^2(\theta)\Delta_r\right)}{\Sigma}d\varphi^2 + \frac{\Sigma}{\Delta_r}dr^2 + \Sigma d\theta^2 \,, \end{aligned} \tag{2.15}$$

where

$$\Sigma = r^2 + a^2\cos^2\theta \,, \qquad \Delta_r = r^2 + a^2 - 2m_c r \tag{2.16}$$

for some real parameters a and m_c, which satisfy $0 < |a| \leq m_c$. Now, the Kerr metric is not diagonal due to the presence of the $dtd\varphi$ term. This term vanishes at $\theta = 0$ and $\theta = \pi$. Since the metric (2.15) posesses a coordinate singularity at these values of θ we change coordinates before making any further statements. Under the change of coordinates $x = \sin\theta\cos\varphi$, $y = \sin\theta\sin\varphi$ the metric (2.15) takes the form

$$\begin{aligned} ds^2 = & -\frac{\Delta_r - a^2(x^2 + y^2)}{\rho^2}dt^2 + 2a\frac{\Delta_r - (a^2 + r^2)}{\rho^2}(xdy - ydx)dt + \frac{\rho^2}{\Delta_r}dr^2 \\ & + a^2\frac{6m_c r + 3\rho^2}{3\rho^2}(xdy - ydx)^2 + \rho^2\left(dx^2 + dy^2 + \frac{(xdx + ydy)^2}{1 - x^2 - y^2}\right) \end{aligned} \tag{2.17}$$

with $\rho^2 = r^2 + a^2(1 - x^2 - y^2)$. This new coordinate system is singular at $x^2 + y^2 = 1$ (a locus which does not correspond to $\theta = 0$, $\theta = \pi$). As we already know that the metric is smooth there, this is of no concern to the current considerations. At $x = y = 0$ the cross-terms vanish and the metric (2.15) again takes the diagonal form

$$ds^2 = -\frac{\Delta_r}{\rho^2}dt^2 + \frac{\rho^2 dr^2}{\Delta_r} \tag{2.18}$$

such that its causal structure can be depicted with a Carter-Penrose diagram. Generic constant θ, constant φ slices do not provide a meaningful representation of the causal structure. The reason for this is that for a generic constant θ, constant φ slice, the property that all spacelike curves in the original spacetime are mapped to spacelike curves in the causal diagram will not hold. This is the case due to the presence of the off-diagonal $dtd\varphi$ term. Hence, the causal diagram that one obtains for the maximally extended Kerr spacetime is highly slice-dependent, a fact which is discussed in detail in [24, subsection 3.3.1].

Apart from the possible slice-dependence that comes with Carter-Penrose diagrams, there are further issues when considering different spacetimes.

1. Conformal Carter-Penrose diagrams rely on the existence of a conformal compactification of spacetime. Generically, for spacetime dimensions $d > 2$ it may not exist.

2. As already discussed above, for many geometries, generic slices do not provide a meaningful representation of the causal structure. In the extreme case, it is impossible to find a slice that meaningfully represents the causal structure of the higher-dimensional spacetime – a statement that should become more clear from what is written below.

We now provide an example for the second point in spacetime dimension three. For this, we consider the metric

$$ds^2 = -F(r)dt^2 + \frac{dr^2}{F(r)} + r^2(N^\varphi(r)dt + d\varphi)^2\,, \tag{2.19}$$

with a discrete identification along ∂_φ and where $N^\varphi(r)$ is nonzero. This metric is considered in detail in section 3.4. We assume that the functions $F(r)$ and $N^\varphi(r)$ decay sufficiently fast and in such a way that a conformal completion exists. In taking a constant φ slice, the term $r^2(2N^\varphi(r)dtd\varphi + d\varphi^2)$ is discarded. This has the undesirable property that some causal curves in the original spacetime are mapped to spacelike curves in the diagram. Therefore, a constant φ slice does not properly represent the causal structure of (2.19). Instead of taking a slice we discard the $r^2(N^\varphi(r)dt + d\varphi)^2$ term, thereby obtaining the metric

$$\gamma_{\mu\nu}dx^\mu dx^\nu = -F(r)dt^2 + \frac{dr^2}{F(r)}\,, \tag{2.20}$$

which shares causal properties with the original spacetime. This procedure of "discarding a slice" can be formalized, as we will see below. We do not discuss the details of the causal structure of (2.19) here but instead postpone the discussion to section 3.4.

The reader is now hopefully convinced that in many situations of interest it is useful, sometimes even necessary, to introduce novel causal diagrams to visualize the causal structure of spacetime. Such diagrams, named *projection diagrams*, were defined in [24]. Constructions similar to projection diagrams appeared already earlier in literature, but a formal definition and a detailed justification of the construction was – as far as I know of – only given in [24].

Definition 2.1. ***Projection diagram***
Let (M, g) be a smooth spacetime. A projection diagram is a pair (π, U), where

$$\pi : M \to W\,, \qquad W \subset \mathbb{R}^{1,1}$$

is a continuous map, differentiable on an open dense set. $U \subset M$ is an open set, assumed to be nonempty, on which π is a smooth submersion, such that

1. *every smooth timelike curve $\sigma \subset \pi(U)$ is the projection of a smooth timelike curve ω in (U, g): $\sigma = \pi \circ \omega$;*

2. *the image $\pi \circ \omega$ of every smooth timelike curve $\omega \subset U$ is a timelike curve in $\mathbb{R}^{1,1}$.*

The two requirements on timelike curves ensure that causal relations on $\pi(U)$ reflect – as accurately as possible – causal relations on U. By continuity, it follows that images of causal curves in U are causal in $\pi(U)$. Many spacelike curves in the original spacetime are mapped to either null or timelike curves in the diagram.

The map π in the definition of the projection diagram is used to systematically construct an auxiliary two-dimensional metric out of spacetime. One then performs a conformal completion, which is always possible in two dimensions, and draws a diagram of the two-dimensional auxiliary metric. This auxiliary metric shares important causal features with the original metric due to the requirements on π.

We discuss a simple example below, but before that let us give some comments on the definition. While it is assumed for simplicity that (M, g), $\pi|_U$ and the causal curves in the definition are smooth, this is unnecessary for most purposes.

It is demanded in the definition 2.1 that π is a submersion which means that π_* is surjective at every point. This guarantees that open sets are mapped to open sets. This ensures that projection diagrams with the same set U are locally unique up to a local conformal isometry of $\mathbb{R}^{1,1}$. In the definition, it is assumed that the map π maps U to a subset of $\mathbb{R}^{1,1}$ but this can be modified. In some applications it might be more natural to consider different two-dimensional manifolds as the target space; an example of such a spacetime is already given in [24] and requires only minimal modification of the definition. For additional explanations with regards to the definition consult [24, section 3.1].

Importantly, the axioms of the definition ensure that if there exists a black hole region in the diagram, there exists a black hole region in the original spacetime. Indeed, if the diagram has a black hole region B, then $B = W - J^-(\mathscr{I}^+(W))$ is nonempty. Here, $J^-(\mathscr{I}^+)$ denotes the causal past of $\mathscr{I}^+$, future null infinity. This implies, that all curves leaving the black hole region B and hitting $\mathscr{I}^+(W)$ at late times are spacelike. We now define a new set $\tilde{B}$ for which it holds that $B = \pi(\tilde{B})$. Assume that there exist causal

curves, moving forward in time, that leave $\tilde{B}$ and that go to future null infinity; then this must also be the case in $B = \pi(\tilde{B})$ via the axioms of the projection diagram. This immediately leads to a contradiction. Therefore, if a black hole region exists in the diagram, a black hole region must exist in the original spacetime.

Note that the standard definition of a black hole region, as given above, needs a well-defined notion of $\mathscr{I}^+$, which is standardly defined through conformal completion. It would be interesting to define a notion of $\mathscr{I}^+$ through the uplift of the conformal boundary in the projection diagram. We hope to return to this in the future.

As announced above, we end this section with a simple example: four-dimensional Minkowski space $\mathbb{R}^{1,3}$.

We first consider Minkowski spacetime in spherical coordinates

$$ds^2 = -dt^2 + dr^2 + r^2\left(d\theta^2 + \sin^2\theta d\varphi^2\right). \tag{2.21}$$

Consider $\pi : (t, r, \theta, \varphi) \to (t, r)$ which maps spacetime to the right half of $\mathbb{R}^{1,1}$ with auxiliary metric γ

$$\gamma_{\mu\nu}dx^\mu dx^\nu = -dt^2 + dr^2\,. \tag{2.22}$$

The map is not differentiable at $r = 0$ and thus $r = 0$ is not a part of

$$U := \{(t, \mathbf{x}) \in \mathbb{R}^{1,3}, |\mathbf{x}| \neq 0\} \in \mathbb{R}^{1,3}\,. \tag{2.23}$$

Hence, the diagram fails to represent the nature of spacetime at $r = 0$ – the locus $r = 0$ looks like a boundary even though it is not. The usual conformal compactification of (2.22) subsequently leads to diagram (a) in Figure 2.1, which coincides with the standard Carter-Penrose diagram of Minkowski spacetime.

A different projection diagram of Minkoswi space is obtained by writing $\mathbb{R}^{1,3} = \mathbb{R}^{1,1} \times \mathbb{R}^2$ and omitting the $\mathbb{R}^2$ part. We have

$$ds^2 = -dt^2 + dx^2 + dy^2 + dz^2\,. \tag{2.24}$$

The map $\pi : (t, x, y, z) \to (t, x)$ maps the spacetime to $\mathbb{R}^{1,1}$ with metric

$$\gamma_{\mu\nu}dx^\mu dx^\nu = -dt^2 + dx^2\,. \tag{2.25}$$

We thus obtain the diagram (b) in Figure 2.1. This diagram has the problem that it fails to represent the connectedness of $\mathscr{I}^+$ and the connectedness of $\mathscr{I}^-$.

These examples show that there is no uniqueness in projection diagrams. It is possible to project in different ways to obtain different projection diagrams. These projection diagrams in turn might carry different information about the causal structure. While the example of Minkowski spacetime exemplifies the definition, it does not yet show the advantage of projection diagrams as the causal diagrams (a) and (b) in Figure 2.1 may also be obtained from conformal compactification of $\mathbb{R}^{1,3}$ and subsequently taking slices. The usefulness of projection diagrams becomes clear in subsection 3.4.4, where we discuss the causal structure of particular metrics of the form (2.19). Their causal structure cannot be meaningfully depicted by taking a slice. Many more projection diagrams are discussed in the paper [24], to which the interested reader is referred to at this point.

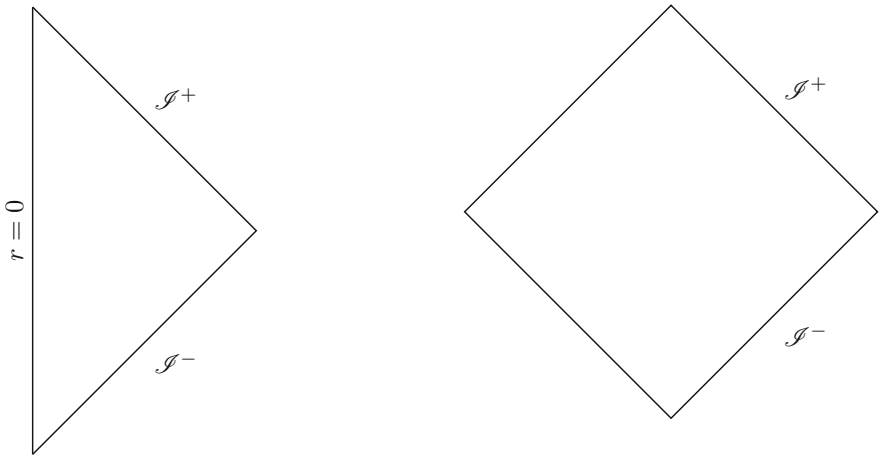

(a) **(b)**

Figure 2.1.: Projection diagrams of Minkowski spacetime. Figure (a) fails to properly depict the nature of spacetime near the set $\mathbf{x} = 0$. Figure (b) fails to properly represent the connectedness of $\mathscr{I}^+$ and the connectedness of $\mathscr{I}^-$.

2.3. Initial Value Formulation of General Relativity

General relativity asserts that the effects of the gravitational field may be described by a spacetime (M, g), where M is an $(n+1)$-dimensional manifold and g is a Lorentzian metric fulfilling Einstein's equations. To obtain an initial value formulation of general relativity, the theory must be viewed as describing the time evolution of some quantity. In classical theories, other than general relativity, we are usually given a fixed spacetime background and consider the time evolution of physical quantities on this fixed background. In general relativity, on the contrary, we want to solve for spacetime itself, making the nature of the initial value formulation less apparent.

We start by reviewing the following theorem [6, theorem 8.3.14]

Theorem 2.2. *Let (M, g) be a globally hyperbolic spacetime. Then, a global time function[1], f, can be chosen such that each surface of constant t is a Cauchy surface. Thus M can be foliated by Cauchy surfaces and the topology of M is $\mathbb{R} \times \Sigma$, where Σ denotes any Cauchy surface.*

In the following, we refer to the Cauchy surface at constant t as Σ_t. Let n^μ be the unit normal vector to the hypersurfaces Σ_t. A spatial metric

$$h_{\mu\nu} = g_{\mu\nu} + n_\mu n_\nu \tag{2.26}$$

is induced on surfaces of constant time. Now, let t^μ be a vector field on M satisfying $t^\mu \nabla_\mu t = 1$. The vector field may be interpreted as representing the flow of time throughout spacetime. The effect of moving forward in time, parametrized by the time function

[1] Recall that a time function t is a differentiable function on M such that $\nabla^\mu t$ is a past directed timelike vector field.

t, then corresponds to going from the surface Σ_0 to the surface Σ_t. Identifying the surfaces Σ_0 and Σ_t by the diffeomorphism that results from the integral curves of t^μ, moving forward in time then corresponds to changing the metric on the n-dimensional manifold Σ from $h_{\mu\nu}(0)$ to $h_{\mu\nu}(t)$. Hence, one expects to regard the spatial metric h on a hypersurface Σ and its "time derivative" as appropriate initial data set. A well-defined notion of the "time derivative" of the spatial metric h is then given by the extrinsic curvature

$$K_{\mu\nu} = h_\mu{}^\sigma \nabla_\sigma n_\nu = \left(\frac{1}{2}\mathcal{L}_n h_{\mu\nu}\right)^{\parallel} = K_{\nu\mu}\,, \tag{2.27}$$

where $\mathcal{L}_n h_{\mu\nu}$ is the Lie derivative of the metric $h_{\mu\nu}$ along the normal vector n^μ and the superscript "$\parallel$" means that the respective tensor is projected to the hypersurface.

It has been shown that appropriate initial data for general relativity consists of the triple (Σ, h, K), where Σ is an $n-$dimensional manifold, h is a Riemannian metric on Σ and K is a symmetric tensor field on Σ. The Einstein equations dictate that this initial data cannot be arbitrary but must satisfy the initial value constraints

$$G_{\mu\nu} n^\nu = 8\pi T_{\mu\nu} n^\nu\,. \tag{2.28}$$

Contracting (2.28) with n^μ or h^ν_μ, respectively, gives

$$D^\mu (K_{\mu\nu} - K^\sigma{}_\sigma h_{\mu\nu}) = J_\nu\,, \tag{2.29a}$$

$${}^{(n)}R + (K^\sigma{}_\sigma)^2 - K_{\mu\nu}K^{\mu\nu} = 2\Lambda + 2\rho\,, \tag{2.29b}$$

where $J_\nu = 8\pi h^\sigma_\nu T_{\sigma\mu}$ is the matter momentum vector, $\rho = 8\pi T_{\mu\nu} n^\mu n^\nu$ is the matter energy density on Σ, ${}^{(n)}R$ is the Ricci scalar of Σ and D^μ is the covariant derivative with respect to the spatial metric h defined as $D_\mu T^{\nu_1\ldots\nu_k}{}_{\sigma_1\ldots\sigma_l} = h^{\nu_1}_{\omega_1}\ldots h^{\zeta_l}_{\sigma_l} h^\kappa_\mu \nabla_\kappa T^{\omega_1\ldots\omega_k}{}_{\zeta_1\ldots\zeta_l}$. The equations (2.29) are referred to as the constraint equations and only depend on quantities intrinsically defined on the surface Σ. While we have considered the extrinsic curvature and the spatial metric on the surface Σ in terms of its embedding into spacetime up until this point, we now introduce their pullback to Σ, referred to as K_{ij} and h_{ij} such that we may write the constraint equations (2.29) as

$$D^i\Big(K_{ij} - K^l{}_l h_{ij}\Big) = J_j\,, \tag{2.30a}$$

$${}^{(n)}R + \Big(K^l{}_l\Big)^2 - K_{ij}K^{ij} = 2\Lambda + 2\rho\,, \tag{2.30b}$$

where indices are raised and lowered with the Riemannian metric h_{ij}. The existence of a well-posed initial value formulation for general relativity in the presence of matter depends upon the dynamical equations satisfied by matter and on the formula for the stress-energy tensor in terms of matter and metric [6].

In principle, the equations of motion of general relativity allow for arbitrary forms of matter, even if the resulting solutions to the equations of motion are typically considered unphysical. It is possible to restrict to physically viable situations by imposing energy conditions on the energy-momentum tensor of the matter. While many such energy

conditions are available in the literature, we consider here only the consequences of the dominant energy condition

$$\rho \geq \sqrt{J_i J_j h^{ij}} \tag{2.31}$$

on the initial value costraints. Equation (2.31) amounts to the requirement that to any observer the local energy–density appears positive and the local energy-flow vector is not spacelike.

An important case, which will be of interest in the following sections is that of time-symmetric initial data, $K_{ij} = 0$ (the "time-symmetric" terminology refers to the fact that a suitable reflection across Σ in the associated spacetime is an isometry). In this case, we have that $J_i = 0$ and the constraint equations (2.30) reduce to

$$^{(n)}R = 2\Lambda + 2\rho\,, \tag{2.32}$$

where ρ vanishes in vacuum. In that case the dominant energy conditions simply translates into the requirement that

$$^{(n)}R - 2\Lambda \geq 0\,. \tag{2.33}$$

Another concept that will be of importance in chapter 4 is that of Killing Initial Data (KIDs). As the terminology already suggests, KIDs are in one-to-one correspondence with Killing vectors in spacetime obtained from the time evolution of the initial data set [27]. We can decompose a Killing vector ξ of spacetime at Σ as

$$\xi = V n^\mu \partial_\mu + Y^i \partial_i\,, \quad V = -\xi^\mu n_\mu\,. \tag{2.34}$$

We will now consider such Killing Initial Data for vacuum spacetimes. From the Killing equations it follows that [28]

$$D_{(i}Y_{j)} + V K_{ij} = 0\,, \tag{2.35a}$$

$$D_i D_j V + \mathcal{L}_Y K_{ij} = \left({}^{(n)}R_{ij} + K K_{ij} - 2K K_{il} K_j{}^l - \frac{2}{n-1}\Lambda h_{ij} \right) V\,, \tag{2.35b}$$

where $K = K^l{}_l$. KIDs are defined as V, Y_i that are solutions to the differential eqations (2.35a)-(2.35b). In the time-symmetric case with $K_{ij} = 0$ and $Y_i = 0$, the equations (2.35) reduce to the *static KIDs equation*

$$D_i D_j V = \left({}^{(n)}R_{ij} - \frac{2}{n-1}\Lambda\, h_{ij} \right) V\,. \tag{2.36}$$

In chapter 4, we consider time-symmetric initial data sets and use KIDs to define the mass associated with these initial data sets.

So far, our discussion has been restricted to globally hyperbolic spacetimes. However, metrics that locally approach Anti-de Sitter spacetime at large distances, are not globally hyperbolic due to the fact that the conformal boundary at infinity is timelike. By definition, (asymptotically locally) Anti-de Sitter spacetimes do therefore not contain a Cauchy hypersurface. In this case, the specification of initial data (K, h, Σ) on a spacelike hypersurface Σ only determines the time evolution completely on the domain

of dependence. Similarly, the KIDs equations only guarantee the existence of Killing vectors on the domain of dependence. The solution, obtained by evolving the initial data set with the Einstein equations, can be uniquely determined by supplementing the initial data set with boundary condition at the conformal boundary. As this is a subtle issue and we will not consider the time evolution of initial data sets in this thesis, we refer the interested reader to [29] for a discussion of the issues occurring in this context.

3. Gravity in 2+1 Dimensions

Studying conceptual problems in general relativity is often hindered by the technical complexity of calculations in higher dimensions. Therefore, it is useful to consider toy models, that capture the relevant features while reducing technical difficulties to a minimum. One such toy model is $(2+1)$-dimensional Einstein gravity.

As we will see in section 3.1, the dynamics of general relativity in three spacetime dimensions is substantially simpler than its higher-dimensional counterparts. In fact, in the absence of local matter sources, we have no dynamical gravitational degrees of freedom and thus there are no gravitational waves in three dimensions. This suggests that Einstein gravity in three dimensions might not be a worthwhile topic to study. However, as we will see in the following this is not the case. In section 3.2 we discuss the simplest solution to three-dimensional Einstein gravity at negative cosmological constant, AdS_3 spacetime. In section 3.3 we discuss the asymptotic behavior of three-dimensional Einstein gravity and its asymptotic symmetry group. Black hole solutions are discussed in section 3.4. In section 3.5 we discuss a modification of Einstein gravity: topologically massive gravity, which propagates one massive graviton. In that section, we discuss particular solutions of this theory which were investigated in [1]. The chapter ends with section 3.6, where we discuss how asymptotic symmetries can be used to perform a microstate counting of three-dimensional black holes.

3.1. Generalities

As already discussed in section 2.1.1, equation (2.5), for $d \geq 3$ the Riemann tensor can be decomposed into Ricci tensor, Ricci scalar and Weyl tensor. This decomposition simplifies in three spacetime dimensions where the Weyl tensor vanishes.

For vanishing Weyl tensor (2.5) reduces to

$$R_{\mu\nu\rho\sigma} = \frac{g_{\mu\rho}R_{\nu\sigma} + g_{\nu\sigma}R_{\mu\rho} - g_{\nu\rho}R_{\mu\sigma} - g_{\mu\sigma}R_{\nu\rho}}{d-2} - R\,\frac{g_{\mu\rho}g_{\nu\sigma} - g_{\mu\sigma}g_{\nu\rho}}{(d-1)(d-2)}\,. \tag{3.1}$$

Upon using vacuum Einstein equations

$$R_{\mu\nu} = \frac{2\Lambda}{d-2}\,g_{\mu\nu} \tag{3.2}$$

this becomes

$$R_{\mu\nu\rho\sigma} = \frac{2\Lambda}{(d-1)(d-2)}(g_{\mu\rho}g_{\nu\sigma} - g_{\mu\sigma}g_{\nu\rho})\,. \tag{3.3}$$

In three dimensions this reduces to

$$R_{\mu\nu\rho\sigma} = \Lambda(g_{\mu\rho}g_{\nu\sigma} - g_{\mu\sigma}g_{\nu\rho})\,. \tag{3.4}$$

It is remarkable that the Riemann tensor of any three-dimensional spacetime satisfying vacuum Einstein equations takes the form (3.4). Equation (3.4) also implies that all sectional curvatures are constant as can be easily checked from the definition of sectional curvature.

Definition 3.1. ***Sectional Curvature***
Let M be a Riemannian manifold with metric g. Suppose $x \in M$ and let E be a nondegenerate plane section (2-dimensional linear subspace) of T_pM. Let $\{X, Y\}$ be a basis of E. Then the sectional curvature of M at x associated with the plane E is given by

$$\kappa(x, E) := \frac{R^{\mu}{}_{\nu\alpha\beta} X^{\alpha} Y^{\beta} X_{\mu} Y^{\nu}}{X^{\mu} X_{\mu} Y^{\nu} Y_{\nu} - (X^{\mu} Y_{\mu})^2} \,. \tag{3.5}$$

One may easily show that the definition of sectional curvature only depends on the plane, but not on the vectors X and Y which span the plane [30, Theorem 2.2.3]. The definition may be extended to pseudo-Riemannian manifolds provided that the plane spanned by X and Y is not null.

Calculating the sectional curvature for any plane E, which is not null, for spacetimes whose Riemann tensor takes the form (3.3), we find that

$$\kappa(x, E) = \frac{2\Lambda}{(d-1)(d-2)} \,. \tag{3.6}$$

We say a manifold M has constant curvature if the sectional curvature is a constant function of x and E. In this thesis, we will also refer to such manifolds as *constant curvature manifolds*. It holds true that all pseudo-Riemannian manifolds of fixed constant curvature are locally isometric [30, Theorem 2.4.11]. In particular, this implies that three-dimensional Lorentzian vacuum solutions to Einstein gravity are, depending on the cosmological constant, either, locally isometric to AdS_3, $\mathbb{R}^{1,2}$ or dS_3. Note that a similar statement can be made in higher dimensions, provided that the Weyl tensor vanishes.

In the following sections we will see that global effects allow for interesting spacetimes in three-dimensional Einstein gravity.

3.2. Global AdS spacetime

The simplest solution to three-dimensional Einstein gravity at negative cosmological constant is AdS_3 spacetime. Global Anti-de Sitter space can be defined in terms of a hyperboloid embedded into $\mathbb{R}^{2,2}$ given by

$$ds^2 = -du^2 - dv^2 + dx^2 + dy^2 \tag{3.7a}$$

through the equation

$$-u^2 - v^2 + x^2 + y^2 = -1 \,. \tag{3.7b}$$

Changing coordinates as

$$u = \cosh\rho \sin t \,, \qquad v = \cosh\rho \cos t \,, \tag{3.8a}$$

$$x = \sinh\rho \cos\varphi \,, \qquad y = \sinh\rho \sin\varphi \tag{3.8b}$$

we obtain

$$ds^2 = -\cosh^2\rho dt^2 + d\rho^2 + \sinh^2\rho d\varphi^2 \,. \tag{3.9}$$

We have the identifications of points $(t, \rho, \varphi) \sim (t + 2\pi j, \rho, \varphi + 2\pi k)$, where $k, j \in \mathbb{Z}$. Because of the identification in t, there exist closed timelike curves through each point in spacetime. A visualization of AdS spacetime, albeit in one dimension lower, is given in Figure 3.1.

A spacetime without closed timelike curves is obtained by unwrapping the t coordinate, i.e. one does not identify t with $t + 2\pi j$. In this manner, one goes from global AdS_3 spacetime to the universal covering space of AdS_3. This space is commonly also referred to as AdS_3 spacetime and we use this ambiguous nomenclature in the following as well. Changing the radial coordinate as

$$\rho = \operatorname{arcsinh}(r) \tag{3.10}$$

the metric (3.9) becomes

$$ds^2 = -\Big(r^2 + 1\Big)dt^2 + \frac{dr^2}{r^2+1} + r^2 d\varphi^2 \,. \tag{3.11}$$

We have the identification of points $(t, r, \varphi) \sim (t, r, \varphi + 2\pi k)$. In the vincinity of $r = 0$ the metric takes the form

$$ds^2 \approx -dt^2 + dr^2 + r^2 d\varphi^2 + \dots \,. \tag{3.12}$$

The locus $r = 0$ is a line and corresponds to the center of the coordinate system. Changing coordinates as $\cosh\rho = 1/\cos q$ we obtain

$$ds^2 = \frac{1}{\cos^2 q}\Big(-dt^2 + dq^2 + \sin^2 q d\varphi^2\Big) \,, \tag{3.13}$$

where $q \in [0, \pi/2)$. The conformal factor $\Omega^2 = \cos^2 q$ vanishes at $\pi/2$ and is positive and non-vanishing elsewhere. The spacetime with metric $\tilde{g}_{\mu\nu} = \Omega^2 g_{\mu\nu}$ and coordinate ranges $q \in [0, \pi/2]$, $t \in (-\infty, \infty)$ and identification $(t, r, \varphi) \sim (t, r, \varphi + 2\pi k)$ is the conformal completion of AdS_3 spacetime. AdS_3 is not conformally compact as $t \in (-\infty, \infty)$. It can be visualized as an infinitely long filled cylinder, see Figure 3.2.

3.2.1. Isometries

The isometry group of AdS_3 is given by $SO(2,2)$. The isometry algebra $so(2,2)$ is spanned by the Killing vectors, which, written in the coordinate system (3.7), read

$$J_{ab} = x_b \frac{\partial}{\partial x^a} - x_a \frac{\partial}{\partial x^b} \,, \tag{3.14}$$

where $x^a = \{v, u, x, y\}$. By definition, J_{ab} is antisymmetric in a and b. Written in detail the Killing vectors read

$$J_{01} = v\,\partial_u - u\,\partial_v \,, \qquad J_{02} = x\,\partial_v + v\,\partial_x \,, \tag{3.15a}$$

$$J_{03} = y\,\partial_v + v\,\partial_y \,, \qquad J_{12} = x\,\partial_u + u\,\partial_x \,, \tag{3.15b}$$

$$J_{13} = y\,\partial_u + u\,\partial_y \,, \qquad J_{23} = y\,\partial_x - x\,\partial_y \,. \tag{3.15c}$$

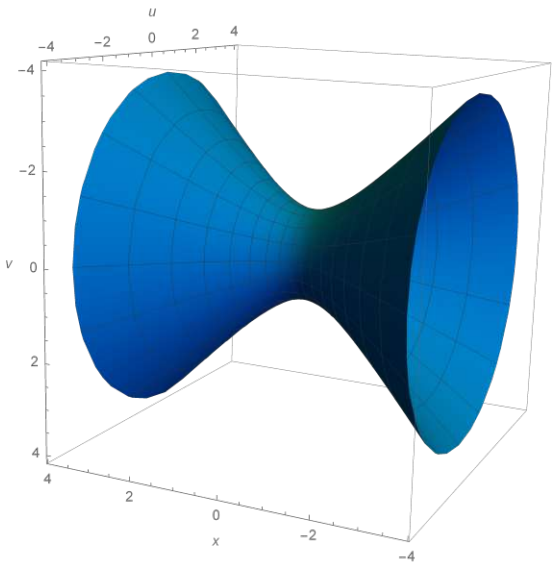

Figure 3.1.: AdS_2 spacetime embedded into $(1+2)$-dimensional flat space $\mathbb{R}^{2,1}$. AdS_2 spacetime is described as the hyperboloid $-u^2 - v^2 + x^2 = -1$ in $\mathbb{R}^{2,1}$ with line element $ds^2 = -du^2 - dv^2 + dx^2$. AdS_2 spacetime has closed timelike curves going through each point. The closed timelike curves wind around the x-axis.

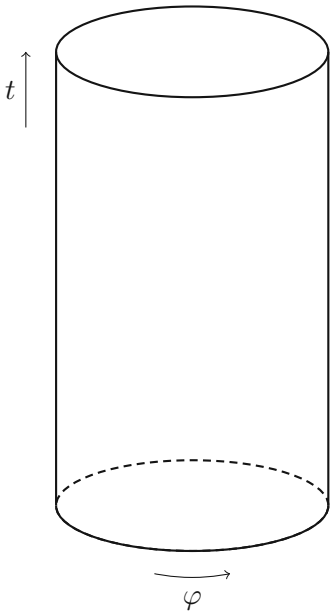

Figure 3.2.: Visualization of AdS_3 as an infinitely long cylinder, which extends from $t = -\infty$ to $t = \infty$.

The vector $J_{01} = \partial_t$ generates time translations, while $J_{23} = -\partial_\varphi$ generates rotations. The algebra spanned by the Killing vectors is $so(2,2)$, defined by the algebraic relations

$$[J_{ab}, J_{cd}] = (g_{ac}J_{bd} + g_{bd}J_{ac} - g_{ad}J_{bc} - g_{bc}J_{ad}) \tag{3.16}$$

with $g_{ab} = \mathrm{diag}\{-1,-1,1,1\}$.

3.3. Asymptotic Behavior

In this section, we discuss the asymptotic behavior of general relativity with a negative cosmological constant. We consider spacetimes that approach AdS_3 – the maximally symmetric vacuum solution to the Einstein equations at negative cosmological constant – at large distances. To compute conserved quantities such as the energy of the gravitational field, it is not only of importance to specify that AdS_3 is approached at large distances, but also at which rate this happens. Brown and Henneaux [21] proposed boundary conditions which achieve this

$$g_{tt} = -\bar{r}^2 + O(1)\,, \tag{3.17a}$$
$$g_{t\bar{r}} = O\left(\frac{1}{\bar{r}^3}\right), \tag{3.17b}$$
$$g_{t\varphi} = O(1)\,, \tag{3.17c}$$
$$g_{\bar{r}\bar{r}} = \frac{1}{\bar{r}^2} + O\left(\frac{1}{\bar{r}^4}\right), \tag{3.17d}$$
$$g_{\bar{r}\varphi} = O\left(\frac{1}{\bar{r}^3}\right), \tag{3.17e}$$
$$g_{\varphi\varphi} = \bar{r}^2 + O(1)\,. \tag{3.17f}$$

They arrived at these boundary conditions by requiring that the isometry group of global AdS_3 spacetime should also be a subgroup of the asymptotic symmetry group of asymptotically AdS_3 spacetimes. This led them to weaken an alternative choice of boundary conditions which was also presented in their paper [21]. The asymptotic Killing vectors that preserve the boundary conditions are defined as solutions of the asymptotic Killing equation which preserve (3.17) up to the terms specified by $O(\dots)$ in (3.17). In the coordinates

$$x^{\pm} = t \pm \varphi \tag{3.18}$$

the asymptotic Killing vectors $\xi = \xi_+ + \xi_-$ preserving (3.17) read

$$\xi_+(v_+) = -\left(\frac{1}{2}\bar{r}v_+' + O\left(\bar{r}^{-1}\right)\right)\partial_{\bar{r}} + \left(v_+ + O\left(\bar{r}^{-4}\right)\right)\partial_+ + \left(\frac{v_+''}{2\bar{r}^2} + O\left(\bar{r}^{-4}\right)\right)\partial_-\,, \tag{3.19}$$
$$\xi_-(v_-) = -\left(\frac{1}{2}\bar{r}v_-' + O(\bar{r}^{-1})\right)\partial_{\bar{r}} + \left(\frac{v_-''}{2\bar{r}^2} + O\left(\bar{r}^{-4}\right)\right)\partial_+ + \left(v_- + O\left(\bar{r}^{-4}\right)\right)\partial_-\,, \tag{3.20}$$

where $v_+ = v_+(x^+)$, $v_- = v_-(x^-)$ and prime denotes derivative with respect to the argument. The functions $v_\pm(x^\pm)$ must respect the identifications

$$(\bar{r}, x^+, x^-) \sim (\bar{r}, x^+ + 2\pi, x^- - 2\pi) \tag{3.21}$$

and thus they must be periodic functions of x^+ and x^- respectively. Expanding $v_\pm\partial_\pm$ into Fourier modes as

$$v_\pm(x^\pm)\partial_\pm = \sum_{n\in\mathbb{Z}} c_\pm^n l_n^\pm\,, \qquad l_n^\pm = e^{inx^\pm}\partial_\pm\,, \tag{3.22}$$

we find the asymptotic symmetry algebra

$$i[l_n^\pm, l_m^\pm] = (n-m)l_n^\pm\,, \quad i[l_n^\pm, l_m^\mp] = 0\,, \tag{3.23}$$

where $[\,,\,]$ denotes the Lie bracket. Note that the definition of basis vectors used in the Fourier decomposition is different than the one used in [21]. The global isometries of AdS_3 spacetime $so(2,2) \cong sl(2,R) \oplus sl(2,R)$ are thus recovered asymptotically and are spanned by the generators $\{l_{-1}^\pm, l_0^\pm, l_1^\pm\}$ where the plus and the minus sector each span one copy of $sl(2,R)$.

To each of these asymptotic Killing vector fields, it is possible to associate a conserved charge. The variation of these charges was computed in [21] using Hamiltonian methods [31]

$$\delta Q^+[v_+] = \frac{1}{8\pi G}\int d\varphi\, v_+(x^+)\delta g^0_{++}\,, \tag{3.24a}$$

$$\delta Q^-[v_-] = \frac{1}{8\pi G}\int d\varphi\, v_-(x^-)\delta g^0_{--}\,, \tag{3.24b}$$

where $g^0_{++} = \frac{1}{4}\left(g^0_{tt} + 2g^0_{t\varphi} + g^0_{\varphi\varphi}\right)$, $g^0_{--} = \frac{1}{4}\left(g^0_{tt} - 2g^0_{t\varphi} + g^0_{\varphi\varphi}\right)$. The index zero refers to the term of order r^0 in the asymptotic expansion (3.17). Note that there are infinitely many charges as $v_+(x^+)$ and $v_-(x^-)$ are arbitrary, smooth functions of the coordinates x^+ and x^- that are well-defined on the entire manifold. Expanding these charges in Fourier modes gives

$$L_n^+ = Q^+[e^{inx^+}] = \frac{1}{8\pi G}\int d\varphi\, e^{inx^+} g^0_{++}\,, \tag{3.25a}$$

$$L_n^- = Q^-[e^{inx^-}] = \frac{1}{8\pi G}\int d\varphi\, e^{inx^-} g^0_{--}\,, \tag{3.25b}$$

where $n \in \mathbb{Z}$. The mass and the angular momentum can then be defined as the charge associated with the generator of time translations $\partial_t = \partial_+ + \partial_-$ and rotations $-\partial_\varphi = -\partial_+ + \partial_-$, respectively

$$m \equiv L_0^+ + L_0^-\,, \quad j \equiv -\left(L_0^+ - L_0^-\right). \tag{3.26}$$

In computing the charges (3.24) we have chosen a background metric b, for which all charges vanish

$$b = -\bar{r}^2 dt^2 + \frac{d\bar{r}^2}{\bar{r}^2} + \bar{r}^2 d\varphi^2\,. \tag{3.27}$$

This is not global AdS_3 spacetime, but a so-called BTZ black hole with – per definition – vanishing mass and angular momentum. We discuss the causal structure of (3.27) in subsection 3.4.7 . Computing the energy of global AdS_3, which has $g^0_{tt} = -1$, $g^0_{\varphi\varphi} = 0$ and $g^0_{t\varphi} = 0$, we find that it is negative

$$m_{AdS_3} = -\frac{1}{8G}\,. \tag{3.28}$$

The negativity is due to the choice of background metric (3.27). It will become clear in the next subsection why this choice of background metric is sensible. The Poisson algebra of the charges (3.25) is isomorphic to the maximal non-trivial central extension of (3.23) and reads

$$i\{L^\pm_n, L^\pm_m\} = (n-m)L^\pm_{n+m} + \frac{c^\pm}{12}(n^3-n)\delta_{n+m,0}\,, \tag{3.29a}$$

$$i\{L^\pm_n, L^\mp_m\} = 0\,, \tag{3.29b}$$

where $\{\,,\,\}$ denote the Poisson brackets. The values of the central extensions in the algebra of the charges can be determined explicitly

$$c^+ = c^- = \frac{3}{2G} \tag{3.30}$$

by computing the Poisson brackets of (3.25). Thus, we have shown that the symmetry transformations that preserve the asymptotic structure of asymptotically AdS_3 spacetimes are given by a direct sum of two copies of the Virasoro algebra. This algebra is well known from a — a priori — completely different context in physics, namely from two-dimensional conformal field theories. The Virasoro algebra (3.29) is the algebra of local conformal transformations in two dimensions and the defining feature of a two-dimensional conformal field theory.

Today, this result is considered to be a precursor of the AdS_3/CFT_2 correspondence which asserts that quantum gravity on AdS_3 spacetimes is dual to a two-dimensional conformal field theory. While many results in favor of the correspondence exist, the result has not been proven, see [32] for a discussion of the issues occurring in this context. In one of his famous papers [13], Strominger states that the fact that the asymptotic symmetries of asymptotically AdS_3 spacetimes comprise two copies of the Virasoro algebra implies that "any consistent quantum theory of gravity on AdS_3 is a conformal field theory". At the minimum, this statement rests on the assumption that the theory of quantum gravity exists (as already pointed out in [13]), but to this day this has not been proven. We present the results of the paper [13] in subsection 3.6 where we also discuss this issue further.

3.3.1. Phase Space

In this subsection we discuss solutions to the vacuum Einstein equations with asymptotically AdS_3 boundary conditions, which we specified above (3.17). For this it is useful to

write the boundary conditions in the Fefferman-Graham coordinate system [33]

$$ds^2 = \frac{d\bar{r}^2}{\bar{r}^2} + g_{AB}(\bar{r}, x^C)dx^A dx^B \tag{3.31}$$

with

$$g(\bar{r}, x^C) = \bar{r}^2\eta + O(1)\,, \tag{3.32}$$

where η is the flat metric on the cylinder, $\eta = -dt^2 + d\varphi^2$. It can be shown by solving the Einstein equations order by order that generic, analytic solutions to the vacuum Einstein equations with negative cosmological constant subject to the fall-off behavior (3.31), (3.32) take the form [34]

$$ds^2 = \frac{d\bar{r}^2}{\bar{r}^2} - \left(\bar{r}dx^+ - \frac{\mathcal{L}_-(x^-)}{\bar{r}}dx^-\right)\left(\bar{r}dx^- - \frac{\mathcal{L}_+(x^+)}{\bar{r}}dx^+\right), \tag{3.33}$$

where $\mathcal{L}_-(x^-)$, $\mathcal{L}_+(x^+)$ are analytic functions of x^+ and x^- respectively. The asymptotic Killing vectors preserving the form of the metric (3.33) to any order read

$$\begin{aligned}\xi = &-\frac{1}{2}\bar{r}(v'_-(x^-) + v'_+(x^+))\partial_{\bar{r}} + \left(v_+(x^+) + \frac{\bar{r}^2 v''_-(x^-) + \mathcal{L}_-(x^-)v''_+(x^+)}{2\bar{r}^4 - 2\mathcal{L}_-(x^-)\mathcal{L}_+(x^+)}\right)\partial_+ \\ &+ \left(v_-(x^-) + \frac{\bar{r}^2 v''_+(x^+) + \mathcal{L}_+(x^+)v''_-(x^-)}{2\bar{r}^4 - 2\mathcal{L}_+(x^+)\mathcal{L}_-(x^-)}\right)\partial_-\,.\end{aligned} \tag{3.34}$$

Expanding (3.34) in large r yields (3.20). The action of (3.34) on the solution space (3.33) reads

$$\delta_\xi\mathcal{L}(x^+) = 2\mathcal{L}_+(x^+)v'_+(x^+) + \mathcal{L}'_+(x^+)v_+(x^+) - v'''_+(x^+)\,, \tag{3.35a}$$
$$\delta_\xi\mathcal{L}_-(x^-) = 2\mathcal{L}_-(x^-)v'_-(x^-) + \mathcal{L}'_-(x^-)v_-(x^-) - v'''_-(x^-). \tag{3.35b}$$

The symmetries in their finite form are

$$x^+ \to \tilde{v}_+(x^+) + O\left(\frac{1}{\bar{r}^2}\right), \tag{3.36a}$$
$$x^- \to \tilde{v}_-(x^-) + O\left(\frac{1}{\bar{r}^2}\right), \tag{3.36b}$$
$$\bar{r} \to \bar{r}\sqrt{\tilde{v}'_+(x^+)\tilde{v}'_-(x^-)} + O\left(\frac{1}{\bar{r}}\right), \tag{3.36c}$$

where $\tilde{v}_\pm$ are the finite symmetry transformations. Here, $\tilde{v}_\pm$ must be diffeomorphisms of S^1. Under these symmetries the metric takes the same form as (3.33), but with

$$\mathcal{L}(x^+) \to \mathcal{L}(\tilde{v}_+(x^+))\tilde{v}'^2_+(x^+) - \frac{c}{12}\{\tilde{v}_+(x^+), x^+\}\,, \tag{3.37a}$$
$$\bar{\mathcal{L}}(x^-) \to \bar{\mathcal{L}}(\tilde{v}_-(x^-))\tilde{v}'^2_-(x^-) - \frac{\bar{c}}{12}\{\tilde{v}_-(x^-), x^-\}\,, \tag{3.37b}$$

where the brackets $\{\,,\,\}$ denote the Schwarzian derivative

$$\{\tilde{v}_+, x^+\} = \frac{\tilde{v}_+(x^+)'''}{\tilde{v}_+(x^+)'} - \frac{3}{2}\left(\frac{\tilde{v}_+(x^+)''}{\tilde{v}_+(x^+)'}\right)^2 . \tag{3.38}$$

The causal structure of the metrics with constant $\mathcal{L}_-(x^-) = \mathcal{L}_-$ and constant $\mathcal{L}_+(x^+) = \mathcal{L}_+$ has been investigated in [35–37], see also [38, section V] for a nice summary.

To examine the causal structure of (3.33) it is useful to switch back to t, r, φ coordinates and parametrize the class of metrics by mass and angular momentum

$$\mathcal{L}_+ = 2G(m-j) \equiv \frac{1}{4}(M-J)\,, \qquad \mathcal{L}_- = 2G(m+j) \equiv \frac{1}{4}(M+J)\,, \tag{3.39}$$

where we have introduced new parameters M and J which are proportional to the mass and angular momentum in such a way that the numerical prefactors in the metric simplify. We furthermore change the radial coordinate

$$\bar{r} = \sqrt{\frac{-\frac{M}{2} + r^2 + \sqrt{\frac{J^2}{4} - Mr^2 + r^4}}{2}} \tag{3.40}$$

to obtain

$$ds^2 = (M - r^2)dt^2 + \frac{4r^2 dr^2}{J^2 - 4Mr^2 + 4r^4} - Jdtd\varphi + r^2 d\varphi^2 \tag{3.41}$$

which may also be written as

$$ds^2 = -F(r)dt^2 + \frac{dr^2}{F(r)} + r^2(N^\varphi(r)dt + d\varphi)^2\,, \tag{3.42}$$

where

$$F(r) = -M + r^2 + \frac{J^2}{4r^2}\,, \qquad N^\varphi(r) = -\frac{J}{2r^2}\,. \tag{3.43}$$

In the case where $M > 0$ and $|J| \leq M$ this metric describes a black hole solution. The horizons are located at the zeros of $F(r)$. The geometry and causal structure of this case will be discussed in detail in the next section 3.4.

To discuss the other cases we change coordinates as $r^2 = \rho$ to obtain

$$(M-\rho)dt^2 + \frac{d\rho^2}{J^2 - 4M\rho + 4\rho^2} - Jdtd\varphi + \rho d\varphi^2\,. \tag{3.44}$$

In the case $|J| > |M| > 0$ the metric is regular everywhere and can be extended to $\rho < 0$. In this case, the geometry has closed timelike curves, that are not being shielded by a horizon. We thereby obtain a nakedly singular spacetime.

In the case $|J| < |M|$, $M < 0$ the spacetime aquires a conical singularity.

In the special case that $M = -1$ and $J = 0$ the geometry is smooth and $r = 0$ is a timelike line

$$ds^2 = -(1 + r^2)dt^2 + \frac{dr^2}{1 + r^2} + r^2 d\varphi^2\,. \tag{3.45}$$

This is just global AdS_3 spacetime with mass given by

$$m_{AdS_3} = \frac{M}{8G} = -\frac{1}{8G}\,. \tag{3.46}$$

The geometric structure of the phase space with constant $\mathcal{L}_+$, $\mathcal{L}_-$ is summarized in Figure 3.3 – the figure has been drawn for the first time in [37].

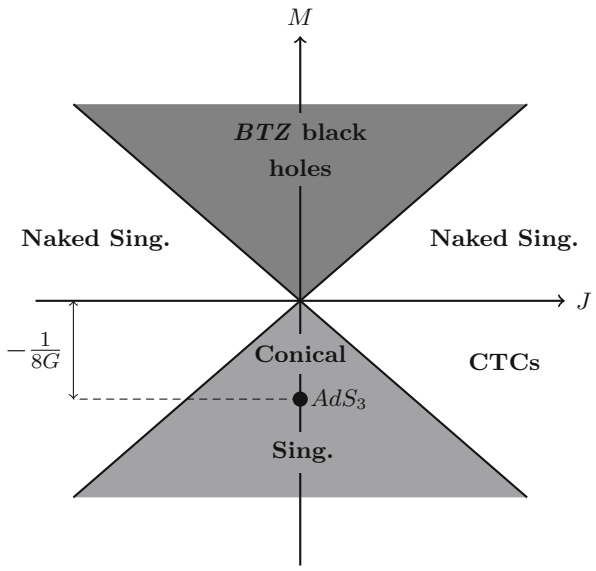

Figure 3.3.: Vacuum solutions (3.33) with constant $\mathcal{L}_\pm$ subject to asymptotically AdS_3 boundary conditions. Figure adapted with permission from [38, 39]

3.4. BTZ Black Hole

In this section, we discuss the so-called BTZ black hole. In subsection 3.4.1 the BTZ black hole is introduced. In subsection 3.4.2 it is discussed how the BTZ black hole can be obtained by identifying points in AdS_3 spacetime. In subsection 3.4.3 the maximal causal extension of the BTZ black hole is discussed. Section 3.4.4 is devoted to the causal structure of the BTZ black hole.

3.4.1. A Surprise in 2+1 Dimensions

As discussed in section 3.1, in three spacetime dimensions all vacuum solutions of the Einstein equations at fixed negative cosmological constant are locally isometric to AdS_3. Hence, if a vacuum black hole solution exists, its local properties must coincide with the local properties of Anti-de Sitter space, implying that it must have constant curvature everywhere. In particular, it must not have a curvature singularity; a property that we typically associate with four-dimensional black holes. For this reason, one might, wrongly,

be tempted to conclude that black holes do not exist in three-dimensional Einstein gravity. In fact, for positive or vanishing cosmological constant this statement is correct: It was shown by Daisuke Ida [40] that black holes in (2+1)-dimensional Einstein gravity do not exist for positive or vanishing cosmological constant.

Given the peculiar features of $(2+1)$-dimensional Einstein gravity it came as a great surprise when Máximo Bañados, Claudio Teitelboim and Jorge Zanelli found a black hole solution in three dimensions [41], which was subsequently named after them. The metric of the BTZ black hole, written in local coordinates t, r and φ, takes the form

$$ds^2 = -N^2 F(r) dt^2 + \frac{dr^2}{F(r)} + r^2 (N^\varphi(r) dt + d\varphi)^2 \,, \tag{3.47}$$

where

$$F(r) = -M + r^2 + \frac{J^2}{4r^2} = \frac{(r^2 - r_+^2)(r^2 - r_-^2)}{r^2} \,, \tag{3.48a}$$

$$N^\varphi(r) = -\frac{J}{2r^2} N + N^\varphi_\infty = -\mathrm{sgn}(J) \frac{r_+ r_-}{r^2} N + N^\varphi_\infty \,, \tag{3.48b}$$

where M, J, r_+, r_-, N and N^φ_∞ are constants and $t \in \mathbb{R}$ and $r \neq \{0, r_-, r_+\}$. The function $F(r)$ vanishes at the location of the Killing horizons

$$r_\pm^2 = \frac{1}{2}\Big(M \pm \sqrt{M^2 - J^2}\Big) \,. \tag{3.49}$$

Therefore, for Killing horizons to exist we must have that

$$M > 0 \,, \quad |J| \leq M \,. \tag{3.50}$$

It holds that $r_- \leq r_+$. Additionally, we have the following identification of points

$$(t, r, \varphi) \sim (t, r, \varphi + 2\pi) \,. \tag{3.51}$$

It is this identification that makes the black hole. If one does not impose the identification (3.51), the metric (3.47) is simply a portion of Anti-de Sitter space and the horizon at $r = r_+$ is just the horizon of an accelerated observer [35] and not an event horizon. On the contrary, if one does impose the identification (3.51) the horizon at $r = r_+$ becomes an event horizon – a fact that is discussed in detail in subsection 3.4.3, where we discuss the causal structure of the BTZ black hole. The constants N and N^φ_∞ can be absorbed by first shifting the angle as

$$\varphi \to \varphi - N^\varphi_\infty t \tag{3.52a}$$

and then rescaling the time as

$$t \to \frac{t}{N} \,. \tag{3.52b}$$

For this reason we set $N = 1$ and $N^{\varphi}_{\infty} = 0$ in the following unless specified otherwise. The two horizons are Killing horizons of the Killing vectors ξ_+ and ξ_-, respectively, which read

$$\xi_{\pm} = \partial_t + \Omega_{\pm}\partial_{\varphi}\,, \tag{3.53}$$

where $\Omega_{\pm}$ are the angular velocities at the inner and the outer horizon

$$\Omega_+ = -\left.\frac{g_{t\varphi}}{g_{\varphi\varphi}}\right|_{r=r_+} = \frac{J}{M+\sqrt{M^2-J^2}}\,, \tag{3.54a}$$

$$\Omega_- = -\left.\frac{g_{t\varphi}}{g_{\varphi\varphi}}\right|_{r=r_-} = \frac{J}{M-\sqrt{M^2-J^2}}\,. \tag{3.54b}$$

Similarly to higher-dimensional black holes, the BTZ black hole possesses a singularity; albeit this singularity is not a curvature singularity, but rather a singularity in the causal structure as we will see below. In coordinates t, r, φ, used in (3.47), this singularity is located at $r = 0$. At first sight, the singularity at $r = 0$ appears to be the standard coordinate singularity that arises at the center of the polar coordinate system. This is however not the case. Changing coordinates as $r^2 = \rho$

$$\begin{aligned} ds^2 &= \Big(r_+^2 + r_-^2 - \rho\Big)dt^2 + \frac{d\rho^2}{4(\rho - r_-^2)(\rho - r_+^2)} - 2\,\mathrm{sgn}(J)\, r_- r_+ dt d\varphi + \rho d\varphi^2 \\ &= (M-\rho)dt^2 + \frac{d\rho^2}{J^2 - 4M\rho + 4\rho^2} - J dt d\varphi + \rho d\varphi^2\,, \end{aligned} \tag{3.55}$$

we find that the metric is regular in the vicinity of $r = 0$ as long as $J \neq 0$. The locus $\rho = 0$ is not a point but rather a surface through which spacetime can be extended. However, if one chooses to allow for $\rho < 0$ closed timelike curves appear, which is why one typically cuts off the spacetime at $r = 0$. The spacetime has constant curvature everywhere, in particular also at $r = 0$. Note that in the case $J = 0$ the black hole aquires a more severe singularity, which is shortly discussed in subsection 3.4.2.

3.4.2. BTZ black hole as a quotient

Given that the black hole can only differ from AdS_3 by global properties, it is natural to expect that it can be obtained from AdS_3 by identifying points in spacetime. It was shown in [35] that the BTZ black hole is a quotient of AdS_3 by a discrete subgroup H of its isometry group. For the quotient space M/H to be a Hausdorff manifold the action of the group H on AdS_3 has to be properly discontinuous (for details see [42]). The quotient is a Hausdorff manifold for the case of the rotating BTZ black hole ($J \neq 0$) but fails to be a Hausdorff manifold when $J = 0$ [35, appendix B]. In the latter case the Hausdorff manifold structure is destroyed at $r = 0$ – leading to a singularity in the manifold structure at this locus. We now shortly discuss the case of the non-extremal rotating BTZ black hole ($r_+^2 - r_-^2 > 0$). In this case the Killing vector along which AdS_3 is identified is given by

$$\xi = r_+ J_{12} - r_- J_{03} = r_+(x\,\partial_u + u\,\partial_x) - r_-(y\,\partial_v + v\,\partial_y) \tag{3.56}$$

in the coordinates (3.7), which describe AdS_3 as a hyperboloid embedded into four-dimensional flat space. The norm of ξ reads

$$\xi^\mu \xi_\mu = r_+^2(u^2 - x^2) + r_-^2(v^2 - y^2)\,, \tag{3.57}$$

which using the identity (3.7b) can also be written as

$$\xi^\mu \xi_\mu = (r_+^2 - r_-^2)(u^2 - x^2) + r_-^2\,. \tag{3.58}$$

The norm of the Killing vector (3.58) becomes negative for $u^2 - x^2 < -r_-^2/(r_+^2 - r_-^2)$, implying that in this region closed timelike curves appear. Conversely, the norm of the Killing vector (3.58) is positive in the region

$$-r_-^2/(r_+^2 - r_-^2) < u^2 - x^2 < \infty \tag{3.59}$$

The region $\xi^\mu \xi_\mu > 0$ can be divided in regions bounded by the null surfaces $u^2 - x^2 = 0$ and $v^2 - y^2 = 1 - (u^2 - x^2) = 0$ where the identity (3.7b) has been used to establish the second equality. In the region $u^2 - x^2 > 1$ and $u, y > 0$ we introduce new coordinates as [35]

$$u = \sqrt{A(r)}\cosh\tilde{\varphi}(t,\varphi)\,, \qquad x = \sqrt{A(r)}\sinh\tilde{\varphi}(t,\varphi)\,, \tag{3.60a}$$

$$y = \sqrt{B(r)}\cosh\tilde{t}(t,\varphi)\,, \qquad v = \sqrt{B(r)}\sinh\tilde{t}(t,\varphi)\,, \tag{3.60b}$$

where

$$A(r) = \frac{r^2 - r_-^2}{r_+^2 - r_-^2}\,, \qquad B(r) = \frac{r^2 - r_+^2}{r_+^2 - r_-^2} \tag{3.60c}$$

and

$$\tilde{t}(t,\varphi) = r_+ t - r_- \varphi\,, \qquad \tilde{\varphi}(t,\varphi) = -r_- t + r_+ \varphi\,. \tag{3.60d}$$

In these coordinates AdS_3 space takes the form

$$ds^2 = -F(r)dt^2 + \frac{dr^2}{F(r)} + r^2(N^\varphi(r)dt + d\varphi)^2 \tag{3.61}$$

with $F(r)$ and $N^\varphi(r)$ given by (3.48). The coordinate system t, r, φ introduced above is distinct from the coordinate system t, r, φ in (3.11). Local coordinate systems in which the metric takes the form (3.61) can also be introduced in the other regions of AdS_3 space, see [35] for the details. Without an additional identification of points, the metric (3.61) is just AdS_3 space in a coordinate system which covers the portion of AdS_3 space where $u, y > 0$ and $u^2 - x^2 > 1$. In the coordinate system (3.60), the Killing vector (3.56) takes the form

$$\xi = \partial_\varphi\,. \tag{3.62}$$

By performing discrete identification along the direction of this Killing vector, we obtain the identification of points

$$\begin{pmatrix} t \\ r \\ \varphi \end{pmatrix} \sim \begin{pmatrix} t \\ r \\ \varphi + 2\pi k \end{pmatrix}, \tag{3.63}$$

where $k \in \mathbb{Z}$. It is the identification (3.63) that gives the black hole spacetime and that differentiates it from AdS_3. In the coordinate system u, v, x, y this identification reads

$$\begin{pmatrix} u \\ x \\ y \\ v \end{pmatrix} \sim \begin{pmatrix} \cosh(2\pi k r_+)u + \sinh(2\pi k r_+)x \\ \cosh(2\pi k r_+)x + \sinh(2\pi k r_+)u \\ \cosh(2\pi k r_-)y - \sinh(2\pi k r_-)v \\ \cosh(2\pi k r_-)v - \sinh(2\pi k r_-)y \end{pmatrix} . \tag{3.64}$$

Indeed, the metric

$$ds^2 = -du^2 - dv^2 + dx^2 + dy^2 \tag{3.65}$$

together with the constraint

$$-u^2 - v^2 + x^2 + y^2 = -1 \tag{3.66}$$

and the identification (3.64) is just the non-extremal BTZ black hole in a different coordinate system.

3.4.3. Kruskal Extension

In the previous subsections, we have discussed some generalities of the BTZ black hole, in this and in the following subsections we focus on its causal structure which was first described in [35]. Consider the BTZ black hole (3.47)–(3.48). The geometry depends upon the sign of $F(r)$, the zeros of $F(r)$ and the order of the zeros of $F(r)$. The zeros are located at $r = r_+$ and $r = r_-$

$$F(r_+) = 0\,, \qquad\qquad F(r_-) = 0\,. \tag{3.67}$$

In the case of the non-extremal rotating BTZ black hole we have that $r_+ \neq r_-$ and

$$F'(r_+) \neq 0\,, \qquad\qquad F'(r_-) \neq 0\,. \tag{3.68}$$

We start by introducing ingoing and outgoing Eddington-Finkelstein coordinates

$$u = t - f(r)\,, \quad v = t + f(r)\,, \tag{3.69}$$

where

$$f'(r) = \frac{1}{F(r)}\,. \tag{3.70}$$

This can be integrated to give

$$f(r) = \frac{1}{r_+^2 - r_-^2}\left(\frac{r_-}{2}\left(\log\left|1 + \frac{r}{r_-}\right| - \log\left|1 - \frac{r}{r_-}\right|\right) - (r_- \leftrightarrow r_+)\right), \tag{3.71}$$

where the integration constant has been chosen such that $f(r)$ vanishes at $r = 0$. The function $f(r)$ diverges at $r = r_+$ and $r = r_-$ where $F(r)$ vanishes and tends to 0 in the limit $r \to \infty$. In Figure 3.4 the function $f(r)$ is plotted for specific values of r_+ and r_-. In coordinates u, r, or v, r, the metric (3.47) reads

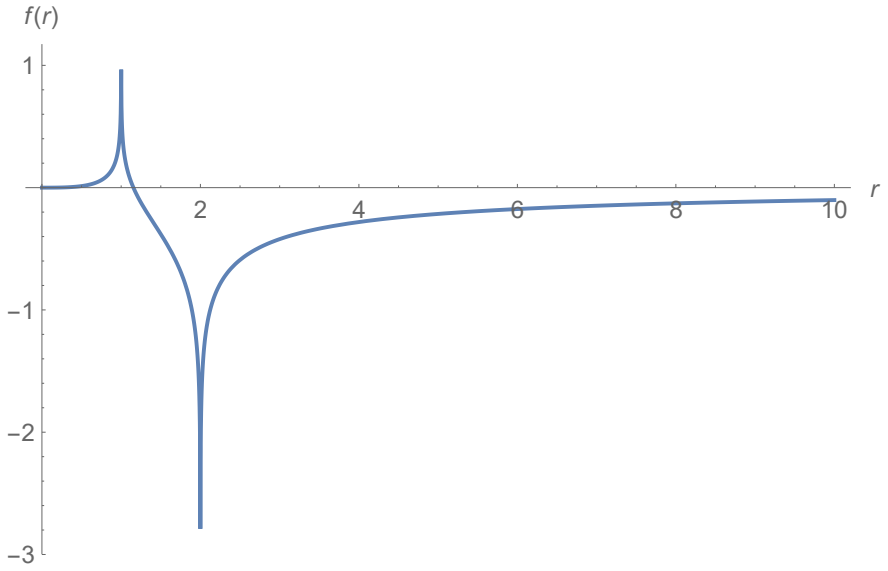

Figure 3.4.: Plot of the function $f(r)$ with $r_- = 1$ and $r_+ = 2$.

$$\begin{aligned} ds^2 &= -F(r)du^2 - 2dudr + r^2\left(N^\varphi(r)\left(du + \frac{dr}{F(r)}\right) + d\varphi\right)^2 \\ &= -F(r)dv^2 + 2dvdr + r^2\left(N^\varphi(r)\left(dv - \frac{dr}{F(r)}\right) + d\varphi\right)^2, \end{aligned} \tag{3.72}$$

which is singular at the zeros of $F(r)$ due to the term $dr/F(r)$ in the brackets. To compensate we use the shift freedom in φ. An extension across the horizon $r = r_+$ can be achieved by choosing the constant $N^\varphi_\infty = \frac{J}{2r_+^2}$. Then

$$N^\varphi(r)dt = \left(\frac{J(r-r_+)}{r_+^3} + O(r-r_+)^2\right)\left(du + \frac{r^2}{(r^2-r_+^2)(r^2-r_-^2)}dr\right). \tag{3.73}$$

For coordinates v, r the same line of argument holds trivially. By fixing $N^\varphi_\infty = -J/(2r_-^2)$ an extension across r_- can be performed. We thus obtain two Eddington-Finkelstein patches – one around $r = r_-$ and one around $r = r_+$. Each patch comes with a different angular coordinate $\varphi_\pm = \varphi + N^\varphi_{\infty\pm}\, t$, where $N^\varphi_{\infty\pm} = -J/(2r_\pm^2)$. The coordinates u, r and v, r, respectively, can be taken to cover two of the quadrants that will be introduced in the following. By taking two Eddington-Finkelstein patches together it is possible to cover almost the entire quadrant except for the bifurcation surface. It is for this reason that we need another coordinate system. Such a coordinate system is provided by Kruskal-Szekeres coordinates. Two Kruskal-Szekeres coordinate systems K_+ and K_- are introduced below, which, taken together, give a maximal causal extension of the spacetime. The Kruskal-Szekeres coordinate system K_+, introduced below, covers the region $r_- < r < \infty$, the Kruskal-Szekeres coordinate system K_- covers the region $0 < r < r_+$. These two patches can be glued together on their overlap $r_- < r < r_+$,

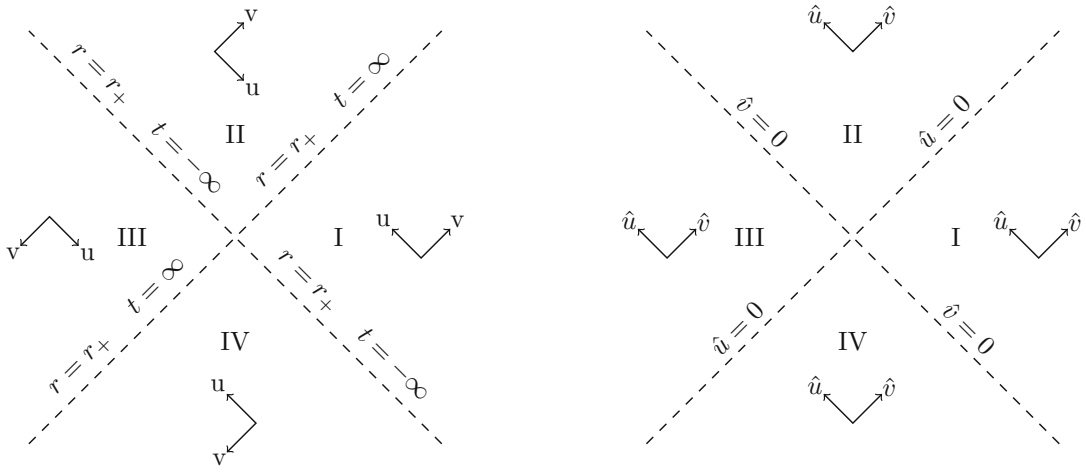

Figure 3.5.: Plot of the four quadrants: The different regions, separated by the horizon at $r = r_+$ are labelled by roman numbers I, II, III, IV. The Eddington-Finkelstein coordinates u, r can be taken to cover either I, IV or II, III. The Eddington-Finkelstein coordinates v, r can be taken to cover either I, II or III, IV. The Kruskal-Szekeres coordinates can be taken to cover all four patches I, II, III, IV at the same time.

yielding a maximal causal extension.

Kruskal-Szekeres patch K_+

To have a well-defined coordinate system that covers the patch $r_- < r < \infty$ we introduce Kruskal-Szekeres coordinates in each of the blocks, which are specified in Figure 3.5 and labeled by a roman number. The Kruskal-Szekeres coordinates read

$$I : \hat{u} = -e^{-c_+ u}, \quad \hat{v} = e^{c_+ v}, \tag{3.74a}$$
$$II : \hat{u} = e^{-c_+ u}, \quad \hat{v} = e^{c_+ v}, \tag{3.74b}$$
$$III : \hat{u} = e^{-c_+ u}, \quad \hat{v} = -e^{c_+ v}, \tag{3.74c}$$
$$IV : \hat{u} = -e^{-c_+ u}, \quad \hat{v} = -e^{c_+ v}. \tag{3.74d}$$

with

$$c_+ = \frac{F'(r_+)}{2} = \frac{r_+^2 - r_-^2}{r_+}. \tag{3.75}$$

The value of the constant c_+ is of utmost importance. Indeed, for any other value of c_+ the coordinates $\hat{u}, \hat{v}$ defined above do not extend smoothly across the horizon, Changing coordinates, to ease the comparison with [35], as

$$\tau = \frac{\hat{u} + \hat{v}}{2}, \qquad \rho = \frac{\hat{v} - \hat{u}}{2}. \tag{3.76}$$

we obtain that the metric (3.47) takes the form [35]

$$ds^2 = \tilde{\psi}_+^2(r)(d\rho^2 - d\tau^2) + r^2(N^\varphi(r)dt + d\varphi)^2, \tag{3.77}$$

where $r = r(\rho,\tau) = r(\hat{u},\hat{v})$ and $t = t(\rho,\tau) = t(\hat{u},\hat{v})$ are implicit functions of the coordinates ρ and τ, or $\hat{u}$ and $\hat{v}$ respectively. We have that $\tilde{\psi}_+$ defined through

$$\tilde{\psi}_+^2(r) = \frac{(r^2 - r_-^2)(r+r_+)^2}{c_+^2 r^2}\left(\frac{r-r_-}{r+r_-}\right)^{\frac{r_-}{r_+}} \tag{3.78}$$

is strictly positive for $r_- < r < \infty$. The explicit expressions for τ and ρ

$$I: \tau = \left(\frac{r-r_+}{r+r_+}\right)^{\frac{1}{2}}\left(\frac{r+r_-}{r-r_-}\right)^{\frac{r_-}{2r_+}}\sinh(c_+t)\,, \qquad \rho = \left(\frac{r-r_+}{r+r_+}\right)^{\frac{1}{2}}\left(\frac{r+r_-}{r-r_-}\right)^{\frac{r_-}{2r_+}}\cosh(c_+t)\,, \tag{3.79a}$$

$$II: \tau = \left(\frac{r_+-r}{r+r_+}\right)^{\frac{1}{2}}\left(\frac{r+r_-}{r-r_-}\right)^{\frac{r_-}{2r_+}}\cosh(c_+t)\,, \qquad \rho = \left(\frac{r_+-r}{r+r_+}\right)^{\frac{1}{2}}\left(\frac{r+r_-}{r-r_-}\right)^{\frac{r_-}{2r_+}}\sinh(c_+t)\,, \tag{3.79b}$$

$$III: \tau = -\left(\frac{r-r_+}{r+r_+}\right)^{\frac{1}{2}}\left(\frac{r+r_-}{r-r_-}\right)^{\frac{r_-}{2r_+}}\sinh(c_+t)\,, \quad \rho = -\left(\frac{r-r_+}{r+r_+}\right)^{\frac{1}{2}}\left(\frac{r+r_-}{r-r_-}\right)^{\frac{r_-}{2r_+}}\cosh(c_+t)\,, \tag{3.79c}$$

$$IV: \tau = -\left(\frac{r_+-r}{r+r_+}\right)^{\frac{1}{2}}\left(\frac{r+r_-}{r-r_-}\right)^{\frac{r_-}{2r_+}}\cosh(c_+t)\,, \quad \rho = -\left(\frac{r_+-r}{r+r_+}\right)^{\frac{1}{2}}\left(\frac{r+r_-}{r-r_-}\right)^{\frac{r_-}{2r_+}}\sinh(c_+t)\,. \tag{3.79d}$$

are the ones given in [35]. Next, it needs to be checked that $r = r(\hat{u},\hat{v})$ is a smooth function. For this we consider the function $G(r)$

$$G(r) = \hat{u}\hat{v} = \tau^2 - \rho^2 = \left(\frac{r+r_-}{r-r_-}\right)^{\frac{r_-}{r_+}}\frac{(r_+-r)}{(r+r_+)} \tag{3.80}$$

which is a real analytic function for $r_- < r < \infty$. This implies that also its inverse $r = G^{-1}(\hat{u}\hat{v})$ is a real analytic function due to the implicit analytic function theorem. In the previous section we have shown that, in Eddington-Finkelstein coordinates, under an appropriate choice of φ the term $N^\varphi(r)dt$ is regular at $r = r_+$. We now check that with this choice of φ the term $N^\varphi(r)dt$ is also regular at $\hat{u} = \hat{v} = 0$ – a locus which is not covered in Eddington-Finkelstein coordinates. Using (3.80) we find that

$$\begin{aligned} N^\varphi(r)dt &= \left(\frac{J(r-r_+)}{2c_+r_+^3} + O(r-r_+)^2\right)\left(\frac{d\hat{v}}{\hat{v}} - \frac{d\hat{u}}{\hat{u}}\right) \\ &= \left(-\frac{J}{c_+r_+^2}\left(\frac{r_++r_-}{r_+-r_-}\right)^{-\frac{r_-}{r_+}}\hat{u}\hat{v} + O(r-r_+)^2\right)\left(\frac{d\hat{v}}{\hat{v}} - \frac{d\hat{u}}{\hat{u}}\right) \end{aligned} \tag{3.81}$$

is regular at $\hat{u} = \hat{v} = 0$. For this reason the coordinates $\hat{u}$ and $\hat{v}$ can be extended to run from $-\infty$ to ∞

$$\hat{u},\hat{v} \in (-\infty,\infty)\,, \quad \text{or} \quad \tau,\rho \in (-\infty,\infty) \tag{3.82}$$

with the restriction

$$\hat{u}\hat{v} = \tau^2 - \rho^2 > -1\,, \tag{3.83}$$

where -1 being the limiting value of $\hat{u}\hat{v}$ for $r \to \infty$.

Therefore, we have shown that the spacetime can indeed be extended through $r = r_+$. The coordinate system τ, ρ, φ with τ and ρ being defined above is well-defined in the region $r_- < r < \infty$. In this coordinate system the metric takes the form (3.77) with (3.78) being smooth and strictly positive for $r_- < r < \infty$. Lastly we introduce compact coordinates X, T as

$$\rho + \tau = \tan\left(\frac{T+X}{2}\right), \qquad \tau - \rho = \tan\left(\frac{T-X}{2}\right), \tag{3.84}$$

such that

$$ds^2 = \frac{1}{\Omega_+^2(r,t)}(dX^2 - dT^2) + r^2(N^\varphi(r)dt + d\varphi)^2\,, \tag{3.85}$$

where $T, X \in (-\pi, \pi)$ and with the restriction

$$\tan\left(\frac{T+X}{2}\right)\tan\left(\frac{T-X}{2}\right) > -1\,. \tag{3.86}$$

The conformal factor

$$\Omega_+^2(r,t) = 4\cos^2\left(\frac{T+X}{2}\right)\cos^2\left(\frac{T-X}{2}\right)\frac{c_+^2 r^2}{(r^2-r_-^2)(r+r_+)^2}\left(\frac{r-r_-}{r+r_-}\right)^{-\frac{r_-}{r_+}}, \tag{3.87}$$

is strictly positive between $r_- < r < \infty$ (X, T are implicit functions of t, r). It vanishes only in the limit $r \to \infty$ or as $t \to \pm\infty$ and diverges at $r = r_-$.

Kruskal-Szekeres patch K_-

The same arguments can be repeated to obtain a Kruskal-Szekeres patch around $r = r_-$. We start from the Eddington-Finkelstein coordinates (3.69) and (3.71). Defining coordinates τ and ρ in an analog way to above, the metric is brought into the form

$$ds^2 = \tilde{\psi}_-(r)^2(d\rho^2 - d\tau^2) + r^2(N^\varphi(r)dt + d\varphi)^2\,, \tag{3.88}$$

with τ and ρ given by

$$I: \tau = \left(\frac{r_- - r}{r + r_-}\right)^{\frac{1}{2}} \left(\frac{r + r_+}{r_+ - r}\right)^{\frac{r_+}{2r_-}} \sinh(c_- t)\,, \qquad \rho = \left(\frac{r_- - r}{r + r_-}\right)^{\frac{1}{2}} \left(\frac{r + r_+}{r_+ - r}\right)^{\frac{r_+}{2r_-}} \cosh(c_- t)\,, \tag{3.89a}$$

$$II: \tau = \left(\frac{r - r_-}{r + r_-}\right)^{\frac{1}{2}} \left(\frac{r + r_+}{r_+ - r}\right)^{\frac{r_+}{2r_-}} \cosh(c_- t)\,, \qquad \rho = \left(\frac{r - r_-}{r + r_-}\right)^{\frac{1}{2}} \left(\frac{r + r_+}{r_+ - r}\right)^{\frac{r_+}{2r_-}} \sinh(c_- t)\,, \tag{3.89b}$$

$$III: \tau = -\left(\frac{r_- - r}{r + r_-}\right)^{\frac{1}{2}} \left(\frac{r + r_+}{r_+ - r}\right)^{\frac{r_+}{2r_-}} \sinh(c_- t)\,, \quad \rho = -\left(\frac{r_- - r}{r + r_-}\right)^{\frac{1}{2}} \left(\frac{r + r_+}{r_+ - r}\right)^{\frac{r_+}{2r_-}} \cosh(c_- t)\,, \tag{3.89c}$$

$$IV: \tau = -\left(\frac{r - r_-}{r + r_-}\right)^{\frac{1}{2}} \left(\frac{r + r_+}{r_+ - r}\right)^{\frac{r_+}{2r_-}} \cosh(c_- t)\,, \quad \rho = -\left(\frac{r - r_-}{r + r_-}\right)^{\frac{1}{2}} \left(\frac{r + r_+}{r_+ - r}\right)^{\frac{r_+}{2r_-}} \sinh(c_- t)\,, \tag{3.89d}$$

where

$$c_- = \frac{F'(r_-)}{2} = \frac{r_-^2 - r_+^2}{r_-}\,. \tag{3.90}$$

The null coordinates $\hat{u}$ and $\hat{v}$ defined by the relations

$$\tau = \frac{\hat{u} + \hat{v}}{2}\,, \qquad \rho = \frac{\hat{v} - \hat{u}}{2}\,. \tag{3.91}$$

are plotted in Figure 3.6. The function

$$\tilde{\psi}_-^2(r) = \frac{(r_+^2 - r_-^2)(r + r_-)^2}{c_-^2 r^2} \left(\frac{r_+ - r}{r_+ + r}\right)^{\frac{r_+}{r_-}} \tag{3.92}$$

is strictly positive in the domain $0 < r < r_+$. In the same manner as for the patch K_+ it can be shown that r is a real analytic function for $0 < r < r_+$ due to the implicit function theorem. Furthermore, the shift freedom in φ can be exploited to obtain a regular $N^\varphi(r)dt$ term at $\tau = \rho = 0$. Therefore, the coordinates τ, ρ can be extended such that

$$\tau, \rho \in (-\infty, \infty) \tag{3.93}$$

with the additional restriction that

$$\tau^2 - \rho^2 > -1 \tag{3.94}$$

where -1 corresponds to the locus $r = 0$, which is the location of the singularity. As already discussed in subsection 3.4.1, an extension to $r \leq 0$ would be, in principle, possible. However, due to the fact that the spacetime exhibits closed timelike curves beyond $r < 0$ it is customary to cut off the spacetime there. The spacetime is then – per construction – geodesically incomplete, as there exist geodesics that go from $r > 0$ to $r \leq 0$. The locus $r = 0$ is regarded as a singularity, as spacetime cannot be continued

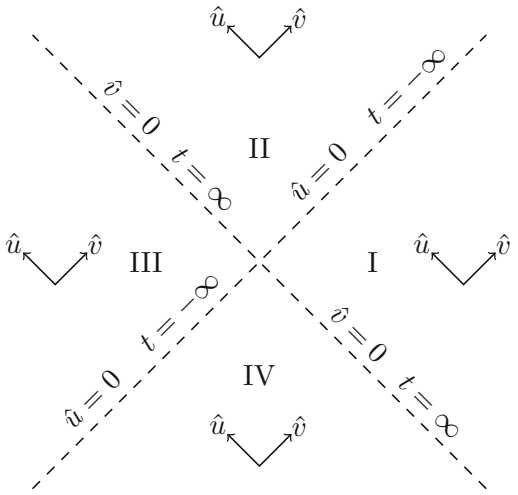

Figure 3.6.: Plot of the four quadrants in the patch K_-. The dashed lines denote the location of the horizon $r = r_-$. Quadrants I and III describe the region inside the horizon $r = r_-$, while quadrants II and IV describe the region $r_- < r < r_+$.

without producing closed timelike curves. If this point of view is taken, as is here and was taken in [35], then the only incomplete geodesics are those that hit the singularity, which is similar to higher-dimensional black holes. Lastly we introduce compact coordinates X, T as

$$\rho + \tau = \tan\left(\frac{T+X}{2}\right), \qquad \tau - \rho = \tan\left(\frac{T-X}{2}\right) \tag{3.95}$$

such that

$$ds^2 = \frac{1}{\Omega_-^2(r,t)}(dX^2 - dT^2) + r^2(N^\varphi(r)dt + d\varphi)^2\,. \tag{3.96}$$

Here, $T, X \in (-\pi, \pi)$ with the restriction that

$$\tan\left(\frac{T+X}{2}\right)\tan\left(\frac{T-X}{2}\right) > -1\,. \tag{3.97}$$

The conformal factor

$$\Omega_-^2(r,t) = 4\cos^2\left(\frac{T+X}{2}\right)\cos^2\left(\frac{T-X}{2}\right)\frac{c_-^2 r^2}{(r_+^2 - r_-^2)(r+r_-)^2}\left(\frac{r_+ - r}{r_+ + r}\right)^{-\frac{r_+}{r_-}}, \tag{3.98}$$

is strictly positive between $0 < r < r_+$ (X, T are implicit functions of t, r).

3.4.4. Causal Diagram of the Non-Extremal BTZ Black Hole

In the last subsection we have seen that the non-extremal BTZ black hole can be extended through $r = r_-$ and $r = r_+$. In this subsection the causal structure of the non-extremal

black hole is visualized with causal diagrams. As we have seen in the previous subsection, the metric can be brought into the form

$$ds^2 = \frac{1}{\Omega^2}(dT^2 - dX^2) + r^2(N^\varphi(r)dt + d\varphi)^2 \tag{3.99}$$

in each patch. The patch K_+ covers the region $r_- < r < \infty$, the patch K_- covers the region $0 < r < r_+$. In the region $r_- < r < r_+$ the patches overlap $K = K_+ \cap K_-$.

The causal structure of the BTZ black hole can now be visualized using so-called projection diagrams reviewed in section 2.2. Indeed, the causal diagrams presented in the 1992 paper by Bañados, Henneaux, Teitelboim and Zanelli [35] are precisely such projection diagrams.

Constant φ slices do not correctly depict the causal structure of spacetime in the case of the rotating BTZ black hole. Indeed, the property that all spacelike curves in the two-dimensional diagram result from spacelike curves in the original spacetime is not preserved in this case. It is impossible to change coordinates such that the second term in (3.99) takes the form $r^2 d\tilde{\varphi}^2$ as

$$d(N^\varphi(r)dt + d\varphi) \neq 0\,. \tag{3.100}$$

Instead of taking a slice, we project to a subset of $\mathbb{R}^{1,1}$ in a way that preserves causal properties and construct a projection diagram.

In each patch K_+, K_- the projection π is defined as the map $(T, X, \varphi) \to (T, X)$. The auxiliary metric in each patch K_+, K_- reads

$$\gamma_{AB}dx^A dx^B = \Omega^2(dX^2 - dT^2) \tag{3.101}$$

with

$$T, X \in (-\pi, \pi)\,, \qquad \tan\left(\frac{T+X}{2}\right)\tan\left(\frac{T-X}{2}\right) > -1\,. \tag{3.102}$$

The two patches K_+ and K_- of the non-extremal rotating BTZ black hole are depicted in Figure 3.7. The patches overlap on the intersection $K = K_+ \cap K_-$. A complete diagram is then obtained by joining an infinite sequence of patches K_+, K_- as is done in Figure 3.7.

3.4.5. $J = 0$, $M > 0$

In the previous subsection, we have considered the non-extremal, rotating BTZ black hole and have discussed its causal structure. Now we discuss the causal structure of the non-rotating BTZ black hole, which corresponds to $J = 0$ or equivalently $r_- = 0$. In this case the metric takes a diagonal form as $N_\varphi(r)$ vanishes

$$ds^2 = -F^2(r)dt^2 + \frac{dr^2}{F^2(r)} + r^2 d\varphi^2\,. \tag{3.103}$$

For $r_- = 0$ there exists only one Kruskal patch, the outer patch, covering the region $0 < r < \infty$. We may use the results from the previous subsections, in which Kruskal-Szekeres coordinates were introduced for the non-extremal rotating black hole. The

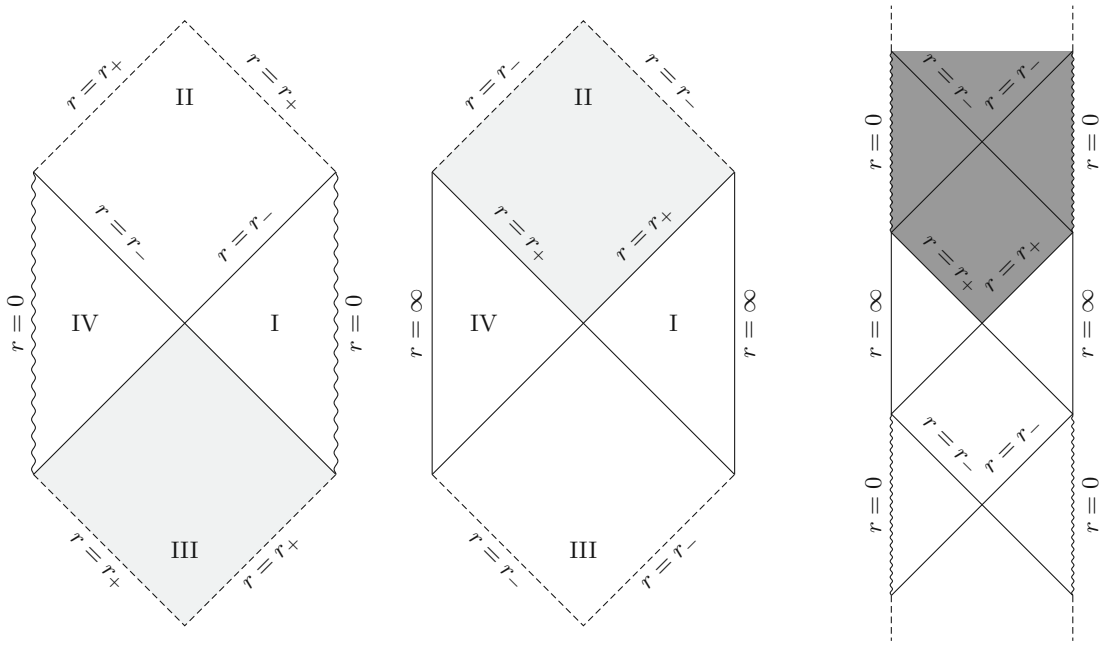

Figure 3.7.: The figure depicts the patches K_+ (left), K_- (middle) and the complete causal diagram of the rotating, non-extremal BTZ black hole. The light grey region denotes the intersection of $K = K_+ \cap K_-$ where the patches are glued together. The dark gray region in the figure to the very right denotes the black hole region where no forward-moving causal curves reach $r = \infty$ anymore. Figure adapted with permission from [39].

Kruskal-Szekeres coordinates in the patch K_+ are regular for $r_- = 0$ and read

$$I : \tau = \left(\frac{r - r_+}{r + r_+}\right)^{\frac{1}{2}} \sinh(c_+ t)\,, \qquad \rho = \left(\frac{r - r_+}{r + r_+}\right)^{\frac{1}{2}} \cosh(c_+ t)\,, \tag{3.104a}$$

$$II : \tau = \left(\frac{r_+ - r}{r + r_+}\right)^{\frac{1}{2}} \cosh(c_+ t)\,, \qquad \rho = \left(\frac{r_+ - r}{r + r_+}\right)^{\frac{1}{2}} \sinh(c_+ t)\,, \tag{3.104b}$$

$$III : \tau = -\left(\frac{r - r_+}{r + r_+}\right)^{\frac{1}{2}} \sinh(c_+ t)\,, \qquad \rho = -\left(\frac{r - r_+}{r + r_+}\right)^{\frac{1}{2}} \cosh(c_+ t)\,, \tag{3.104c}$$

$$IV : \tau = -\left(\frac{r_+ - r}{r + r_+}\right)^{\frac{1}{2}} \cosh(c_+ t)\,, \qquad \rho = -\left(\frac{r_+ - r}{r + r_+}\right)^{\frac{1}{2}} \sinh(c_+ t) \tag{3.104d}$$

with $c_+ = r_+$. Similarly to before the limit $r \to \infty$ corresponds to $\rho^2 - \tau^2 \to 1$, however, the limit $r \to 0$ corresponds now to $\tau^2 - \rho^2 \to 1$. In compact coordinates we obtain

$$\rho + \tau = \tan\left(\frac{T + X}{2}\right), \qquad \tau - \rho = \tan\left(\frac{T - X}{2}\right), \tag{3.105a}$$

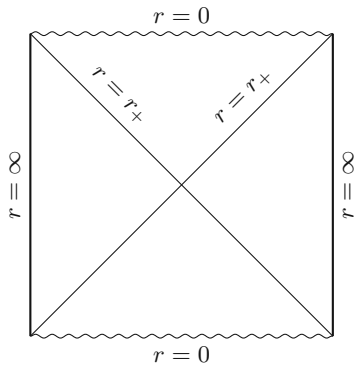

Figure 3.8.: Diagram of the non-rotating BTZ black hole. The wiggled line denotes the location of the singularity.

$$\gamma_{AB}dx^A dx^B = \Omega^2(r,t)(dX^2 - dT^2) \tag{3.105b}$$

with

$$\frac{1}{\Omega^2(r,t)} = \frac{1}{4\cos^2\left(\frac{T+X}{2}\right)\cos^2\left(\frac{T-X}{2}\right)}\frac{(r+r_+)^2}{r_+^2} \tag{3.106}$$

and $T, X \in \left(-\frac{\pi}{2}, \frac{\pi}{2}\right)$. The singularity $r = 0$ is mapped to the lines $T = \pm\pi/2$, $r = \infty$ is mapped to $X = \pm\pi/2$ yielding the diagram in figure 3.8.

3.4.6. Extremal Case $M = |J|$

Up until this point, we have assumed that $M \neq |J|$, i.e. we have considered the non-extremal black hole. In the extremal case $M = |J|$ the function $F(r)$ in (3.47) takes the form

$$F(r) = \frac{(r^2 - r_+^2)^2}{r^2}\,. \tag{3.107}$$

As discussed before, the order of the zeros of $F(r)$ is important for the geometry of spacetime and its extendability. In the extremal case $F(r)$ has a zero of second order

$$F(r_+) = 0\,, \quad F'(r_+) = 0\,, \tag{3.108}$$

implying that it cannot be Kruskal extended through $r = r_+$. We introduce the null coordinates (in the same way as [35])

$$u = t + f(r) \tag{3.109}$$

with $f'(r) = \frac{1}{F(r)}$. This can be solved explicitly to give

$$f(r) = -\frac{r}{2(r^2 - r_+^2)} + \frac{1}{4r_+}\log\left|\frac{r - r_+}{r + r_+}\right|, \tag{3.110}$$

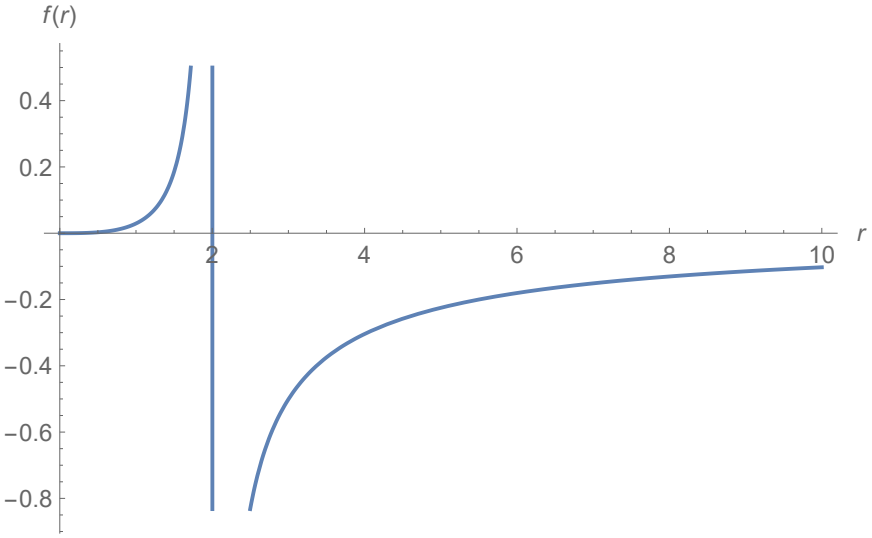

Figure 3.9.: Plot of the function $f(r)$ in case of the extremal BTZ black hole with $r_- = r_+ = 2$

where the integration constant has been chosen such that $f(r=0)=0$. The function $f(r)$ is plotted in Figure 3.9. In Eddington-Finkelstein coordinates the metric (3.47) takes the form

$$ds^2 = -F(r)du^2 + 2dudr + r^2(N_\varphi(r)dt + d\varphi)^2\,, \tag{3.111}$$

where t is an implicit function of u and r. Next we introduce the compact coordinates T, X

$$u = \tan\left(\frac{T+X}{2}\right), \qquad v = -t + f(r) = \tan\left(\frac{X-T}{2}\right) \tag{3.112}$$

to obtain

$$\begin{aligned} ds^2 &= F(r)dudv + r^2(N_\varphi(r)dt + d\varphi)^2 \\ &= F(r)\frac{(dX^2 - dT^2)}{(\cos(T)+\cos(X))^2} + r^2(N_\varphi(r)dt + d\varphi)^2\,. \end{aligned} \tag{3.113}$$

Expressed in coordinates X, T equation (3.110) becomes

$$f(r) = -\frac{r}{2(r^2 - r_+^2)} + \frac{1}{4r_+}\log\left|\frac{r-r_+}{r+r_+}\right| = \frac{\sin(X)}{\cos(T)+\cos(X)}\,. \tag{3.114}$$

The horizon $r = r_+$ is at 45 degrees angle. From equation (3.114) we see that at $r=\infty$ and $r=0$ the function $f(r)$ vanishes. However, while $r=0$ corresponds to $X = (k\pi)^+$, $r=\infty$ corresponds to $X = (k\pi)^-$. Here, the plus denotes that as $r \to 0$ the function $f(r)$ tends to zero from above $f(r) \to 0^+$ and the coordinate X tends to π from above $X \to k\pi^+$. The minus denotes that as $r \to \infty$ the function $f(r)$ tends to 0 from below $f(r) \to 0^-$ and the coordinate X tends to π from below $X \to k\pi^-$. In fact, the region

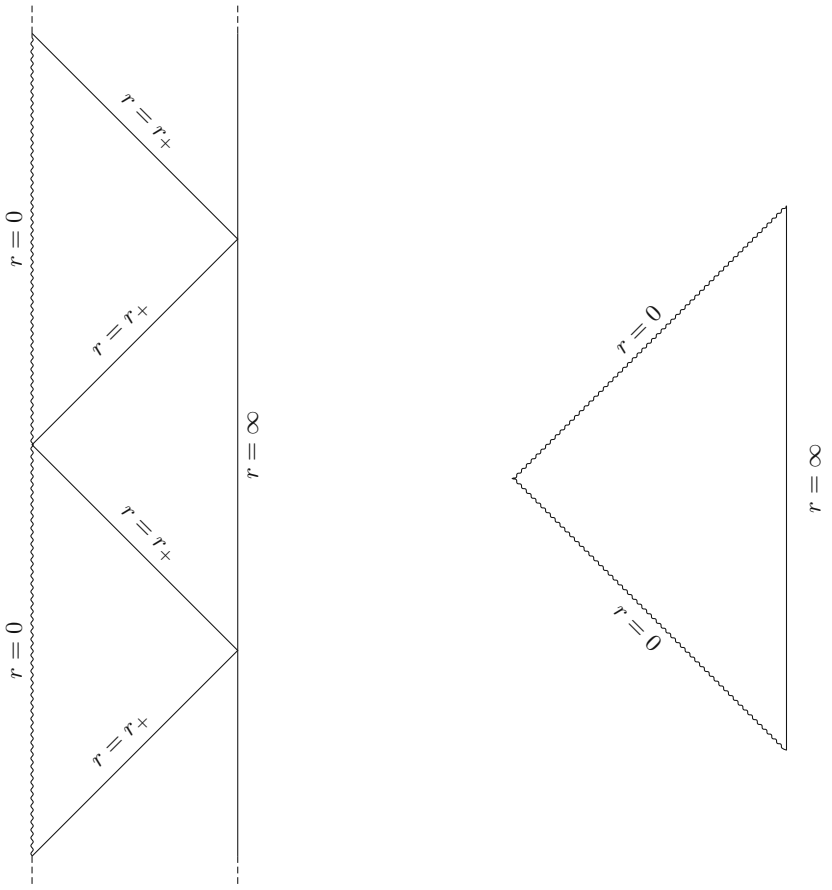

(a) $M = |J| \neq 0$ **(b)** $M = |J| = 0$

Figure 3.10.: Plot of the extremal BTZ black hole with $M = |J|$ and the special case $M = |J| = 0$. The wiggled lines denote the location of the singularity.

$r > r_+$ and the region $r < r_+$ correspond to different determinations of the arctangent. This is apparent from Figure 3.9 where the function $f(r)$ is plotted. The triangles $r > r_+$ and the triangle $0 < r < r_+$ are glued along $r = r_+$. To achieve a maximal extension one must glue an infinite sequence of these triangles as is shown in diagram 3.10a.

3.4.7. Special Case $M = J = 0$

In the special case $M = J = 0$ the metric is

$$ds^2 = -r^2 dt^2 + \frac{1}{r^2} dr^2 + r^2 d\varphi^2 \,. \tag{3.115}$$

Changing coordinates as

$$u = t - \frac{1}{r} \,, \quad v = -t - \frac{1}{r} \tag{3.116}$$

we obtain

$$ds^2 = \frac{4}{(u+v)^2}\Big(dudv + d\varphi^2\Big)\,. \tag{3.117}$$

Changing to coordinates T, X as

$$u = \tan\frac{T+X}{2}\,, \quad v = \tan\frac{X-T}{2} \tag{3.118}$$

we obtain

$$\begin{aligned} ds^2 &= \frac{1}{\sin^2(X)}\Big(-dT^2 + dX^2 + (\cos(T)+\cos(X))^2 d\varphi^2\Big) \\ &= \frac{1}{\Omega^2}\Big(-dT^2 + dX^2 + (\cos(T)+\cos(X))^2 d\varphi^2\Big) \end{aligned} \tag{3.119}$$

The conformal factor $\Omega^2(X) = \sin^2(X)$ is smooth and strictly positive and vanishes only at $X = k\pi$ with $k \in \mathbb{Z}$. In coordinates T, X the origin $r = 0$ is located at $\cos(T)+\cos(X) = 0$ and $r = \infty$ corresponds to $\sin(X) = 0$. A constant φ slice thus corresponds to a triangle bounded by the lines

$$T = \pi + X\,, \quad T = -\pi - X\,, \quad X = 0\,. \tag{3.120}$$

Such a constant φ slice is depicted in Figure 3.10b.

3.5. Introducing Degrees of Freedom: An Example

As we have seen at the beginning of this chapter, general relativity in three dimensions is a topological theory; it has no local degrees of freedom. There are many theories beyond Einstein gravity – for a review see [43]. We discuss one possibility to introduce degrees of freedom: topologically massive gravity. The theory was introduced by Deser, Jackiw and Templeton in 1981 [44]. In subsection 3.5.1 we introduce the theory and discuss general features. In subsection 3.5.2 we discuss particular solutions to the theory. Subsection 3.5.3 includes parts of my paper [1] and discusses the causal structure of so-called warped flat spacetimes, the nomenclature of which is explained in subsection 3.5.2.

3.5.1. Topologically Massive Gravity

A simple model of gravity in three dimensions which is not pure Einstein gravity but propagates one degree of freedom is topologically massive gravity.[1] This theory is obtained by adding a Chern-Simons term to the Einstein-Hilbert action built out of the Christoffel symbols

$$S[g] = \frac{1}{16\pi G}\int d^3x\sqrt{-g}(R - 2\Lambda) + \frac{1}{32\pi G\mu}\int d^3x\sqrt{-g}\epsilon^{\lambda\mu\nu}\Gamma^{\rho}{}_{\lambda\sigma}\Big(\partial_\mu\Gamma^{\sigma}{}_{\rho\nu} + \frac{2}{3}\Gamma^{\sigma}{}_{\mu\tau}\Gamma^{\tau}{}_{\nu\rho}\Big)\,. \tag{3.121}$$

[1] It might seem confusing that a theory that possesses local degrees of freedom is called topological; the "topological" in the name stems from the fact that the modification of the action is a Chern-Simons term.

The Chern-Simons term is not invariant under diffeomorphisms, but changes into a total derivative of a local expression of the metric [43]. Topologically massive gravity has one propagating massive degree of freedom with mass proportional to μ. Varying the action with respect to the metric gives the equations of motion

$$G_{\mu\nu} + \Lambda g_{\mu\nu} + \frac{1}{\mu} C_{\mu\nu} = 0\,, \tag{3.122}$$

where

$$C_{\mu\nu} = \epsilon_{\mu}^{\ \rho\sigma} \nabla_\rho (R_{\sigma\nu} - \frac{1}{4} g_{\sigma\nu} R) \tag{3.123}$$

is the Cotton tensor with $\epsilon_{\mu\nu\rho}$ being the epsilon tensor. The Cotton tensor is symmetric, traceless and covariantly conserved. Similarly to the Weyl tensor in higher dimensions, the Cotton tensor vanishes iff the metric is conformally flat.

Any vacuum solution of the Einstein equations of motion

$$G_{\mu\nu} + \Lambda g_{\mu\nu} = 0 \tag{3.124}$$

also solves (3.122) as can be easily checked: If (3.124) is fulfilled, then (3.123) simplifies to

$$C_{\mu\nu} = \frac{\Lambda}{2} \epsilon_{\mu}^{\ \rho\sigma} \nabla_\rho g_{\sigma\nu} = 0\,. \tag{3.125}$$

While any solution to Einstein gravity is a solution of topologically massive gravity, the gravitational Chern-Simons term allows for new classes of solutions, some of which are described in the next section.

3.5.2. Warped Spacetimes

In this subsection, we briefly discuss three spacetimes, which are solutions of topologically massive gravity (but not of Einstein gravity): warped AdS_3, warped dS_3 and warped flat space. The latter and quotients thereof were the subject of my publication [1] and will be discussed in the following subsections. One reason why these spacetimes are interesting is because of their relation to extremal four-dimensional black holes. A quotient of warped AdS_3 appears in the near-horizon limit of extremal Kerr black holes at fixed polar angle [15]. A quotient of warped flat space appears as near-horizon geometry at fixed polar angle of "ultra-cold" extremal Kerr-dS black holes where the inner, outer and cosmological horizons coincide [45]. The name of warped AdS_3, warped dS_3 and warped flat space stems from the fact that these spacetimes can be seen as fibrations over AdS_2, dS_2 and $\mathbb{R}^{1,1}$, similarly to the Hopf fibration which describes the fact that S^3 may be understood as a fibration over S^2. The suitable mathematical terminology in this context is (pseudo-)Riemannian submersion. In appendix A it is described in detail how warped AdS_3, warped dS_3 and warped flat space may be understood as pseudo-Riemannian submersions with base manifold AdS_2, dS_2 and $\mathbb{R}^{1,1}$.

Warped AdS_3 is given by the metric

$$ds^2 = \frac{1}{\nu^2 + 3\epsilon} \left(-d\tau^2 (1 + r^2) + \frac{dr^2}{1 + r^2} + \frac{4\nu^2}{\nu^2 + 3\epsilon} (du + r d\tau)^2 \right), \tag{3.126}$$

where $\epsilon = \{-1, 0, 1\}$, $\mu = 3\nu$ and $\Lambda = -\epsilon$. Unlike the name seems to suggest, depending on the value of ϵ it can be supported by a positive, vanishing or negative cosmological constant. The sign of μ depends on the choice of orientation, which we have chosen here as $\epsilon_{\tau ru} = -\sqrt{-\det \mathrm{g}}$. The first two terms in the bracket (3.126) describe AdS_2. For $\Lambda = -\epsilon = -1$ and $\nu^2 = 1$ the metric (3.126) reduces to AdS_3

$$ds^2 = \frac{1}{4}\left(\frac{dr^2}{1+r^2} + du^2 + 2r du d\tau - d\tau^2\right), \tag{3.127}$$

albeit in an unusual coordinate system. Changing coordinates as $r = \sinh\sigma$, equation (3.127) becomes

$$\begin{aligned} ds^2 &= \frac{1}{4}\Big(-d\tau^2 + du^2 + d\sigma^2 + 2\sinh\sigma du d\tau\Big) \\ &= \frac{1}{4}\Big(-\cosh^2 u d\tau^2 + du^2 + (d\sigma + \sinh u d\tau)\Big)\,. \end{aligned} \tag{3.128}$$

When considering AdS_3 as a hyperboloid embedded into $\mathbb{R}^{2,2}$

$$ds^2 = -du^2 - dv^2 + dx^2 + dy^2\,, \qquad -u^2 - v^2 + x^2 + y^2 = -1 \tag{3.129}$$

the coordinate transformation that relates (3.129) to (3.128) is given by [46]

$$v = \cosh\left(\frac{\sigma}{2}\right)\sin\left(\frac{\tau}{2}\right)\cosh\left(\frac{u}{2}\right) - \sinh\left(\frac{\sigma}{2}\right)\cos\left(\frac{\tau}{2}\right)\sinh\left(\frac{u}{2}\right), \tag{3.130a}$$

$$u = \sinh\left(\frac{\sigma}{2}\right)\sin\left(\frac{\tau}{2}\right)\sinh\left(\frac{u}{2}\right) + \cosh\left(\frac{\sigma}{2}\right)\cos\left(\frac{\tau}{2}\right)\cosh\left(\frac{u}{2}\right), \tag{3.130b}$$

$$x = \cosh\left(\frac{\sigma}{2}\right)\cos\left(\frac{\tau}{2}\right)\sinh\left(\frac{u}{2}\right) - \sinh\left(\frac{\sigma}{2}\right)\sin\left(\frac{\tau}{2}\right)\cosh\left(\frac{u}{2}\right), \tag{3.130c}$$

$$y = \sinh\left(\frac{\sigma}{2}\right)\cos\left(\frac{\tau}{2}\right)\cosh\left(\frac{u}{2}\right) + \cosh\left(\frac{\sigma}{2}\right)\sin\left(\frac{\tau}{2}\right)\sinh\left(\frac{u}{2}\right). \tag{3.130d}$$

Warped dS_3 on the contrary can only be supported by a positive cosmological constant and is given by the metric [47]

$$ds^2 = \frac{1}{3-\nu^2}\left(-\left(1-r^2\right)d\tau^2 + \frac{dr^2}{1-r^2} + \frac{4\nu^2}{3-\nu^2}(du + r d\tau)^2\right). \tag{3.131}$$

Another difference with warped AdS_3 is that there is no value of ν for which the metric (3.131) reduces to de Sitter space. The first two terms in (3.131) describe two-dimensional de Sitter space. The metric (3.131) solves the equations of motion of topologically massive gravity for $\mu = 3\nu$ and $\Lambda = 1$. Here, the orientation has been chosen as $\epsilon_{\tau ru} = -\sqrt{-\det \mathrm{g}}$.

3.5.3. Warped Flat Space

The following subsections are taken from [1] with minor modifications (co-authored with Stéphane Detournay, Wout Merbis and Gim Seng Ng)

We consider the following three-dimensional spacetime [22, 47]

$$ds^2 = dx^2 - d\tau^2 + 12(dy + x d\tau)^2 \,, \tag{3.132}$$

which solves the equations of motion of topologically massive gravity at $\Lambda = 1$ and $\mu = 3\sqrt{3}$. Here, the orientation has been chosen as $\epsilon_{\tau xy} = -\sqrt{-\det \mathrm{g}}$. As already discussed above, the name warped flat space stems from the fact that this spacetime is a fibration over two-dimensional flat space $\mathbb{R}^{1,1}$, but the cosmological constant is positive for this spacetime.

One can now obtain warped flat space as a limit of global warped AdS_3 or warped dS_3 (both with positive cosmological constant) by taking the limit $\nu^2 \to 3$ in an adequate way. Taking the warped AdS_3 metric (3.126) with positive cosmological constant, sending $r \to \sqrt{\nu^2 - 3}x$, $\tau \to \sqrt{\nu^2 - 3}\tau$, $u \to (\nu^2 - 3)y$ and then taking the $\nu^2 \to 3$ we obtain warped flat space. Alternatively, for $\nu^2 < 3$ we start with warped dS_3 (3.131) and repeat the same limit but replace $(\nu^2 - 3)$ with $(3 - \nu^2)$ in the transformations to obtain (3.132).

The metric (3.132) has constant curvature scalars $R = 6$, $R_{\mu\nu}R^{\mu\nu} = 108$. The Cotton tensor

$$C_{\mu\nu}dx^\mu dx^\nu = 12\sqrt{3}\Big[\Big(24x^2 + 1\Big)d\tau^2 + 48x d\tau dy - dx^2 + 24dy^2\Big] \,. \tag{3.133}$$

yields $C_{\mu\nu}C^{\mu\nu} = 2592$. In computing the Cotton tensor we have chosen the following orientation of the epsilon tensor $\epsilon^{\tau xy} = 1/(\sqrt{-\mathrm{det}g})$ and this is the convention that we stick with in the following.

The inverse metric in coordinates (τ, x, y) reads

$$g^{\mu\nu} = \begin{pmatrix} -1 & 0 & x \\ 0 & 1 & 0 \\ x & 0 & \frac{1}{12}(1 - 12x^2) \end{pmatrix} . \tag{3.134}$$

From (3.134) it can be seen that the normal vector to constant τ surfaces is always timelike while the one to constant x surfaces is spacelike. However, for constant y surfaces, $12 n_\mu n^\mu = 1 - 12x^2$; so it is a spacelike surface for $|x| > 1/\sqrt{12}$, while for $|x| < 1/\sqrt{12}$ it is a timelike surface. The $x = \pm 1/\sqrt{12}$ surfaces are null surfaces.

The isometries are generated by the four Killing vectors

$$I_0 = -2\partial_y \,, \tag{3.135a}$$
$$a_\pm = \partial_\tau \mp \partial_x \pm \tau\partial_y \,, \tag{3.135b}$$
$$H = -\tau\partial_x - x\partial_\tau + \frac{1}{2}\Big(x^2 + \tau^2\Big)\partial_y \,, \tag{3.135c}$$

satisfying the following algebra:

$$[a_+, a_-] = I_0, \quad [H, a_\pm] = \mp a_\pm \,, \tag{3.136}$$

where I_0 commutes with all other generators. The algebra is precisely the one of the Hamiltonian, annihilation and creation operator of a harmonic oscillator in quantum mechanics, where I_0 is a c-number. The algebra (3.136) is known under the name P_2^c, as it is the 2-dimensional centrally extended Poincaré algebra. We may bring the commutation relations into a well-known form through the following change of basis $\sqrt{2}a_+ = P_1 + P_0$, $\sqrt{2}a_- = P_1 - P_0$ leading to

$$[P_0, P_1] = I_0, \quad [H, P_1] = -P_0, \quad [H, P_0] = -P_1 \,. \tag{3.137}$$

Here, H denotes the boost, P_0 and P_1 are the 2-dimensional translations and I_0 denotes the central extension.

We see that some of these isometries have a natural geometric interpretation. For I_0 and $a_+ + a_- = 2\partial_\tau$, the finite coordinate transformations are translations in y and τ. For $-\frac{1}{2}(a_+ - a_-) = -\tau\partial_y + \partial_x$, we have the simultaneous transformation

$$x' = x + C \,, \qquad y' = y - C\tau \,, \qquad \tau' = \tau \,. \tag{3.138}$$

Here, C is an arbitrary constant. Finally the finite transformation generated by H is the most complicated one:

$$\begin{aligned} \tau' &= \tau \cosh C - x \sinh C \,, \\ x' &= -\tau \sinh C + x \cosh C \,, \\ y' &= y + \frac{1}{2}\sinh(C)\Big[\cosh(C)\Big(\tau^2 + x^2\Big) - 2\tau x \sinh(C)\Big] \,. \end{aligned} \tag{3.139}$$

We see that the τ' and x' transformations are simply a boost transformation, while the y' transformation is non-trivial.

3.5.4. Quotienting Warped Flat Space

Following [22], we start with the warped flat spacetime (3.132) and consider the region $x^2 - \tau^2 > 0$, $x > 0$. We perform the coordinate transformation

$$\begin{aligned} x &= \sqrt{\frac{\rho}{6\xi}} \cosh(12\xi\varphi) \,, \\ \tau &= \sqrt{\frac{\rho}{6\xi}} \sinh(12\xi\varphi) \,, \\ y &= u + (\xi + \omega)\varphi - \frac{\rho}{24\xi} \sinh(24\xi\varphi) \,, \end{aligned} \tag{3.140}$$

where ξ and ω are two real constants and $\rho/\xi > 0$. We obtain

$$\begin{aligned} ds^2 &= \frac{d\rho^2}{24\xi\rho} + 12du^2 + 24(\rho+\omega+\xi)d\varphi du + 12\Big[(\rho+\omega)^2 + \xi(\xi+2\omega)\Big]d\varphi^2 \\ &= \frac{d\rho^2}{24\xi\rho} - 24\xi\rho d\varphi^2 + 12[du + (\rho+\xi+\omega)d\varphi]^2\,, \end{aligned} \tag{3.141}$$

which upon identification of $(u,\rho,\varphi) \sim (u,\rho,\varphi+2\pi)$ gives the warped flat quotient. This amounts to perform discrete identifications in the global warped flat geometry (3.132) along orbits of the Killing vector

$$\partial_\varphi = -12\xi H - \frac{\xi+\omega}{2} I_0. \tag{3.142}$$

In equation (3.141) the coordinate u runs from $-\infty$ to ∞. Depending on the sign of ξ, ρ runs from $-\infty$ to 0 or from 0 to ∞. If we send $\rho \to -\rho, \xi \to -\xi, \omega \to -\omega$ and $\varphi \to -\varphi$ the metric, the identifications, and the orientation stay the same. Thus, (ξ,ω) and $(-\xi,-\omega)$ describe spacetimes which are isometric with the same orientation. Hence, in the following, we restrict to $\xi > 0$ without loss of generality.

The inverse metric (in (u,ρ,φ) coordinates) reads

$$g^{\mu\nu} = \begin{pmatrix} -\frac{(\rho+\omega)^2+\xi(\xi+2\omega)}{24\xi\rho} & 0 & \frac{\rho+\xi+\omega}{24\xi\rho} \\ & 24\xi\rho & 0 \\ & & -\frac{1}{24\xi\rho} \end{pmatrix}. \tag{3.143}$$

The global Killing vectors H and I_0, as well as the local Killing vectors $a_\pm$ are given by

$$H = \frac{1}{12\xi}((\xi+\omega)\partial_u - \partial_\varphi), \quad I_0 = -2\partial_u, \tag{3.144a}$$

$$a_\pm = \frac{e^{\pm 12\xi\varphi}}{2\sqrt{6\xi\rho}}[\partial_\varphi + (\rho-\xi-\omega)\partial_u \mp 24\xi\rho\partial_\rho] \tag{3.144b}$$

and satisfy (3.136).

The inverse transformation of (3.140) reads

$$\begin{aligned} \rho(x,\tau) &= 6\xi(x^2-\tau^2)\,, \\ u(\tau,x,y) &= y + \frac{1}{4}\Big(x^2-\tau^2\Big)\sinh\left(2\operatorname{arctanh}\left(\frac{\tau}{x}\right)\right) - \frac{(\xi+\omega)\operatorname{arctanh}\left(\frac{\tau}{x}\right)}{12\xi}\,, \\ \varphi(\tau,x) &= \frac{\operatorname{arctanh}\left(\frac{\tau}{x}\right)}{12\xi}\,. \end{aligned} \tag{3.145}$$

For the parameter range $\omega \le -\xi/2$ the metric component $g_{\varphi\varphi}$ becomes negative and closed timelike curves occur in the region $\rho > 0$ between $\rho_1 = -\omega - \sqrt{-\xi(\xi+2\omega)}$ and $\rho_2 = -\omega + \sqrt{-\xi(\xi+2\omega)}$. In the following we differentiate between two cases of interest:

1. For $\omega > -\xi/2$: no closed timelike curves appear
2. For $\omega \leq -\xi/2$: closed timelike curves appear in the region $-\omega - \sqrt{-\xi(\xi+2\omega)} < \rho < -\omega + \sqrt{-\xi(\xi+2\omega)}$

In the case $\xi + \omega = 0$, closed timelike curves start to occur at $\rho = 0$, which is why we often restrict to $\xi + \omega > 0$ in the following. The surface $\rho = 0$ is a Killing horizon of the following Killing vector

$$K^\mu \partial_\mu = \partial_u - \frac{1}{\xi + \omega}\partial_\varphi \tag{3.146}$$

if $\xi + \omega \neq 0$. For $\xi + \omega = 0$ the Killing horizon is generated by the Killing vector ∂_φ.

3.5.5. Causal Structures

In this section, we discuss the causal structure of warped flat space (3.132) and the warped flat quotient (3.141), using methods developed in [24]. These methods are discussed in detail in section 2.2 and have also been applied in section 3.4 where we discussed the causal structure of the BTZ black hole.

Warped Flat Space

First, we consider warped flat space (3.132). The map π from the definition of the projection diagram is given by the projection $(\tau, x, y) \mapsto (\tau, x)$. This is the same map used in appendix A to explain the name warped flat space. The auxiliary metric

$$\gamma_{\mu\nu} dx^\mu dx^\nu := dx^2 - d\tau^2 \,, \tag{3.147}$$

is two-dimensional Minkowski space $R^{1,1}$, whose conformal compactification and conformal boundaries are well-known.

We want to answer the question of whether the geometry (3.132) possesses a non-zero black hole region. Our notion of future asymptotic infinity $\mathscr{I}^+$ of (3.147) is defined with respect to the conformal boundary of the two-dimensional metric. The two-dimensional spacetime (3.147) obviously does not have a black hole region.

We now show that also the three-dimensional spacetime does not have a black hole region. This can be seen explicitly by considering the family of null curves $(\tau(s), x(s)) = (\tau_0 + s, x_0 + s)$ going from each point in spacetime all the way to $\mathscr{I}^+$. These curves can be lifted to null curves in the three-dimensional spacetime going through every point: $(\tau(s), x(s), y(s)) = (\tau_0 + s, x_0 + s, y_0 - x_0 s + \frac{s^2}{2})$. Therefore, there is no black hole region in the three-dimensional spacetime.[a]

Warped Flat Quotient

Next, we consider the warped flat quotient. Here we distinguish between two cases, the case where closed timelike curves are present and the case without closed timelike curves.

[a] I thank Piotr Chruściel for pointing this out to me.

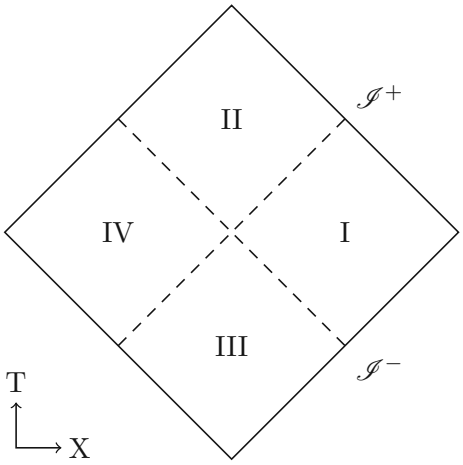

Figure 3.11.: Here, we depict the split of the spacetime into the four sectors in the compact coordinates T and X, which are introduced below. Each coordinate patch u, ρ, φ covers one such sector. The dashed lines denote the location of the Killing horizon. They intersect at the point $T = X = 0$.

As the coordinate system (u, ρ, φ) used in the previous section cannot be extended beyond $\rho = 0$, we work with the coordinates (τ, x, y) which are everywhere well-defined. We split our spacetime into four sectors:

I $x^2 - \tau^2 > 0$, $\tau - x < 0$

II $x^2 - \tau^2 < 0$, $\tau - x > 0$

III $x^2 - \tau^2 < 0$, $\tau - x < 0$

IV $x^2 - \tau^2 > 0$, $\tau - x > 0$

This split is depicted in Figure 3.11. The coordinate transformation in sector I has already been discussed in the previous section (see equation (3.140)). In the sectors II, III, IV we introduce new coordinates u, ρ and φ as follows

$$II: x = \sqrt{-\frac{\rho}{6\xi}}\sinh(12\xi\varphi), \tag{3.148a}$$

$$\tau = \sqrt{-\frac{\rho}{6\xi}}\cosh(12\xi\varphi), \tag{3.148b}$$

$$y = \frac{\rho\sinh(24\xi\varphi)}{24\xi} + \varphi(\xi + \omega) + u\,, \tag{3.148c}$$

$$III: x = -\sqrt{-\frac{\rho}{6\xi}}\sinh(12\xi\varphi), \tag{3.148d}$$

$$\tau = -\sqrt{-\frac{\rho}{6\xi}}\cosh(12\xi\varphi), \tag{3.148e}$$

$$y = \frac{\rho\sinh(24\xi\varphi)}{24\xi} + \varphi(\xi+\omega) + u\,, \tag{3.148f}$$

$$IV: x = -\sqrt{\frac{\rho}{6\xi}}\cosh(12\xi\varphi), \tag{3.148g}$$

$$\tau = -\sqrt{\frac{\rho}{6\xi}}\sinh(12\xi\varphi), \tag{3.148h}$$

$$y = -\frac{\rho\sinh(24\xi\varphi)}{24\xi} + \varphi(\xi+\omega) + u\,. \tag{3.148i}$$

This leads to the metric (3.141) in each sector, which upon identification of $(u,\rho,\varphi) \sim (u,\rho,\varphi+2\pi)$ gives the warped flat quotient. Here, u runs from $-\infty$ to ∞. Depending on the sector ρ runs from $-\infty$ to 0 or from 0 to ∞. The inverse transformation of (3.148) reads

$$\rho = 6\xi(x^2-\tau^2)\,, \tag{3.149a}$$

$$x^2-\tau^2<0: u = y - \frac{1}{4}\left(x^2-\tau^2\right)\sinh\left(2\operatorname{arctanh}\left(\frac{x}{\tau}\right)\right) - \frac{(\xi+\omega)\operatorname{arctanh}\left(\frac{x}{\tau}\right)}{12\xi}, \tag{3.149b}$$

$$\varphi = \frac{\operatorname{arctanh}\left(\frac{x}{\tau}\right)}{12\xi}, \tag{3.149c}$$

$$x^2-\tau^2>0: u = y + \frac{1}{4}\left(x^2-\tau^2\right)\sinh\left(2\operatorname{arctanh}\left(\frac{\tau}{x}\right)\right) - \frac{(\xi+\omega)\operatorname{arctanh}\left(\frac{\tau}{x}\right)}{12\xi}, \tag{3.149d}$$

$$\varphi = \frac{\operatorname{arctanh}\left(\frac{\tau}{x}\right)}{12\xi}\,. \tag{3.149e}$$

The starting point of the construction is to write the metric (3.141) in the following form:

$$\begin{aligned} g_{\mu\nu}dx^\mu dx^\nu = &-\frac{24\xi\rho}{\xi^2+2\xi\omega+(\rho+\omega)^2}du^2 + \frac{d\rho^2}{24\xi\rho} \\ &+ 12\Big((\rho+\omega)^2+2\xi\omega+\xi^2\Big)\left(d\varphi + \frac{\rho+\xi+\omega}{\xi^2+2\xi\omega+(\rho+\omega)^2}du\right)^2. \end{aligned} \tag{3.150}$$

We see that the last term is positive everywhere, except for in the region where closed timelike curves are present (compare with (3.141)). We discuss the case without closed timelike curves first for which the last term is manifestly positive. We project in such a

way that the auxiliary metric $\gamma_{\mu\nu}$ reads

$$\gamma_{\mu\nu}dx^\mu dx^\nu := -\frac{24\xi\rho}{\xi^2+2\xi\omega+(\rho+\omega)^2}du^2+\frac{d\rho^2}{24\xi\rho}\,. \tag{3.151}$$

Then we perform the following coordinate transformation in each of the four sectors

$$I: \qquad V=e^{cf(\rho)-cu}, \qquad U=-e^{cf(\rho)+cu}\,, \tag{3.152a}$$
$$II: \qquad V=e^{cf(\rho)-cu}, \qquad U=e^{cf(\rho)+cu}\,, \tag{3.152b}$$
$$III: \qquad V=-e^{cf(\rho)-cu}, \qquad U=-e^{cf(\rho)+cu}\,, \tag{3.152c}$$
$$IV: \qquad V=-e^{cf(\rho)-cu}, \qquad U=e^{cf(\rho)+cu}\,, \tag{3.152d}$$

where $c=\frac{12\xi}{\xi+\omega}$ and $f(\rho)$ is the solution to the differential equation

$$f'(\rho)=\frac{\sqrt{\xi^2+2\xi\omega+(\rho+\omega)^2}}{24\xi\rho}\,. \tag{3.153}$$

The solution satisfies that $f(\rho=\pm\infty)=\infty$ and $f(\rho=0)=-\infty$. The coordinates V, U both run from $(-\infty,\infty)$. We introduce two more coordinates

$$V=\tan\left(\frac{X+T}{2}\right), \quad U=\tan\left(\frac{T-X}{2}\right), \tag{3.154}$$

so that $(T-X)/2\in(-\pi/2,\pi/2)$ and $(T+X)/2\in(-\pi/2,\pi/2)$. Now we can rewrite $\gamma_{\mu\nu}$ as

$$\begin{aligned}\gamma_{\mu\nu}dx^\mu dx^\nu =& -\operatorname{sgn}(\rho)\frac{e^{-2cf(\rho)}\rho(\xi+\omega)^2}{6\xi(\xi^2+2\xi\omega+(\rho+\omega)^2)}\,dU\,dV\\ =&\frac{1}{\Omega^2}(-dT^2+dX^2)\,.\end{aligned} \tag{3.155}$$

The projection π is then defined as the map $(\tau,x,y)\to(X(\tau,x,y),T(\tau,x,y))$. The map is differentiable everywhere. The conformal factor reads

$$\Omega^2=4\operatorname{sgn}(\rho)\frac{6\xi e^{2cf(\rho)}(\xi^2+2\xi\omega+(\rho+\omega)^2)}{\rho(\xi+\omega)^2}\frac{1}{(1+U^2(\rho,u))(1+V^2(\rho,u))}\,. \tag{3.156}$$

The conformal factor goes to 0 as ρ,u go to $\pm$ infinity, is regular at $\rho=0$ and is positive everywhere. The projection diagram of the warped flat quotient in the case where no closed timelike curves occur looks like the one of two-dimensional Minkowski space and is depicted in Figure 3.12. The above derivation is valid for the case where no closed timelike curves appear. In the case where closed timelike curves appear, the construction is valid everywhere except for in the region $-\omega-\sqrt{-\xi(\xi+2\omega)}<\rho<-\omega+\sqrt{-\xi(\xi+2\omega)}$ which must be excised from the diagram. We thus cut off our spacetime at $\rho=-\omega-\sqrt{-\xi(\xi+2\omega)}$.

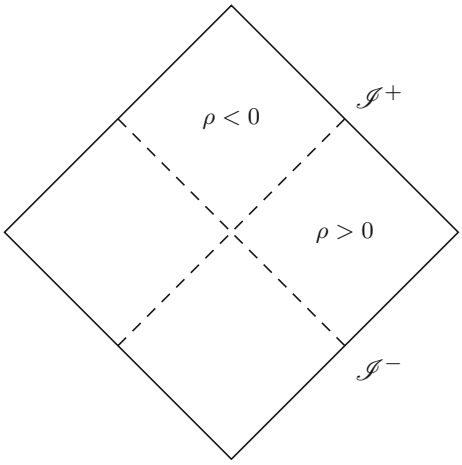

Figure 3.12.: Projection diagram of the warped flat quotient in the case where no closed timelike curves are present ($\omega > -\xi/2$). The upper and lower sectors correspond to $\rho < 0$, while the left and right sectors correspond to $\rho > 0$. The dashed lines that divide these sectors are the $\rho = 0$ lines. The four vertices correspond to $\rho \to \pm\infty, u = \text{const}$.

The resulting diagram is depicted in Figure 3.13. This projection diagram looks like the Penrose diagram of flat space cosmologies [48].

We now want to answer the question of whether the geometry (3.141) possesses a non-zero black hole region. As before, our notion of future null infinity $\mathscr{I}^+$ is defined with respect to the conformal boundary of the two-dimensional auxiliary metric. The two-dimensional spacetime (3.151) does not have a black hole region. To show that the three-dimensional geometry does not possess a black hole region either we proceed as follows. In each sector we consider null curves in the two-dimensional geometry (3.151). These curves $(u(\rho), \rho)$ are solutions to the differential equation

$$\left(\frac{\partial u(\rho)}{\partial \rho}\right)^2 = \left(\frac{\xi^2 + 2\xi\omega + (\rho+\omega)^2}{(24\xi\rho)^2}\right), \tag{3.157}$$

and may be lifted to null curves $(u(\rho), \rho, \varphi(\rho))$ in the three-dimensional geometry provided

$$\frac{\partial \varphi(\rho)}{\partial \rho} = -\frac{\rho + \xi + \omega}{\xi^2 + 2\xi\omega + (\rho+\omega)^2}\frac{\partial u(\rho)}{\partial \rho}\,. \tag{3.158}$$

The differential equations can be solved to give two curves emanating from every point in spacetime, except at $\rho = 0$, where the coordinate system breaks down. Considering the curves in the global coordinate system (τ, x, y) (see (3.140) and (3.148)), we find that the coordinates $(\tau(\rho), x(\rho), y(\rho))$ are finite and continuous for any ρ if one patches the curves in the sectors I, II, III, IV together appropriately. As there exist such null curves going

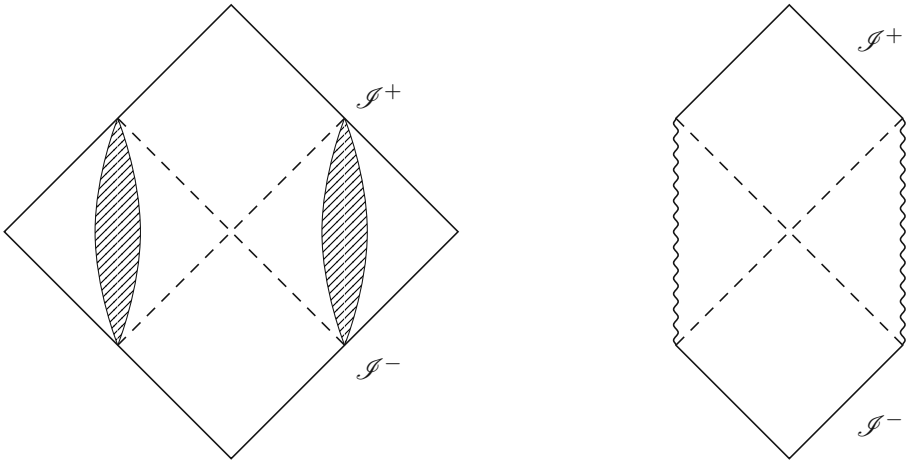

Figure 3.13.: Projection diagram of the warped flat quotient in the case where closed timelike curves are present $\omega \leq -\xi/2$. The closed timelike curves appear in the shaded region in the left picture: $-\omega - \sqrt{-\xi(\xi+2\omega)} < \rho < -\omega + \sqrt{-\xi(\xi+2\omega)}$. In the right picture we have cut off the spacetime at the place where the closed timelike curves appear. The vertical, wiggly line is the singularity. The right figure looks the same as the causal diagram of flat space cosmologies [48].

through every point this shows there is no black hole region in our three-dimensional spacetime.

Warped Flat Quotient: $\xi + \omega = 0$

The causal analysis in the previous section holds true for all ξ, ω except for the case $\xi + \omega = 0$. Reconsidering (3.152) for $\xi + \omega = 0$ we see that $c = \frac{12\xi}{\xi+\omega}$ diverges if $\xi + \omega = 0$. The case $\xi + \omega = 0$ is special because – as already briefly mentioned at the end of section 2.2 – for this case closed timelike curves appear between the horizon $\rho = 0$ and $\rho = 2\xi$. As causality is not represented in any useful way in this region, we must excise it from the diagram. We thus cut off our spacetime at $\rho = 0$. The metric (3.141) for $\xi + \omega = 0$ reads

$$ds^2 = \frac{d\rho^2}{24\xi\rho} + \frac{24\xi}{2\xi - \rho}du^2 - \frac{12\rho(du + (\rho - 2\xi)d\varphi)^2}{2\xi - \rho} \tag{3.159}$$

Performing the coordinate transformation $\rho = -6r^2\xi$ we obtain

$$ds^2 = -dr^2 + \frac{12du^2}{1+3r^2} + \frac{36r^2}{1+3r^2}\Big(du - \Big(2\xi + 6r^2\xi\Big)d\varphi\Big)^2 . \tag{3.160}$$

Here, the last term is positive. We project in such a way that the auxiliary metric $\gamma_{\mu\nu}$ reads

$$\gamma_{\mu\nu}dx^\mu dx^\nu = -dr^2 + \frac{12du^2}{1+3r^2} . \tag{3.161}$$

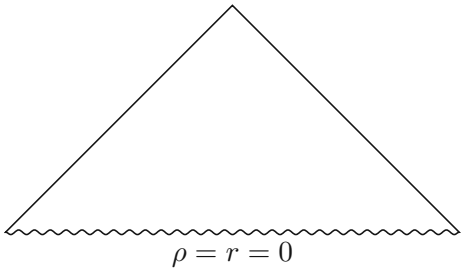

Figure 3.14.: Projection diagram of the warped flat quotient in the case where $\xi + \omega = 0$. Due to the occurence of closed timelike curves the spacetime is cut off at $\rho = r = 0$, resulting in a singularity (wiggled line).

Here, r runs from $(0, \infty)$ and $u \in (-\infty, \infty)$. Performing the subsequent coordinate transformations

$$V = \arctan(x + u)\,, \quad U = \arctan(u - x)\,, \tag{3.162}$$

with

$$x = \int \frac{\sqrt{1 + 3r^2}}{\sqrt{12}} dr \tag{3.163}$$

and $V = T + X$, $U = T - X$ we obtain

$$\gamma_{\mu\nu} dx^\mu dx^\nu = \frac{1}{\Omega^2}\left(-dX^2 + dT^2\right) \tag{3.164}$$

with

$$\Omega^2 = \frac{(1 + 3r^2)}{12(1 + (u - x(r))^2)(1 + (u + x(r))^2)}\,. \tag{3.165}$$

As $x \in (0, \infty)$ it follows that $V \geq U$ which in turn implies $X \geq 0$. This leads to the projection diagram 3.14 for the $\xi + \omega = 0$ warped flat quotient. The conformal factor Ω^2 goes to 0 for $r \to \infty$ or $u \to \pm\infty$ and is regular at $r = 0$. In analogy to the other cases it can be shown that the three-dimensional $\xi + \omega = 0$ warped flat quotient is not a black hole.

3.6. Black Hole Entropy and Microstate Counting

In subsection 3.4 we have discussed the geometry of BTZ black holes and found that they share several features with $(3 + 1)$-dimensional Kerr black holes: The non-extremal BTZ black hole has two Killing horizons, the outer Killing horizon is an event horizon. While it does not have a curvature singularity, it can be shown that upon the introduction of matter the causal singularity becomes a curvature singularity [35]. Importantly, not only the classical features of the BTZ black hole are similar to the classical features of the Kerr black hole, but the similarities also continue on the quantum level. Indeed, the BTZ black hole exhibits non-trivial thermodynamics. It Hawking evaporates at the

temperature

$$T_H = \frac{r_+^2 - r_-^2}{2\pi r_+} \tag{3.166}$$

and it has a Bekenstein-Hawking entropy

$$S = \frac{A}{4G} = \frac{2\pi r_+}{4G}\,, \tag{3.167}$$

where A denotes the horizon area. Understanding the quantum origin of the Bekenstein-Hawking entropy is one of the main quests in theoretical high-energy physics nowadays. The hope is that this quest will not only give information about the microscopic structure of black holes but also provide novel information about quantum gravity.

Vafa and Strominger [12] were the first ones to derive the entropy of certain black holes in string theory through a microscopic derivation. Shortly after, Strominger [13] provided a microscopic derivation of black hole entropy for the BTZ black hole, which was in the same spirit as his earlier work with Vafa. The idea was to give a microscopic counting of black hole microstates in a similar manner as we know it from statistical mechanics.

Strominger's work is based on the observation made by Brown and Henneaux that the asymptotic symmetry algebra of asymptotically AdS_3 spacetimes is given by two copies of the Virasoro algebra. He asserted that *if a theory of quantum gravity exists on asymptotically AdS_3 spacetimes, it must be a conformal field theory* and *then the physical states of quantum gravity must fall into representations of the Virasoro algebra.*

More specifically, he used the idea of holography, which – in this context – conjectures that quantum gravity on asymptotically AdS_3 spacetimes is dual to a two-dimensional conformal field theory (AdS_3/CFT_2 correspondence) with symmetry algebra

$$[\hat{L}_n^\pm, \hat{L}_m^\pm] = (n-m)\hat{L}_{n+m}^\pm + \frac{c^\pm}{12}(n^3 - n)\delta_{n+m,0}\,, \tag{3.168a}$$

$$[\hat{L}_n^\pm, \hat{L}_m^\mp] = 0\,, \tag{3.168b}$$

and central charge given by

$$c^+ = c^- = \frac{3\ell}{2G} \equiv c\,, \tag{3.169}$$

where ℓ is the AdS_3 radius which we only restore for the purpose of this subsection, but which is otherwise set to 1. The essence of Strominger's paper was to apply Cardy's formula for the asymptotic growth of states in a two-dimensional conformal field theory [49] to derive the entropy of the three-dimensional BTZ black hole. The derivation of the Cardy formula is performed in the Euclidean and the underlying manifold on which the conformal field theory is defined is a torus. Now, provided that the conformal field theory is modular invariant and the energy spectrum is bounded from below and possesses a gapped ground state, it is possible to derive an entropy expression from the partition function in the conformal field theory in the large temperature limit. The entropy expression, intrinsic to two-dimensional conformal field theories on the torus, is

given by

$$S_{CFT} = 2\pi\sqrt{\frac{c_+ \langle \hat{L}_0^+ \rangle}{6}} + 2\pi\sqrt{\frac{c_- \langle \hat{L}_0^- \rangle}{6}}\,, \tag{3.170}$$

where c_+, c_- are the central charges in the two-dimensional conformal field theory and $\langle \hat{L}_0^\pm \rangle$ are the expectation values of the operators $\hat{L}_0^\pm$ in the two-dimensional conformal field theory, which fulfill the commutation relations (3.168). The entropy expression (3.170) is obtained by counting states in a two-dimensional conformal field theory.

Now, employing the AdS_3/CFT_2 correspondence, the entropy (3.170) should be related to an entropy expression in three-dimensional quantum gravity. To make use of the results for energy derived in subsection 3.3, equation (3.26), and the entropy result (3.167), we must work in the semi-classical regime where the cosmological constant is small in Planck units, or equivalently

$$\ell \gg G\,. \tag{3.171}$$

From (3.169) we obtain

$$c \gg 1\,. \tag{3.172}$$

Expressing the entropy of the black hole in terms of the *classical* charges L_0^+ and L_0^- which are related to the mass m and the angular momentum j as (3.26) the black hole entropy reads

$$S_{BH} = 2\pi\sqrt{\frac{c_+ L_0^+}{6}} + 2\pi\sqrt{\frac{c_- L_0^-}{6}}\,, \tag{3.173}$$

where $c^\pm$ are given by (3.169). Identifying the classical charges with the expectation values of the operators $\hat{L}_0^\pm$, the expression (3.173) precisely coincides with (3.170):

$$S_{BH} = S_{CFT}\,. \tag{3.174}$$

Therefore, the entropy of the three-dimensional BTZ black hole can be reproduced from a counting in a two-dimensional conformal field theory. The fact that not just the functional form of the entropy, but also the prefactors precisely match is evidence in favor of the AdS/CFT correspondence.

Some further comments are in order: Due to the fact that the energy in the conformal field theory $E = \langle \hat{L}_0^+ \rangle + \langle \hat{L}_0^- \rangle$ has to be bounded from below for the Cardy formula to apply, the same has to hold true for asymptotically AdS_3 spacetimes. Boundedness of the energy for asymptotically AdS_3 spacetimes and a gap in the energy spectrum is needed for the derivation of the Cardy formula. It is clear from the discussion in subsections 3.3.1 that there does not exist a "literal gap" in the energy of solutions to the Einstein equations. By this, we mean that for any value of the energy there exist vacuum solutions to the Einstein equations for negative cosmological constant. However, at least when considering only vacuum solutions to the Einstein equations with constant $\mathcal{L}_+$ and $\mathcal{L}_-$ one can argue for the existence of such a gap. When restricting to this particular subset of vacuum solutions which are asymptotically AdS_3, one observes that the BTZ black holes are separated from AdS_3 by solutions with conical singularities. These are excluded

from the phase space in Strominger's derivation. The value of the gap is given by the energy of AdS_3

$$\Delta_{gap} = m_{AdS_3} = -\frac{1}{8G}\,. \tag{3.175}$$

The energy is bounded from below, if one restricts the phase space to smooth vacuum solutions with constant $\mathcal{L}_+$ and $\mathcal{L}_-$ without closed timelike curves and conical singularities. This fact is visualized in Figure 3.3. At the time of this writing, it is unclear to me whether one can still argue for this gap and boundedness of the energy by considering asymptotically AdS_3 spacetimes in the presence of matter satisfying some energy condition such as the dominant energy condition. Progress regarding the positivity of energy in asymptotically AdS_3 spacetimes has been made in the paper [50] by studying coadjoint orbits of the Virasoro group. While positive energy theorems for negatively curved spacetimes exist in higher dimensions and are a subject of active research in mathematical general relativity, we do not know of results pertaining to $(2+1)$ dimensions (aside from [50]). This is a question that I would like to return to in the near future.

Lastly, we discuss microstate countings that go beyond the derivation by Strominger [13]. This derivation has been the basis of many microstate countings and it is believed by many in the community that such a microstate counting should be possible for generic black holes. Again, the underlying assumption of most of these constructions is that the theory of quantum gravity exists and is of holographic nature - i.e. that quantum gravity in d dimensions is dual to a quantum field theory in $(d-1)$ dimensions.

Many of the microstate countings available in literature can not be seen as completely independent derivations of (black hole) entropy, as they are often based on extremal or near-extremal black holes, whose near horizon region includes an AdS_3 or AdS_2 factor. Notable exceptions include e.g. [17,18] where the entropy of three-dimensional flat space cosmologies was calculated by performing a microstate counting in another two-dimensional quantum field theory with infinitely many symmetries – a BMS_3 field theory. Another notable exception discusses asymptotically Lifshitz black holes whose entropy can be derived from a field theory with anisotropic scaling in two dimensions [19,51].

In the paper [1], our goal was to reproduce the entropy of the warped flat quotients (3.141) which we discussed in section 3.5. The spacetimes (3.141) have a Killing horizon at $\rho = 0$ which was claimed to be a black hole horizon in [22]. The reason we originally got interested in this two-parameter family of solutions to topologically massive gravity was that we thought that they describe black hole spacetimes with curious isometries. As discussed in subsection 3.5.5, there does not exist a value of ξ and ω for which the spacetime has an event horizon. However, the causal diagram of warped flat quotients in the regime where $\omega \leq -\xi/2$ shares similarities to the one of flat space cosmologies, which suggests that the horizon is of cosmological nature, see Figure 3.13.

In [1] we derived the entropy of these warped flat quotients using a microstate counting in yet another two-dimensional field theory that possesses infinitely many symmetries – a so-called warped conformal field theory.

The structure of warped conformal field theories (WCFTs) was first investigated by Hofman and Strominger [52]. Generalizing the arguments by Zamolodchikov [53] and Polchinski [54], Hofman and Strominger considered a two-dimensional unitary quantum

field theory without Lorentz symmetry, which is invariant under chiral global scaling symmetry and translations

$$x^- \to x^- + a\,, \qquad x^+ \to x^+ + b\,, \qquad x^- \to \lambda_- x^-\,. \tag{3.176}$$

They found that these quantum field theories must have an extended local algebra. The two minimal options for this algebra are either two copies of the Virasoro algebra or a semi-direct sum of a Virasoro algebra and a $u(1)$ Kac-Moody algebra. We call the latter case a warped conformal field theory. The symmetry algebra of a warped conformal field theory is given by

$$\begin{aligned}
[L_m, L_n] &= (m-n)L_{m+n} + \frac{c}{12}(m^3 - m)\delta_{n+m,0} \\
[L_m, P_n] &= -nP_{m+n} + \kappa(m^2 + m)\delta_{m+n,0} \\
[P_m, P_n] &= Kn\delta_{n+m,0}\,,
\end{aligned} \tag{3.177}$$

where n, m run over all integers and c, κ and K denote central terms of the algebra. First examples for putative holographic warped conformal field theories were given in [16, 55]. In a similar manner as in the case of two-dimensional conformal field theories, it is possible to derive an intrinsic entropy expression for warped conformal field theories [16].

By studying the asymptotic symmetries of warped flat spacetimes we found that their algebra is given by a semi-direct sum of a Virasoro algebra and a $u(1)$ Kac-Moody algebra – the symmetry algebra of a warped conformal field theory. This gives the link between the gravitational setup and the warped conformal field theory. Provided that certain assumptions regarding boundedness of the spectrum and the vacuum state are fulfilled, for details see [1, 16], it is possible to argue that the calculation within the warped conformal field theory can be applied to the gravitational setup. In our paper, we give arguments in favor of these assumptions. The gravitational entropy then precisely coincides with the entropy expression in warped conformal field theories, thereby providing evidence in favor of a holographic description of spacetime – independently of the value of the cosmological constant and the theory of gravity one is considering.

4. Positivity of Mass at Negative Cosmological Constant

The question of the positivity of energy of the gravitational field has played a key role in many investigations in mathematical general relativity [56]. So far these questions have predominantly been considered (and answered) in the context of asymptotically locally flat spacetimes where the metric (locally) approaches the Minkowski metric at large distances. When the cosmological constant is negative, which corresponds to asymptotically locally AdS spacetimes, much fewer results are known and only a few bounds exist. For time-symmetric initial data sets, this becomes the question of whether the energy of asymptotically locally hyperbolic spaces is bounded from below. In this chapter, the contents of my work (co-authored with Piotr Chruściel and Erwann Delay) [2] and its relation to positive energy theorems for asymptotically locally hyperbolic spaces is discussed. In section 4.1, we introduce two classes of spacetimes that will be of importance in this chapter: the Birmingham–Kottler spacetimes and the Horowitz–Myers spacetimes. In section 4.2, we give a short overview of positive mass theorems for general relativity with negative cosmological constant and discuss the Horowitz–Myers conjecture. Sections 4.3-4.8 are concerned with the paper and are taken with only minimal modifications from [2].

4.1. Solutions of Interest

In this section, we introduce two static vacuum solutions of Einstein gravity with negative cosmological constant in $(n+1)$ spacetime dimensions, which will be of relevance in the following. The space dimension n is always assumed to be greater or equal to two. In this chapter, we will use $\tilde{g}$ for the line element of Lorentzian spacetime metrics and g for the line element of Riemannian metrics. We also recall our conventions summarized at the beginning of this thesis, in chapter 0: Greek letters $(\mu, \nu, \sigma, ...)$ are used as spacetime indices and run from 1 to $n+1$, small Latin letters $(a, b, c, ..., i, j, k, ...)$ are used for spatial indices and run from $1, ...n$. Big Latin letters from the beginning of the alphabet $(A, B, C, ...)$ run from $1, ...n-1$. Big Latin letters from the middle of the alphabet $(I, J, ...)$ run from $1, ...n-2$.

4.1.1. Birmingham–Kottler metrics

The Birmingham–Kottler metrics [57, 58] are solutions to the vacuum Einstein equations with negative cosmological constant in $(n+1)$ spacetime dimensions. Their line element

is given by

$$\tilde{g} = -f dt^2 + f^{-1} dr^2 + r^2 h_k \,, \qquad f = r^2 + k - \frac{2m_c}{r^{n-2}} \,, \tag{4.1}$$

where m_c is a constant which we refer to as the *coordinate mass parameter*, and where h_k is an Einstein metric[1] on an $(n-1)$-dimensional compact manifold N^{n-1} with scalar curvature equal to

$$R(h_k) = k(n-1)(n-2) \,, \qquad k \in \{0, \pm 1\} \,. \tag{4.2}$$

The collection of (N^{n-1}, h_k)'s is quite rich — there exist many Einstein metrics on higher-dimensional spheres, including exotic ones [59]. The spacetime (4.1) is also often referred to as Schwarzschild–AdS or Schwarzschild–Tangherlini–AdS when the boundary manifold (N^{n-1}, h_k) is the round sphere.

In space dimension $n = 2$, the constant k can be absorbed via a redefinition of m_c. The resulting spacetime reads

$$\tilde{g} = -\Big(r^2 - 2m_c\Big) dt^2 + \frac{dr^2}{r^2 - 2m_c} + r^2 d\varphi^2 \,. \tag{4.3}$$

For $m_c > 0$ the metric (4.3) describes a non-rotating BTZ black hole. The geometry of (4.3) has been discussed in detail in section 3.4 and subsection 3.3.1.

In 3+1 spacetime dimensions, which will be the main case of interest in the following, the boundary manifold (N^{n-1}, h_k) is two–dimensional and thus the Poincaré uniformization theorem applies. The Poincaré uniformization theorem, compare e.g. [60, Proposition 8.1], asserts that any compact, orientable Riemannian 2-manifold is conformal to either: the Riemann sphere, a flat torus or a compact higher-genus surface with constant curvature. Note that there exist an infinite number of distinct tori with conformal structure, each parametrized by a distinct complex number (the modular parameter). A similar statement holds true with regards to higher-genus surfaces with constant curvature metric.

In the following, we focus on space dimension $n \geq 3$. The Riemann tensor of the metric (4.1) reads [57]

$$\tilde{R}_{trtr} = \frac{f''}{2} \,, \quad \tilde{R}_{tAtB} = \frac{r}{2} f f' h_{AB} \,, \quad \tilde{R}_{rArB} = -\frac{r}{2}\frac{f'}{f} h_{AB} \,, \tag{4.4}$$

$$\tilde{R}_{ABCD} = r^2 R_{ABCD}(h) - r^2 f (h_{AC} h_{BD} - h_{AD} h_{BC}) \,. \tag{4.5}$$

For $m_c = 0$ this reduces to

$$\tilde{R}_{\mu\nu\rho\sigma} = -(g_{\mu\rho} g_{\nu\sigma} - g_{\mu\sigma} g_{\nu\rho}) \tag{4.6}$$

provided that the metric h_k fulfills that

$$R_{ABCD}(h) = k(h_{AC} h_{BD} - h_{AD} h_{BC}) \,. \tag{4.7}$$

[1] The Ricci tensor is proportional to the metric, with the proportionality factor being a constant.

The condition (4.7), that (N^{n-1}, h_k) be a constant curvature manifold, is automatically fulfilled for $n-1 \leq 3$. In generic dimensions $n-1 > 3$ Einstein spaces of non-constant curvature exist. The Kretschmann scalar of $\tilde{g}$

$$\begin{aligned} R_{\mu\nu\rho\sigma}R^{\mu\nu\rho\sigma} &= (f'')^2 + \frac{2(f')^2(n-1)}{r^2} + \frac{2f^2}{r^4}(n-1)(n-2) - \frac{4fR(h)}{r^4} \\ &\quad + \frac{R_{ABCD}(h)R^{ABCD}(h)}{r^4} \\ &= 2n(n+1) - \frac{2k^2(n-1)(n-2)}{r^4} + \frac{4m_c^2(n-2)(n-1)^2 n}{r^{2n}} \\ &\quad + \frac{R_{ABCD}(h)R^{ABCD}(h)}{r^4}\,. \end{aligned} \tag{4.8}$$

generically blows up at $r = 0$ for space dimension $n \geq 3$. If $m_c = 0$ and the boundary manifold is of constant curvature, then the Kretschmann scalar does not diverge at $r = 0$.

In the following, we restrict ourselves to $n = 3$, where the boundary manifold is two-dimensional and the spacetimes $(M, \tilde{g})$ with $m_c = 0$ are manifolds of constant curvature.

To discuss the causal structure of $\tilde{g}$, we use projection diagrams, which were introduced in this thesis in section 2.2. The map π from the definition of the projection diagram is given by $(t, r, \varphi) \mapsto (t, r)$ and maps $(M, \tilde{g})$ to a subset of $\mathbb{R}^{1,1}$ with metric

$$\gamma = -f dt^2 + f^{-1} dr^2\,. \tag{4.9}$$

The causal structure of the spacetime depends upon the zeros of the function $f(r)$ and the order of the zeros. A systematic study of conformal diagrams for two-dimensional metrics has been carried out by Walker [61], which was reviewed in [24]. In [61], one considers separately maximal intervals ("blocks") on which f is finite and does not change sign. These intervals define the ranges of r and lead to connected Lorentzian manifolds on which γ is defined everywhere. The conditions under which such manifolds can be patched together were discussed in [61]. Following [24, 61], we first bring the metric (4.9) into a manifestly conformally flat form by choosing a value r^* such that $f(r^*) \neq 0$ and introduce a new coordinate

$$x(r) = \int_{r^*}^{r} \frac{ds}{f(s)}\,, \tag{4.10}$$

which yields

$$\gamma = f(-dt^2 + dx^2)\,. \tag{4.11}$$

When $x(r)$ ranges over $\mathbb{R}$ on the block, we obtain that γ is conformal to a diamond. When $x(r)$ is only diverging at one end, we obtain that the metric within the block is conformal to a triangle. When $x(r)$ is finite at both ends, we obtain a strip. It was shown that [61] four blocks can be glued together across a boundary where

$$f(r_0) = 0\,, \qquad f'(r_0) \neq 0 \tag{4.12}$$

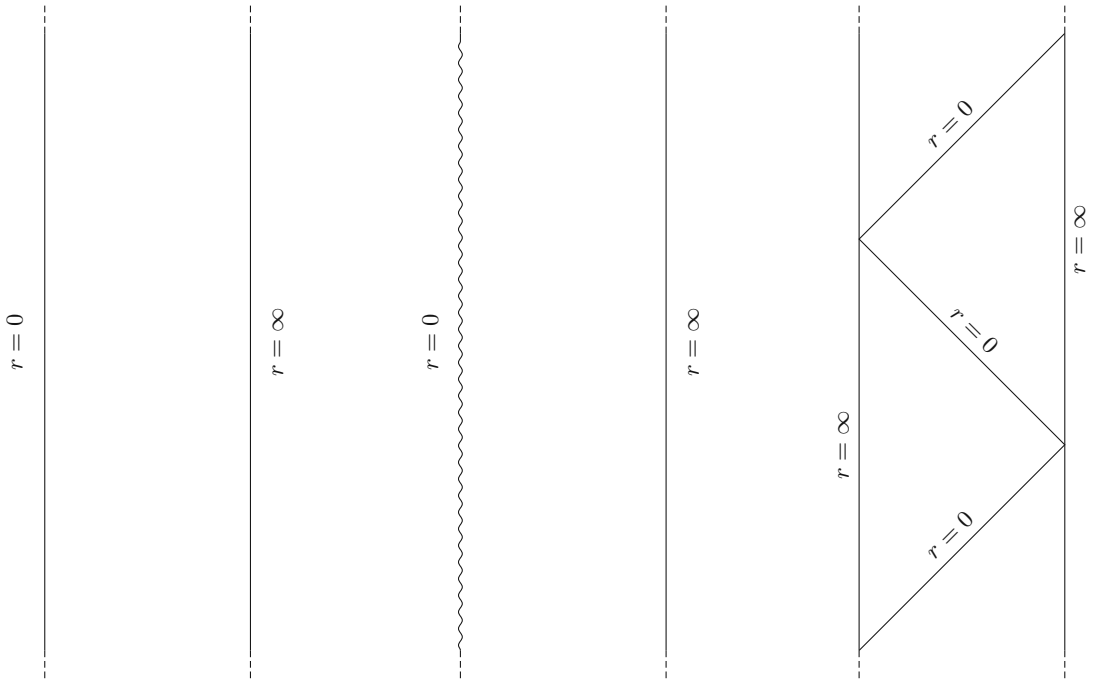

(a) no singularity **(b)** nakedly sing. **(c)** no singularity

Figure 4.1.: Projection diagrams of Birmingham–Kottler metrics when $f(r)$ has no zeros for $r > 0$. In all three cases the projection diagram is an infinitely long strip. In Figure 4.1a $r = 0$ corresponds to an axis of rotation, in Figure 4.1b $r = 0$ corresponds to a singularity. Figure 4.1c is an infinitely long strip with both sides of the strip corresponding to $r = \infty$ except for at the tip of the triangles.

such that the Kruskal extension so obtained is real analytic. As shown in [24], r is a real analytic function in terms of the Kruskal coordinates and therefore also the spacetime metric $\tilde{g}$ extends smoothly across $r = r_0$.

If the function $f(r)$ has a higher-order zero at $r = r_0$

$$f(r_0) = 0\,, \qquad f'(r_0) = 0\,, \tag{4.13}$$

one may only glue together two-blocks, as was shown in [61] by performing an Eddington-Finkelstein extension. Again, r is a real analytic function in terms of the Eddington-Finkelstein coordinates and therefore also the spacetime metric $\tilde{g}$ extends smoothly across $r = r_0$.

$k \in \{0, 1\}$

For $k \in \{0, 1\}$, we must differentiate between the cases $m_c > 0$, $m_c < 0$ and $m_c = 0$.

1. $m_c > 0$: The function $f(r)$ aquires a zero of first order at $r_0 > 0$. The function $x(r)$ diverges at $r = r_0$ and is finite at $r = \infty$ and $r = 0$. The blocks $0 < r < r_0$ and

$r_0 < r < \infty$ therefore both correspond to triangles. Gluing four blocks together across $r = r_0$ as described above, we obtain a causal diagram that looks the same as the causal diagram of the non-rotating BTZ black hole, Figure 3.8. The locus $r = 0$ corresponds to a singularity as the Kretschmann scalar of $\tilde{g}$ diverges there. Thus, in this regime, the metric $\tilde{g}$ describes a black hole.

2. $m_c = 0$: The metric $\tilde{g}$ is locally maximally symmetric and corresponds to global Anti-de Sitter spacetime ($k = 1$) or locally Anti-de Sitter spacetime with toroidal conformal infinity ($k = 0$). The geometry of constant time slices corresponds to global hyperbolic space ($k = 1$) or locally hyperbolic space ($k = 0$). For $k = 1$, the locus $r = 0$ corresponds to an axis of rotation and the causal diagram of γ is that of a strip, see Figure 4.1a. For $k = 0$, the function $f(r)$ has a zero of second order at $r = 0$. The function $x(r)$ diverges at $r = 0$ but stays finite as r tends to infinity such that the block $0 < r < \infty$ corresponds to a triangle. By gluing triangles together we obtain the diagram of an infinitely long strip with both sides of the strip being given by $r = \infty$ except for at the tips of the triangles, see Figure 4.1c.

3. $m_c < 0$: For $m_c < 0$, the function $f(r)$ has no zeros at positive values of r and the metric $\tilde{g}$ is nakedly singular, as the singularity at $r = 0$ is not shielded by a horizon. The function $x(r)$ is finite at both ends such that we obtain an infinitely long strip as the projection diagram, see Figure 4.1b.

$k = -1$

For $k = -1$ we must discriminate between five cases, which are seperated in the parameter space by the loci $m_c = \pm m_c^{\text{crit}} = \pm 1/(3\sqrt{3})$.

1. $m_c < -m_c^{\text{crit}}$: The function $f(r)$ does not possess zeros for positive values of r. The spacetime is nakedly singular, as the curvature singularity at $r = 0$ is unshielded. Since the function $x(r)$ is finite at $r = 0$ and $r = \infty$, the projection diagram is given by an infinitely long strip, see Figure 4.1b.

2. $m_c = -m_c^{\text{crit}}$: The function $f(r)$ aquires a zero of second order at $r = r_0$. The function $f(r)$ is finite at $r = 0$ and $r = \infty$. The block $r_0 < r < \infty$ and the block $0 < r < r_0$ are therefore both conformal to triangles. The maximal causal extension is obtained by gluing an infinite sequence of these triangles across their boundaries $r = r_0$, thereby obtaining a causal diagram which coincides with the one of the extremal BTZ black hole, Figure 3.10a. The spacetime $\tilde{g}$ describes a non-rotating black hole.

3. $-m_c^{\text{crit}} < m_c < 0$: The function $f(r)$ has two distinct zeros of first order for $r > 0$, $r = r_+$ and $r = r_-$. The function $x(r)$ stays finite at $r = 0$ and $r = \infty$. The metric γ is therefore conformal to a triangle in the region $0 < r < r_-$ and in the region $r_+ < r < \infty$. In the region $r_- < r < r_+$ the metric is conformal to a diamond. Gluing the patches together through a four block gluing, we obtain a causal diagram

which looks the same as the one of the rotating, non-extremal BTZ black hole, see Figure 3.7. The spacetime $\tilde{g}$ describes a non-rotating black hole.

4. $m_c = 0$: The metric is locally AdS spacetime and the geometry of constant time slices is locally hyperbolic space. The function $f(r)$ has a first order zero at $r_0 = 1$. The locus $r = 0$ is regular and corresponds to an axis of rotation. The function $x(r)$ is finite at $r = 0$ and $r = \infty$. The blocks $0 < r < r_0$ and $r_0 < r < \infty$ therefore both corresponds to triangles. We obtain a diagram which looks similar to the non-extremal, non-rotating BTZ black hole (compare with Figure 3.8), only that in this case $r = 0$ corresponds to a center of (local) rotational symmetry.

5. $m_c > 0$: The function $f(r)$ has a first order zero at $r = r_0 > 0$, $x(\infty)$ and $x(0)$ are both finite. The case is analogous to the previous case $m_c = 0$ with the difference that $r = 0$ now corresponds to a curvature singularity. The metric describes a black hole spacetime with causal diagram given by Figure 3.8.

4.1.2. Horowitz–Myers metrics

The Horowitz–Myers metrics [20] are vacuum solutions to general relativity with negative cosmological constant. The spacetime manifolds underlying the Horowitz–Myers metrics have topology $\mathbb{R} \times \mathbb{R}^2 \times \mathbb{T}^{n-2}$, where $\mathbb{T}^{n-2}$ denotes a $(n-2)$-dimensional torus. The conformal boundary at infinity is diffeomorphic to $\mathbb{R} \times S^1 \times \mathbb{T}^{n-2} = \mathbb{R} \times \mathbb{T}^{n-1}$.

In $n+1$ dimensions the Horowitz–Myers metrics read

$$\tilde{g} = -r^2 dt^2 + \frac{dr^2}{f(r)} + f(r) d\psi^2 + r^2 h_{IJ} d\theta^I d\theta^J \tag{4.14}$$

with

$$f(r) = r^2 - \frac{2m_c}{r^{n-2}} \tag{4.15}$$

and where $h_{IJ} d\theta^I \theta^J$, $I, J \in \{1, \dots n-2\}$ is a flat metric on $\mathbb{T}^{n-2}$. In the following, we will be interested in the case $m_c > 0$, for which the function $F(r)$ has zeros located at

$$r_0^n = 2m_c \,, \tag{4.16}$$

which corresponds to an axis of rotation. To guarantee smoothness at $r = r_0$ the period of the coordinate ψ has to be chosen appropriately. When $m_c > 0$, the coordinate ψ is redefined as

$$\psi = \frac{2}{f'(r_0)} \phi = \lambda^{-1} \phi \,, \tag{4.17}$$

where

$$\lambda = \frac{n r_0}{2} \tag{4.18}$$

and where ϕ has to be 2π periodic. To see why this is the case, we define a new coordinate ρ as

$$\rho = \int \frac{dr}{\sqrt{f(r)}} = \sqrt{r - r_0} \left(\frac{2}{\sqrt{f'(r_0)}} + O(r - r_0) \right) \tag{4.19}$$

such that

$$\begin{aligned}\frac{dr^2}{f(r)}+f(r)d\psi^2 &= d\rho^2+(\frac{1}{4}f'(r_0)^2\rho^2+O(\rho^4))d\psi^2\\ &= d\rho^2+(\rho^2+O(\rho^4))d\phi^2\,.\end{aligned}\tag{4.20}$$

The Horowitz–Myers spacetime thus has the curious property that the conformal structure of the boundary manifold depends upon the coordinate mass parameter m_c, provided we keep $h_{IJ}d\theta^I d\theta^J$ fixed (recall that ψ is one of the coordinates parametrizing the boundary manifold which at fixed time is given by $\mathbb{T}^{n-2}$). A conformal completion of the Horowitz–Myers metric is obtained by introducing a new coordinate $x=1/r$ such that (4.14) becomes

$$\tilde{g}=x^{-2}\Big(-dt^2+dx^2(1+O(x^n))+(1+O(x^n))d\psi^2+h_{IJ}dx^I dx^J\Big)\,,\tag{4.21}$$

where $x\in(0,x_0]$, where $x_0^n=1/(2m_c)$. A fixed ψ,x^I slice corresponds to an infinitely long strip.

For positive coordinate mass parameter m_c, the energy of spacetime is in fact negative as the mass is proportional to $-m_c$. We will calculate the mass in section 4.6, where we give a precise definition of the energy used in this context. Horowitz and Myers claimed that the metric (4.14) minimizes the mass amongst the class of metrics with the same conformal structure at infinity. This statement was refined in [62] and is a subject of current research, see e.g. [56]. We discuss the Horowitz–Myers conjecture in more detail in section 4.2.

Lastly, we comment on $m_c\leq 0$. When $m_c=0$, $\tilde{g}$ is locally AdS and smooth at $r=0$, independently of the period of ψ. When $m_c<0$, $\tilde{g}$ is nakedly singular as the function $f(r)$ does not possess any zeros at $r>0$ and the Kretschmann scalar

$$\begin{aligned}R_{\mu\nu\rho\sigma}R^{\mu\nu\rho\sigma} &= (f'')^2+\frac{2(f')^2(n-1)}{r^2}+\frac{2f^2(n-1)(n-2)}{r^4}\\ &= 2n(n+1)+\frac{4m_c(n-2)(n-1)^2n}{r^{2n}}\end{aligned}\tag{4.22}$$

diverges at $r=0$ unless $n=2$ — this special case is discussed below. Note that when $m_c>0$, the locus $r=0$ is not part of spacetime, as the manifold smoothly caps off at the axis of rotation.

In the following sections, the Horowitz–Myers metric will feature prominently. When we say Horowitz–Myers metric or Horowitz–Myers instanton, we always refer to (4.14) with $m_c>0$.

$n=2$

Consider the Horowitz–Myers metric with $n=2$,

$$\tilde{g}=-r^2dt^2+\frac{dr^2}{r^2-2m_c}+(r^2-2m_c)d\psi^2\,.\tag{4.23}$$

When $m_c > 0$, regularity at the rotation axis requires that ψ is periodic with period $2\pi/\sqrt{2m_c}$, while for $m_c \leq 0$ any period of ψ is allowed. We now consider the case where $m_c > 0$. Setting

$$\rho^2 = r^2 - 2m_c \tag{4.24}$$

one finds

$$\tilde{g} = -(\rho^2 + 2m_c)dt^2 + \frac{d\rho^2}{\rho^2 + 2m_c} + \rho^2 d\psi^2\,, \tag{4.25}$$

which would be a BK metric with mass $-m_c$ if the period of ψ were 2π. To correct for this it suffices now to set

$$\bar{\psi} = \lambda\psi\,, \quad \bar{t} = \lambda t\,, \quad \bar{\rho} = \lambda^{-1}\rho\,, \tag{4.26}$$

with $\lambda = \sqrt{2m_c}$ chosen so that (4.23) is regular at $r = \sqrt{2m_c}$ and that the period of $\bar{\psi}$ is 2π, leading to

$$\tilde{g} = -(\bar{\rho}^2 + 2\bar{m}_c)d\bar{t}^2 + \frac{d\bar{\rho}^2}{\bar{\rho}^2 + 2\bar{m}_c} + \bar{\rho}^2 d\bar{\psi}^2 = -(\bar{\rho}^2 + 1)d\bar{t}^2 + \frac{d\bar{\rho}^2}{\bar{\rho}^2 + 1} + \bar{\rho}^2 d\bar{\psi}^2\,, \tag{4.27}$$

which is AdS_3 spacetime.

4.2. Positivity of Mass and the AdS/CFT Correspondence

This section reviews and motivates why the positivity of the mass for general relativity with negative cosmological constant is an interesting open question. The precise definitions of the mass and fall-off conditions used in this context will not be given here, but we postpone these definitions to subsection 4.6.1 where we also calculate the mass of the Horowitz–Myers and Birmingham–Kottler metrics.

Positive energy theorems are widely regarded as one of the most powerful achievements in mathematical general relativity [70] and have found many applications to this date. In particular, they have been used in proofs of uniqueness of asymptotically flat black holes [71, 72] or to resolve the Yamabe problem [73], the latter will also be of relevance in the following sections of this thesis. The Yamabe problem was first posed in 1960 by Hidehiko Yamabe who asked whether, given a metric g on a manifold M, there exists a metric $\tilde{g}$ conformal to g which has constant scalar curvature. Yamabe claimed to have found a proof when M is compact. However, Yamabe's proof was later found to be erroneous and it took two decades until the proof was finally completed by Richard Schoen after the combined efforts of Yamabe, Trudinger and Aubin. Unexpectedly, a key point in Schoen's proof was the application of the positive mass theorem of general relativity which back in the 1980s had only recently been proven by Schoen and Yau [74]. When M is non-compact, the Yamabe problem is much more subtle and much of current research focuses on determining which conformal classes contain metrics of constant scalar curvature. The relevant equation to consider in the context of the Yamabe problem is the transformation behavior of the Ricci scalar under conformal transformations (2.4). In the following sections, the Yamabe problem for two-dimensional manifolds will be

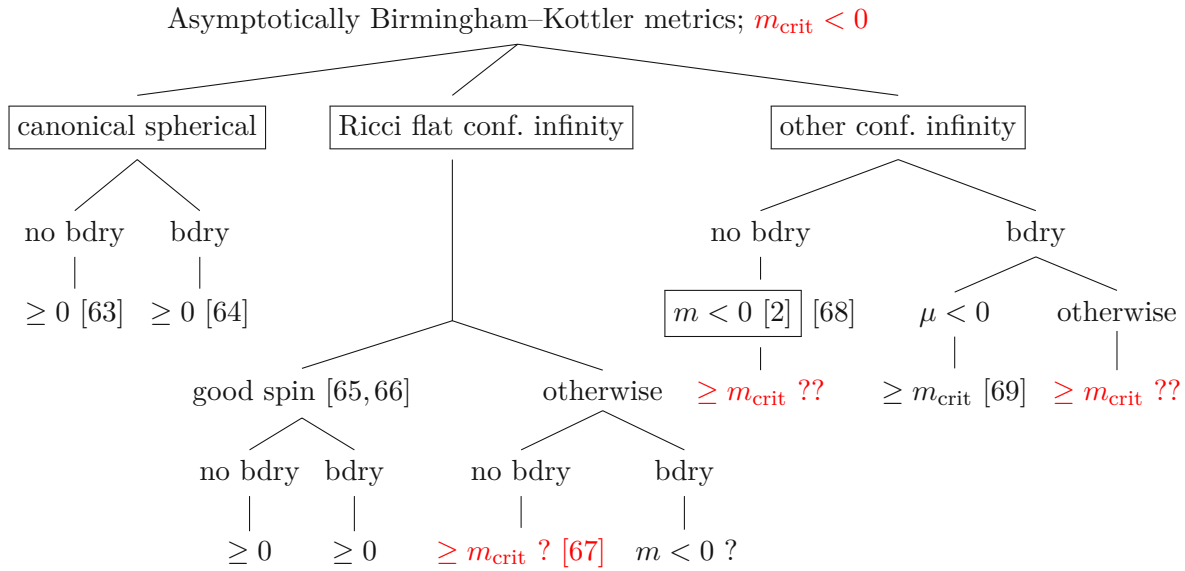

Table 4.1.: Mass inequalities for asymptotically Birmingham–Kottler metrics. The mass is normalized in such a way, that the Birmingham–Kottler metric with coordinate mass parameter $m_c = 0$ which lies in the appropriate conformal class at infinity has mass zero, $m = 0$. A double question mark indicates that no results are available; a single one indicates the existence of partial results. The shorthand "bdry" refers to a black-hole boundary. "Good spin" denotes a topology where the manifold is spin *and* the spin structure admits asymptotic Killing spinors. The case "other conformal infinity" includes higher genus topologies when the boundary is two-dimensional, but also e.g. quotients of spheres in higher dimensions. Reference [2] is the publication I co-authored together with Piotr Chruściel and Erwann Delay. The case [67] corresponds to the Horowitz–Myers conjecture. Finally, μ is the mass aspect function which is defined in subsection 4.6.1. The critical value of the mass m_{crit}, assuming it exists, is expected to be determined by the conformal structure of the boundary at infinity.

of importance. In two dimensions and with $\tilde{g} = e^f g$, where f is a smooth real-valued function, equation (2.4) reads

$$\tilde{R} = e^{-f}(R - \Delta_g f)\,. \tag{4.28}$$

When $\tilde{R}$ is a constant this is the Yamabe equation. The example of the Yamabe problem goes to show that positive energy theorems have wide-ranging applicability that go even beyond the scope of general relativity.

To this date, the question of positivity of mass has been predominantly considered in the context of asymptotically flat spacetimes where the metric (locally) approaches the Minkowski metric at large distances. When the cosmological constant is negative, some progress has been made, but the problem is essentially wide open. In the Lorentzian setting, we would like to answer whether the energy of spacetimes, which locally approach AdS, is bounded from below. As these spacetimes are the main object of study within the AdS/CFT correspondence, it is clear that bounds on the energy for such spaces could have potential implications for the correspondence. Boundedness of energy for

negative cosmological constant is often required within the framework of the AdS/CFT correspondence. In the derivation of the Cardy formula, which was shortly discussed in section 3.6 and most generalizations thereof, it is assumed that the energy spectrum of the conformal field theory is bounded from below — which in turn implies that also the energy in asymptotically AdS spacetimes must be bounded from below. Hence, for the Cardy formula to apply, a positive energy theorem in general relativity for negative cosmological constant must hold. On the one hand, positive energy theorems in general relativity for negative cosmological constant can be used to restrict the energy spectrum in a conformal field theory and make predictions regarding aspects of the AdS/CFT correspondence. On the other hand, the duality may be used to form conjectures regarding the boundedness of energy in general relativity. One example of this is the Horowitz–Myers conjecture [20] which has received much attention over the last twenty years, both in the AdS/CFT, as well as in the mathematical general relativity community. Horowitz and Myers studied the consequences of a potential non-supersymmetric AdS/CFT correspondence in five spacetime dimensions, under the assumption that such a correspondence exists. They considered a novel solution to the vacuum Einstein equations with negative cosmological constant, which they referred to as the AdS soliton and which we refer to as the Horowitz–Myers metric or Horowitz–Myers instanton.[2] The geometric properties of this solution have been discussed in subsection 4.1.2 and we discuss a precise definition of the mass of Horowitz–Myers metrics in section 4.6. Horowitz and Myers computed the mass of their new solution and found that it is negative in comparison to the mass of locally AdS spacetimes with the same toroidal conformal infinity.

In their paper [20], Horowitz and Myers estimated the ground state Casimir energy of a conformal field theory and compared it to the energy of the Horowitz–Myers metric. They found that these values indeed matched up to a factor of 3/4 which was not unexpected due to the estimation method used for the calculation of the ground state [62]. Due to the fact that the Casimir energy is the ground state energy in the conformal field theory, they asserted that a new positive energy conjecture in general relativity must hold. In the original paper this conjecture reads [20, Conjecture 2]

Conjecture 4.1. ***Horowitz–Myers Conjecture*** *Consider all solutions to Einstein's equations in five spacetime dimensions with cosmological constant* $\Lambda = -6$ *which satisfy*

$$g_{\mu\nu} = \bar{g}_{\mu\nu} + h_{\mu\nu} \tag{4.29}$$

with

$$h_{\alpha\gamma} = \mathcal{O}(r^{-4}), \quad h_{\alpha r} = \mathcal{O}(r^{-4}), \quad h_{rr} = \mathcal{O}(r^{-6}) \quad \text{with}\, \alpha, \gamma \neq r \tag{4.30}$$

and where $\bar{g}_{\mu\nu}$ *denotes the Horowitz–Myers metric in five spacetime dimensions in coordinates* (4.14)*. Then, the mass* $m \geq 0$ *with equality if and only if* $g_{\mu\nu} = \bar{g}_{\mu\nu}$*.*

While the original conjecture was formulated in five spacetime dimensions, the conjecture can be posed in any spacetime dimension $d = n + 1 \geq 4$ and this was in fact done in [75]. The conjecture has been formulated in Riemannian terms by Woolgar

[2] In literature this metric is also often referred to as Horowitz–Myers geon [62].

in [62, Conjecture 1.1]. It is this version of the conjecture that is mostly used throughout the mathematical general relativity literature because the methods for proofing positivity of mass have been predominantly developed in the Riemannian setting. We now give the conjecture in the form stated in [62] using the terminology of [2]

Conjecture 4.2. *Let (M, g) be an n-dimensional complete asymptotically locally hyperbolic manifold with flat toroidal infinity, with compact, totally geodesic, possibly empty boundary, with well defined mass m and with scalar curvature satisfying $R \geq -n(n-1)$. Then the mass m of (M, g) obeys $m \geq m_0$ where m_0 is the mass of the Horowitz–Myers metric which has the least mass amongst all Horowitz–Myers metrics with the same conformal boundary at infinity.*

Some comments regarding the conjecture are in order: We say that (M, g) is *asymptotically locally hyperbolic (ALH)* if the Ricci scalar of g approaches a negative constant when the conformal boundary at infinity is approached. The precise falloff conditions used in this context will be specified in section 4.6, where we will also give a definition of the mass. There is a countable infinity of non-isometric Horowitz–Myers metrics that share the same conformal boundary at infinity [62, 76, 77]. The Horowitz–Myers metric with the lowest mass m_0 is chosen in such a way that the shortest non-trivial cycle on the boundary at infinity bounds a disk in the bulk [62]. In the original conjecture, there is no mention of inner boundaries, but in [62] they are included to allow for horizons. With regards to initial data, it is natural to regard a black hole horizon as a boundary, as initial data is only prescribed outside of the horizon. We will take this viewpoint in this work. In the following, we will also often use the terminology black hole boundary for this locus.

While some evidence in favor of the Horowitz–Myers conjecture exists, the conjecture remains unproven to this day. The difficulty stems from the fact that many methods which are typically used in positive mass theorems cannot be applied in this case. In particular, spinorial methods cannot be applied as the Horowitz–Myers metric does not admit the right spin structure. Other standard methods fail as well, as they often rely implicitly on comparisons with the potential minimal energy metric. These comparisons work well when this metric is of constant curvature, but this is not the case for the Horowitz–Myers metric [62].

Before closing this section, we shortly review the currently known energy bounds for general relativity with negative cosmological constant. To compute the mass, one typically considers spaces that asymptote to the Birmingham–Kottler metrics with $m_c = 0$.

In the case of space dimension $n = 3$, which we consider in the following sections, requiring that a metric be asymptotically Birmingham Kottler is equivalent to requiring that it be asymptotically locally hyperbolic. As discussed in subsection 4.1.1, there is a variety of asymptotically Birmingham–Kottler metrics, which differ by the existence of black hole boundaries or the lack thereof and by the topology of the boundary at infinity (N, h_k). The current knowledge of bounds on the energy for such metrics is summarized in table 4.1. The theorems available in literature, typically distinguish between the case where there exists an interior boundary and the case where no interior boundary exists. In the case of a spherical boundary at infinity, it has been shown that

the energy is bounded from below [63, 64] and that the energy only vanishes when (M, g) is isometrically diffeomorphic to hyperbolic space. Note that while there exists a notion of mass for general asymptotically locally hyperbolic metrics which admit asymptotic static potentials [78], nothing is known about the sign of the mass for those which are not asymptotically Birmingham–Kottler. See also [79] for a discussion of the issues occurring in this context.

In the following sections, we discuss the explicit construction of three-dimensional conformally compact asymptotically locally hyperbolic manifolds without boundary, with connected conformal infinity of higher genus, with constant negative scalar curvature and with negative mass [2]. Such spaces were previously not known to exist. In four space dimensions negative-mass asymptotically locally hyperbolic metrics were found in [68, 80] (compare [81, 82]), where conformal infinity is a quotient of a sphere.

4.3. Introduction to the Problem

The following sections are from [2] with minor modifications (co-authored with Piotr Chruściel and Erwann Delay)

In [83] Isenberg, Lee and Stavrov, inspired by [84], have shown how to glue together two ALH general relativistic initial data sets by performing a boundary connected sum, which they referred to as a "Maskit gluing". The resulting initial data set has a conformal boundary at infinity which is a connected sum of the original ones. A variation of this construction has been presented in [23]. It is of interest to analyze the properties of the initial data sets so obtained. This work aims to address this question in the time-symmetric case, with vanishing extrinsic curvature tensor K_{ij}.

We start with a short presentation of the boundary-gluing construction of [23] in section 4.4. The construction involves a certain amount of freedom which we make precise, showing that the gluing results in whole families of new ALH metrics. As a particular case, in section 4.5 we apply the construction to Birmingham–Kottler metrics. This provides new families of ALH metrics with apparent-horizon boundaries with more than one component, and with locally explicit metric when the mass parameter is zero. One thus obtains time-symmetric vacuum initial data for spacetimes containing several apparent horizons; such initial data sets evolve to spacetimes with multiple black holes.

Next, an important global invariant of asymptotically hyperbolic general relativistic initial data sets is the total energy-momentum vector $\mathbf{m} \equiv (m_\mu)$ [65, 66, 85] (compare [78, 86, 87]) when the conformal metric at infinity is that of the round sphere (we talk of *AH metrics* then), and the total mass m for the remaining topologies at infinity; this is reviewed in subsection 4.6. It turns out that the formulae for the mass after the gluings of both [83] and [23] are relatively simple. This is analyzed in Section 4.6.4, where we derive formulae (4.80)-(4.83). This is the first main result of the paper [2].

A quick glance at (4.81) suggests very strongly that the boundary-gluing of two

Horowitz–Myers metrics, which both have negative mass aspect functions, will lead to a manifold with higher-genus boundary at infinity and with *negative mass*. This turns out, however, to be subtle because of correction terms that are inherent to the constructions. In fact, negativity of the total mass is far from clear for the Isenberg-Lee-Stavrov gluings, because these authors use the conformal method, which changes the mass integrand in a way that appears difficult to control in the neck region. Things are clearer when the localized boundary-gluing of [23] is used, and in section 4.7 we show that negativity indeed holds. We thus construct *three-dimensional conformally compactifiable ALH manifolds with constant scalar curvature, without boundaries at finite distance, with connected boundary at infinity of higher genus topology and with negative mass.* This is the second main result of this paper. As already hinted to, such manifolds correspond to time-symmetric initial data surfaces in vacuum spacetimes with negative cosmological constant. Here one should keep in mind that the Horowitz–Myers metrics have toroidal topology at infinity, and that the higher-genus Birmingham–Kottler metrics with negative mass are either nakedly singular, or have a totally geodesic boundary with the same genus as the boundary at infinity, or acquire a conformal boundary at infinity with two components, and contain an apparent horizon, after a doubling across the boundary.

4.4. Localized boundary-gluing of ALH metrics

Before entering the subject, some comments on our terminology are in order. We say that an ALH manifold is *asymptotically hyperbolic* (AH) if the conformal class of $\bar{g} = \Omega^2 g$ on the conformal boundary at infinity is that of a round sphere. *Asymptotically Birmingham–Kottler (ABK) metrics* are defined as metrics that asymptote to the Birmingham–Kottler metrics. The Birmingham–Kottler metrics themselves are ALH, which can be seen by setting $\Omega = 1/r$ in (4.34), and noting that they have constant scalar curvature since they solve the time-symmetric general relativistic scalar constraint equation with negative cosmological constant.

Differentiability requirements of $\bar{g}$ at the conformal boundary at infinity often need to be added in the definitions above and depend upon the problem at hand. Here we will be interested in a class of manifolds with well-defined mass, as will be made precise in subsection 4.6.1.

An ABK metric can equivalently be defined as an ALH metric such that the conformal class of its conformal metric at infinity contains an Einstein metric. Note that this is always the case for three-dimensional manifolds, hence two-dimensional conformal boundaries, by the uniformization theorem; thus ALH metrics are necessarily ABK in three dimensions, but this is not the case anymore in higher dimensions. For ABK metrics we can introduce Fefferman-Graham coordinates based on the Einstein representative of the conformal metric at infinity. In these coordinates, the asymptotic expansion of g will coincide with that of a BK metric, say b, written in the same coordinate system, up to some order. This decay order can be measured using b-orthonormal frames; equivalently, by measuring the decay of the b-norm of $g - b$; the g-norm of $g - b$ would give an

equivalent result too. The mass integrals of section 4.6.1 are well defined and convergent if the decay of $g - b$ so understood is, roughly speaking, $o(r^{-n/2})$, where r is the radial coordinate in (4.34).

The reader is warned that there is no consistency in the literature concerning terminology. While our definition of ALH coincides with that of several authors, some other authors use AH for what we call ALH here. However, we find it natural to reserve the name AH for the special case where the metric is asymptotic to that of hyperbolic space.

Our analysis below is motivated by the localized boundary-gluings of ALH manifolds, or initial data sets, as in [23, Section 3.5]. In this section, we present a somewhat more general version of these gluings.

We start with points p_1, p_2, lying on the conformal boundary of two ALH vacuum initial data sets (M_1, g_1, K_1) and (M_2, g_2, K_2). (An identical construction applies when p_1 and p_2 belong to the same manifold; then the construction provides instead a handle connecting a neighborhood of p_1 with a neighborhood of p_2. Instead of vacuum initial data one can also take e.g. data satisfying the dominant energy condition; the construction will preserve this. Further, if $K_1 \equiv 0 \equiv K_2$, then one can have $K \equiv 0$ throughout the construction.) We assume that both (M_1, g_1, K_1) and (M_2, g_2, K_2) have extrinsic curvature tensors asymptoting to zero, and have well-defined total energy-momentum, cf. section 4.6. As shown in [23] for deformations of data sets preserving the vacuum condition or for scalar curvature deformations preserving an inequality, or in [63, Appendix A] for deformations of data sets preserving the dominant energy condition, for all $\varepsilon > 0$ sufficiently small we can construct new initial data sets $(M_i, g_{i,\varepsilon}, K_{i,\varepsilon})$, $i = 1, 2$, such that the metrics coincide with the hyperbolic metric in coordinate half-balls $\mathscr{U}_{1,\varepsilon}$ of radius ε around p_1 and $\mathscr{U}_{2,\varepsilon}$ around p_2, and the $K_{i,\varepsilon}$'s are zero there. Here the coordinate half-balls refer to coordinates on the upper half-space model of hyperbolic space $\mathcal{H}^n$, in which we have

$$\mathcal{H}^n = \mathbb{R}^n_+ = \{x = (\omega, z) \in \mathbb{R}^{n-1} \times]0, \infty[\} \,, \tag{4.31}$$

with the metric

$$b = \frac{|d\omega|^2 + dz^2}{z^2} \,. \tag{4.32}$$

In order to avoid a proliferation of indices we now choose ε so that the deformation described above has been carried out, with corresponding ALH metrics $(M_i, g_{i,\varepsilon}, K_{i,\varepsilon})$, $i = 1, 2$, and coordinate half-balls $\mathscr{U}_{i,\varepsilon}$, which we write from now on as (M_i, g_i, K_i), and $\mathscr{U}_i$. It should be kept in mind that different values of ε lead to different initial data sets near the gluing region, but the data sets remain the original ones, hence identical, away from the gluing region, which can be chosen as small as desired.

The above shows in which sense the exterior curvature tensor K is irrelevant to the problem at hand. Therefore, from now on, we will only consider initial data sets with $K \equiv 0$ in the gluing region.

The gluing construction uses *hyperbolic hyperplanes* $\mathfrak{h}$ in the hyperbolic-space region of (M_i, g_i). These are defined, in the half-space model, as half-spheres with centers on the hyperplane $\{z = 0\}$ in the coordinates of (4.32) which, for our purposes, are entirely contained in the half-balls $\mathscr{U}_i$. The conditionally compact, in $\mathbb{R}^n$, component of $\mathcal{H}^n$

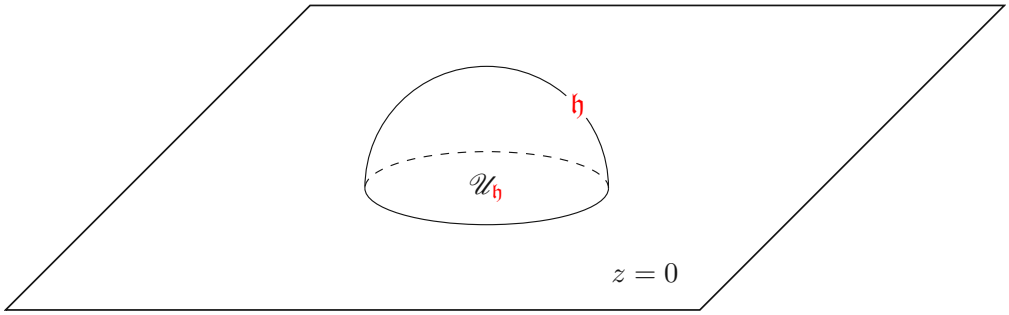

Figure 4.2.: The "thin component" $\mathscr{U}_{\mathfrak{h}}$ and its boundary $\mathfrak{h}$ in the half-space model, where hyperbolic space is represented as a half-space $\{z > 0\}$, and the conformal boundary at infinity is the hyperplane $\{z = 0\}$. After an "exotic gluing" has been performed, the metric becomes exactly hyperbolic inside $\mathscr{U}_{\mathfrak{h}}$.

separated by $\mathfrak{h}$ will be referred to as the *thin component*, denoted by $\mathscr{U}_{\mathfrak{h}}$, and the remaining one will be called the *fat component*; see Figure 4.2.

In what follows we will also invoke the *Poincaré ball* model, which represents the n-dimensional hyperbolic space $\mathcal{H}^n$ as the open unit ball B^n endowed with the metric

$$b = \frac{4}{(1 - |\vec{x}|^2)^2}\delta\,, \tag{4.33}$$

where δ is the Euclidean metric.

A basic fact is that for every hyperbolic hyperplane $\mathfrak{h}$ as above there exist two isometries of the hyperbolic space, which we denote by $\Lambda_{\mathfrak{h},\pm}$, such that $\Lambda_{\mathfrak{h},+}$ maps $\mathfrak{h}$ to the equatorial hyperplane of the Poincaré ball, with the fat region being mapped to the upper hemisphere, while $\Lambda_{\mathfrak{h},-}$ again maps the hyperbolic hyperplane to the equatorial hyperplane but it maps the fat region into the lower hemisphere. Using physics terminology, an example of $\Lambda_{\mathfrak{h},+}$ is provided by a boost along the axis passing through the origin of the Poincaré ball and the barycenter of the hyperbolic hyperplane. Given $\Lambda_{\mathfrak{h},+}$, a map $\Lambda_{\mathfrak{h},-}$ can be obtained by applying to $\Lambda_{\mathfrak{h},+}$ a rotation by π around any axis lying on the equatorial plane.

It should be clear that there are many such pairs $\Lambda_{\mathfrak{h},\pm}$: consider, e.g., the isometries $R_\pm\Lambda_{\mathfrak{h},\pm}$, where the $R_\pm$'s are some rotations along the axis joining the north pole and the south pole.

Let $\mathscr{P}$ denote the collection of pairs of isometries (Λ_1, Λ_2) of hyperbolic space with the following property: There exist hyperbolic hyperplanes $\mathfrak{h}_i \subset \mathring{\mathscr{U}}_i$, $i = 1, 2$, such that Λ_1 is a $\Lambda_{\mathfrak{h}_1,+}$ and Λ_2 is a $\Lambda_{\mathfrak{h}_2,-}$. Here $\mathring{\mathscr{U}}_i$ denotes the interior of $\mathscr{U}_i$.

For each such pair of hyperbolic hyperplanes $\mathfrak{h}_i$ the manifolds $M_i \setminus \mathscr{U}_{\mathfrak{h}_i}$ are manifolds with a non-compact boundary component $\partial\mathscr{U}_{\mathfrak{h}_i} = \mathfrak{h}_i$ extending to the conformal boundary at infinity of M_i, with the hyperbolic metric near the boundary $\mathfrak{h}_i$.

Given $(\Lambda_1, \Lambda_2) \in \mathscr{P}$ we construct a boundary-glued manifold M_{Λ_1,Λ_2} by gluing the boundaries $\mathfrak{h}_i$ as follows: We map the thin complement $\mathscr{U}_{\mathfrak{h}_1}$ of $\mathfrak{h}_1$ to the lower half of the Poincaré ball using Λ_1. We map the thin complement $\mathscr{U}_{\mathfrak{h}_2}$ of $\mathfrak{h}_2$ to the upper half of

the Poincaré ball using Λ_2. We then identify the two manifolds with boundary $M_i \setminus \mathscr{U}_{\mathfrak{h}_i}$ along the equatorial plane of the Poincaré ball using the identity map.

The metrics on $M_i \setminus \mathscr{U}_{\mathfrak{h}_i}$ coincide with the original ones (one can think of the maps $\Lambda_{\mathfrak{h}_i}$ as changes of coordinates), hence are ALH there by hypothesis. Both metrics are exactly hyperbolic at both sides of the gluing boundary, namely the equatorial plane of the Poincaré ball, and extend smoothly there. Hence for every pair $(\Lambda_1, \Lambda_2) \in \mathscr{P}$ the manifold M_{Λ_1,Λ_2} is a smooth ALH manifold.

4.5. Boundary-gluing of Birmingham–Kottler solutions

An obvious candidate to which our construction can be applied is the space-part of the Birmingham–Kottler (BK) metrics, introduced in subsection 4.1.1. The line element of the Birmingham–Kottler metrics induced at constant time slices reads

$$g = f^{-1}dr^2 + r^2 h_k\,, \qquad f = r^2 + k - \frac{2m_c}{r^{n-2}}\,, \tag{4.34}$$

where m_c is a constant which will be referred to as the *coordinate mass parameter*, and where h_k is an Einstein metric on an $(n-1)$-dimensional manifold N^{n-1} with scalar curvature equal to

$$R(h_k) = k(n-1)(n-2)\,, \qquad k \in \{0, \pm 1\}\,. \tag{4.35}$$

We will assume that m_c is in a range so that f has positive zeros, with the largest one, denoted by r_0, of first order. The metric is then smooth on the product manifold $[r_0, \infty) \times N^{n-1}$, with a totally geodesic boundary at $r = r_0$.

The construction of section 4.4 applied to two such manifolds,

$$(M_i = [r_i, \infty) \times N_i^{n-1}, g_i)\,, \tag{4.36}$$

leads to manifolds with a conformal boundary at infinity with connected-sum topology $N_1^{n-1} \# N_2^{n-1}$ and a totally geodesic boundary that has two connected components, one diffeomorphic to N_1^{n-1} and the second to N_2^{n-1}.

One can double each of the original manifolds across their totally geodesic boundaries, in which case the doubled manifolds have no boundaries but each has a conformal infinity with two components.

One can iterate the construction, obtaining ALH manifolds with an arbitrary number of components of the boundary at infinity, and an arbitrary number of totally geodesic compact boundary components. The maximal globally hyperbolic development of the resulting time-symmetric general relativistic vacuum Cauchy data will have a Killing vector field defined in a neighborhood of each such boundary (but not globally in general), which becomes the bifurcation surface of a bifurcate Killing horizon for this vector field. The case $m_c = 0$ is of special interest here, as then the metric is exactly hyperbolic, locally, everywhere, so that the construction of [88] which glues in a hyperbolic half-ball

is trivial. All the boundary gluing constructions described here apply without further due to this case. Some of the metrics constructed above likely evolve to the spacetimes considered in [89, 90], so it might be of some interest to explore this.

4.6. Hyperbolic mass

4.6.1. The definition

We recall the definition of hyperbolic mass from [66]. We consider a family of Riemannian metrics g which approach a "background metric" b with constant scalar curvature $-n(n-1)$ as the conformal boundary at infinity is approached. We assume that b is equipped with a non-empty set of solutions of the *static Killing Initial Data (KID)* equations, introduced in this thesis in section 2.3:

$$\mathring{\Delta} V - nV = 0\,, \tag{4.37}$$

$$\mathring{D}_i \mathring{D}_j V = V(\mathring{R}_{ij} + n b_{ij})\,, \tag{4.38}$$

where $\mathring{R}_{ij}$ denotes the Ricci tensor of the metric b, $\mathring{D}$ the Levi-Civita connection of b, the operator $\mathring{\Delta} := b^{k\ell}\mathring{D}_k\mathring{D}_\ell$ is the Laplacian of b, and we use D for the Levi-Civita connection of g. Nontrivial triples (M, b, V), where V solves (4.37)-(4.38), are called *static Killing Initial Data*. Killing Initial Data and their connection to Killing vectors in spacetime were explained in section 2.3. We recall that solutions of (4.37)-(4.38) are in one-to-one correspondence with timelike Killing vectors in the associated spacetime on the domain of dependence of the initial data set.

Strictly speaking, for the purpose of defining the mass only the geometry of a neighborhood of the conformal boundary at infinity of M is relevant. A tuple (b, V) will also be called a static KID when M or its conformal boundary are implicitly understood. The functions V will be interchangeably referred to as *static potentials* or static KIDs. The (finite-dimensional) vector space of static potentials of (M, b) will be denoted by $\mathscr{K}_b$. All static potentials for the BK and Horowitz–Myers metrics are derived in Appendix C. Under conditions on the convergence of g to b spelled-out in (4.42)-(4.46) below, well defined global geometric invariants can be extracted from the integrals [66]

$$H(V, b) := \lim_{R\to\infty} \int_{r=R} \mathbb{U}^i(V) dS_i \tag{4.39}$$

where $V \in \mathscr{K}_b$, with

$$\mathbb{U}^i(V) := 2\sqrt{\det g}\,\Big(V g^{i[k} g^{j]l} \mathring{D}_j g_{kl} + D^{[i} V g^{j]k}(g_{jk} - b_{jk})\Big)\,, \tag{4.40}$$

and where dS_i are the hypersurface forms $\partial_i \rfloor dx^1 \wedge \cdots \wedge dx^n$.

From now on, until explicitly indicated otherwise the background metric b will be a BK metric with $m_c = 0$. In the coordinates of (4.34) we set

$$M_{\text{ext}} := [R, \infty) \times N^{n-1}\,, \tag{4.41}$$

for some large $R \in \mathbb{R}^+$, and we consider the following orthonormal frame $\{f_i\}_{i=1,n}$ on M_{ext}:

$$f_i = r^{-1}\epsilon_i\,, \quad i = 1, \dots, n-1\,, \quad f_n = \sqrt{r^2 + k}\,\partial_r\,, \tag{4.42}$$

where the ϵ_i's form an orthonormal frame for the metric h_k. We set

$$g_{ij} := g(f_i, f_j)\,, \quad b_{ij} := b(f_i, f_j) = \begin{cases} 1, & i = j; \\ 0, & \text{otherwise.} \end{cases} \tag{4.43}$$

Assuming that

$$\int_{M_{\text{ext}}} \Big(\sum_{i,j} |g_{ij} - b_{ij}|^2 + \sum_{i,j,k} |f_k(g_{ij})|^2\Big) r\, d\mu_g < \infty\,, \tag{4.44a}$$

$$\int_{M_{\text{ext}}} |R_g - R_b|\, r\, d\mu_g < \infty\,, \tag{4.44b}$$

$$\exists\, C > 0 \;\text{ such that }\; C^{-1} b(X, X) \le g(X, X) \le C b(X, X)\,, \tag{4.45}$$

where $d\mu_g$ denotes the measure associated with the metric g, one finds that the limit in (4.39) exists and is finite. If moreover one requires that

$$\sum_{i,j} |g_{ij} - b_{ij}| + \sum_{i,j,k} |f_k(g_{ij})| = \begin{cases} o(r^{-n/2})\,, & \text{if } n > 2, \\ O(r^{-1-\epsilon}), & \text{if } n = 2, \text{ for some } \epsilon > 0\,, \end{cases} \tag{4.46}$$

then the "mass integrals" (4.39) are well-defined, in the following sense: Consider any two background metrics b_i, $i = 1, 2$, of the form (4.34), *with the same boundary manifold* (N^{n-1}, h_k) *with* $m_c = 0$, in particular with the same value of k. Assume that g approaches both b_1 and b_2 at the rates presented above. Then there exists an isometry Φ of b_1 such that [66]

$$H(V, b_1) = H(V \circ \Phi, b_2)\,. \tag{4.47}$$

From now on we assume that the space dimension n is larger than or equal to three. Consider a background b of the form (4.34). The function

$$V_{(0)}(r) = \sqrt{r^2 + k} \tag{4.48}$$

satisfies the static KID equations (4.37). Assuming (4.44)-(4.46), a somewhat lengthy calculation shows that the mass integral

$$H(V_{(0)}) := H(\sqrt{r^2 + k}, b) \tag{4.49}$$

equals [87]

$$H(V_{(0)}) = \lim_{R\to\infty} R^{n-1}(R^2+k)\times \\ \int_{\{r=R\}} \left(-\sum_{i=1}^{n-1} \left\{ \frac{\partial e_{ii}}{\partial r} + \frac{k e_{ii}}{r(r^2+k)} \right\} + \frac{(n-1)e_{nn}}{r} \right) d^{n-1}\mu_{h_k} \,. \tag{4.50}$$

Here

$$e_{ij} := g_{ij} - b_{ij} \tag{4.51}$$

denotes the frame components in a b-ON frame, with the n'th component corresponding to the direction orthogonal to the level sets of r. In space dimension 3, which will be of main interest below, under the decay conditions spelled above this simplifies to

$$H(V_{(0)}) = \lim_{R\to\infty} R^4 \int_{\{r=R\}} \left(\frac{2e_{33}}{r} - \sum_{i=1}^{2} \frac{\partial e_{ii}}{\partial r} \right) d^2\mu_{h_k} \,. \tag{4.52}$$

A class of ALH metrics of interest are those for which

$$e_{ij} = r^{-n}\mu_{ij} + o(r^{-n}) \,, \tag{4.53}$$

where the μ_{ij}'s depend only upon the coordinates x^A on ∂M. One can further specialize the coordinates in which $\mu_{nn} \equiv 0$, but this choice might be unnecessarily restrictive for some calculations. Metrics with these asymptotics are dense in the space of all AH metrics in suitable circumstances [91, Theorem 5.3]. The tensor μ_{ij} will be referred to as the *mass aspect tensor*.

For metrics for which (4.53) holds, Equation (4.50) reads

$$H(V_{(0)}) = \int_{\partial M} \Big((n-1)\mu_{nn} + n \sum_{i=1}^{n-1} \mu_{ii} \Big) d^{n-1}\mu_{h_k} =: \int_{\partial M} \mu \, d^{n-1}\mu_{h_k} \,, \tag{4.54}$$

where μ is the *mass aspect function* mentioned in Table 4.1. An elegant formula for mass can be derived by integration by parts in (4.39)-(4.40), leading to the following: To every KID (b, V) and conformal-boundary component ∂M one associates a mass

$$m = m(V) = m(V, \partial M) \equiv H(V, b) \tag{4.55}$$

by the formula [92] (compare [93, Equation (IV.40)])

$$m(V, \partial M) \quad = \quad -\lim_{x\to 0} \int_{\{x\}\times\partial M} D^j V (R^i{}_j - \frac{R}{n}\delta^i_j) \, d\sigma_i \,, \tag{4.56}$$

where R_{ij} is the Ricci tensor of the metric g, R its trace, and we have ignored an overall dimension-dependent positive multiplicative factor which is typically included in the

physics literature. Here ∂M is a component of conformal infinity, x is a coordinate near ∂M so that ∂M is given by the equation $\{x = 0\}$, and $d\sigma_i := \sqrt{\det g} dS_i$.

Equation (4.56) will be used predominantly in the following sections. To make contact with usual spacetime methods, we comment on the derivation of (4.56) in [93]. There, (4.56) was obtained by calculating the Hamiltonian associated with a timelike Killing vector field of the background and expressing the result in terms of initial data. In this work, we will only consider static KIDs or timelike Killing vector fields which do not depend on the coordinate mass parameter m_c.

As a special case, consider a triple $(M, g, \hat{V})$ satisfying (4.37)-(4.38); thus both $(M, g, \hat{V})$ and (M, b, V) are static KIDs. Assume that g asymptotes to b as above, and that $\hat{V}$ asymptotes to V. One checks that V can be replaced by $\hat{V}$ in the integrand of (4.56), so that

$$\begin{aligned} D^j\hat{V}(R^i{}_j - \frac{R}{n}\delta^i_j) &= \frac{1}{\hat{V}} D^j\hat{V}(D^iD_j\hat{V} - \frac{1}{n}\Delta\hat{V}\delta^i_j) \\ &= \frac{1}{\hat{V}} D^j\hat{V}(D^iD_j\hat{V} - \hat{V}\delta^i_j) \\ &= \frac{1}{2\hat{V}} D^i(|d\hat{V}|^2) - D^i\hat{V}\,. \end{aligned} \tag{4.57}$$

Letting $r = 1/x$, (4.56) becomes

$$m(\hat{V}) = \lim_{R\to\infty} \int_{r=R} (D^i\hat{V} - \frac{1}{2\hat{V}} D^i(|d\hat{V}|^2))\, d\sigma_i\,. \tag{4.58}$$

As an application, and for further use, we apply (4.58) to the space-part of the Horowitz-Myers metric,

$$g = \frac{dr^2}{r^2 - \frac{2m_c}{r^{n-2}}} + (r^2 - \frac{2m_c}{r^{n-2}})d\psi^2 + r^2\mathsf{h}_{IJ}d\theta^I d\theta^J\,, \tag{4.59}$$

where $\mathsf{h}_{IJ}d\theta^I d\theta^J$, $I, J \in \{1, \dots n-2\}$ is a flat $(n-2)$-dimensional metric, $m_c > 0$ is a constant and ψ has a suitable period to guarantee smoothness at $r^n = 2m_c$. The background is taken to be g with $m_c = 0$, thus $\hat{V} = r$, $|d\hat{V}|^2 = (r^2 - \frac{2m_c}{r^{n-2}})$, which gives an integrand in (4.58) equal to

$$(D^r\hat{V} - \frac{1}{2\hat{V}} D^r(|d\hat{V}|^2))\, r^{n-2}\sqrt{\det\mathsf{h}} = -(n-2)m_c(1 - \frac{2m_c}{r^n})\sqrt{\det\mathsf{h}}\,, \tag{4.60}$$

and thus total mass

$$m = -(n-2)m_c\,, \tag{4.61}$$

where we have assumed that the area of the conformal boundary at infinity in the metric $d\psi^2 + \mathsf{h}_{IJ}dx^I dx^J$ has been normalized to 1. Applying (4.58) to the space-part of the

toroidal Birmingham–Kottler metric

$$g = \frac{dr^2}{r^2 - \frac{2m_c}{r^{n-2}}} + r^2 \mathsf{h}_{AB} d\theta^A d\theta^B \,, \tag{4.62}$$

which has $\hat{V} = \sqrt{r^2 - \frac{2m_c}{r^{n-2}}}$, gives

$$(D^r \hat{V} - \frac{1}{2\hat{V}} D^r(|d\hat{V}|^2)) \frac{r^{n-1}}{\hat{V}} = m_c(n-2)(n-1)\Big(1 + \frac{m_c(n-2)}{r^n}\Big) \,, \tag{4.63}$$

and

$$m = (n-1)(n-2)m_c \,. \tag{4.64}$$

4.6.2. The spherical case

The question then arises, what happens with the mass under the boundary gluings of section 4.4. The case when both manifolds have a conformal boundary with spherical topology and a metric conformal to the standard round metric is simplest because then the maps $(\Lambda_1, \Lambda_2) \in \mathscr{P}$ act globally on collar neighbourhoods of N_1^{n-1} and N_2^{n-1} in M_1 and M_2. The initial energy-momenta $\mathbf{m}_1$ of N_1^{n-1} and $\mathbf{m}_2$ of N_2^{n-1} are transformed to $\Lambda_1\mathbf{m}_1$ of $\Lambda_2\mathbf{m}_2$. Since the mass integrands are zero in the neck region, where the metric is exactly hyperbolic, one finds that the energy-momentum $\mathbf{m}$ of the boundary-glued manifold is additive:

$$\mathbf{m} = \Lambda_1\mathbf{m}_1 + \Lambda_2\mathbf{m}_2 \,. \tag{4.65}$$

This is true for all dimensions $n \geq 3$.

A more detailed presentation of the spherical case can be found in [63], and note that most of the work there arose from the necessity to control the direction of the momenta $\mathbf{m}_a$.

4.6.3. Conformal rescaling of h_k

The remaining cases, as well as the Isenberg-Lee-Stavrov gluings, require more effort. After the gluing has been done, the initial "boundary metric" h_k of (4.34) will have to be conformally rescaled in general. Thus, there will be a function $\psi > 0$, defined on a subset of the boundary at infinity, such that

$$h_k = \psi^2 h_{\bar{k}} \,, \tag{4.66}$$

for some constant $\bar{k} \in \{0, \pm 1\}$. The following can be justified by considerations revolving around the Yamabe problem.

First, if (N^{n-1}, h_k) is a round sphere, there exist globally defined non-trivial such conformal factors with $k = \bar{k} = 1$, and they all arise from conformal isometries of the sphere.

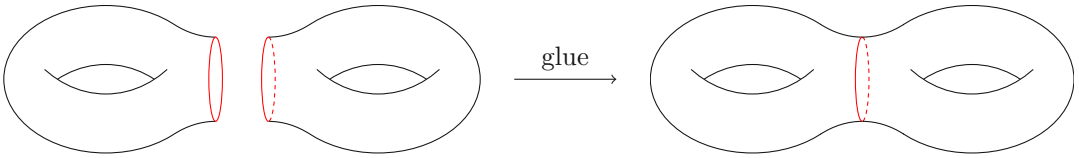

Figure 4.3.: Gluing two solid tori along a disc, the boundary of which becomes a closed geodesic on the boundary of the glued manifold.

Next, when (N^{n-1}, h_k) is a closed manifold with $k = 0$ and (4.66) holds globally, then $\bar{k}$ must also be zero and ψ must be constant. Of course, any constant will do, and there does not seem to be a geometrically preferred value for this constant. When calculating the mass of the Horowitz–Myers metric we will normalize the volume of (N^{n-1}, h_k) to one, which removes the ambiguity.

In all other cases, $\psi \equiv 1$ and $k = \bar{k}$ is the only possibility for globally defined functions ψ on closed manifolds.

However, we will also need (4.66) on subsets of N^{n-1}. Then non-trivial functions ψ are possible with $k \neq \bar{k}$ in dimension $n = 3$. By way of example, let N^2 be the connected sum of two tori, i.e.

$$N^2 = \mathbb{T}^2 \# \mathbb{T}^2 \,, \tag{4.67}$$

with the gluing occurring across a closed geodesic, cf. Figure 4.3. If we cut the connecting neck along the closed geodesic, each of the factors in (4.67) can be viewed as a torus $\mathbb{T}^2 \setminus D^2$ with an open disc removed, and there we can write

$$h_{-1} = e^{\omega} h_0 \,, \tag{4.68}$$

where ω is a solution of the two-dimensional Yamabe equation (4.28), which for (4.68) reads

$$\Delta_{h_0} \omega = 2 e^{\omega} \,, \tag{4.69}$$

with vanishing Neumann data at ∂D^2.

Now, our definition of mass requires that the glued manifold admits non-trivial static potentials. This is guaranteed when both the initial manifolds (N_i^{n-1}, h_{k_i}), $i = 1, 2$, and the new metric on $N_1^{n-1} \# N_2^{n-1}$ are Einstein manifolds. The gluing construction itself does not care about this, but the existence of a static potential on a collar neighborhood of the glued manifold is not clear, except when the boundary is two-dimensional, or when at least one boundary metric is a round sphere in all dimensions. The existence of further higher-dimensional such examples is unlikely, see [94].

Here one should keep in mind that there exist large families of *smoothly compactifiable stationary vacuum* solutions (M, g) of (Riemannian) Einstein equations such that (N^{n-1}, h_k) is *not* Einstein [95–99]. Each such metric comes equipped with a definition of mass [78] for metrics with the same conformal infinity. Whether or not our weighted addition formula (4.80) below applies in these more general circumstances is not clear; we plan to address this in the future.

Returning to our main line of thought, suppose thus that (4.66) holds on a subset of N^{n-1}. We extend ψ to a neighbourhood of the conformal boundary by requiring $\partial_r \psi = 0$. Let us denote by $(\bar{r}, \bar{x}^A)$ coordinates such that the new background metric $h_{\bar{k}}$ takes the form

$$\bar{b} := \frac{d\bar{r}^2}{\bar{r}^2 + \bar{k}} + \bar{r}^2 h_{\bar{k}} \,. \tag{4.70}$$

We can write

$$b = \frac{dr^2}{r^2 + k} + r^2 h_k = \frac{dr^2}{r^2 + k} + r^2 \psi^2 h_{\bar{k}} = \frac{d\bar{r}^2}{\bar{r}^2 + \bar{k}} + \bar{r}^2 (h_{\bar{k}} + \delta h) \,, \tag{4.71}$$

with

$$\delta h(\partial_r, \cdot) = 0 \,. \tag{4.72}$$

Let us denote by x^A the local coordinates at ∂M. As shown in Appendix D below (cf. (D.21) and (D.24)) we find for large r

$$\bar{x}^A = x^A + \frac{\mathscr{D}^A \psi}{2\psi r^2} + O(r^{-4}) \,, \tag{4.73}$$

$$\bar{r} = \psi r \left(1 + \frac{\left(-\mathscr{D}^A \mathscr{D}_A \log \psi + (n-2) \mathscr{D}^A \log \psi \mathscr{D}_A \log \psi \right)}{2(n-1) r^2} + O(r^{-4}) \right) , \tag{4.74}$$

where $\mathscr{D}$ is the Levi-Civita connection of h_k.

It follows from (4.73)-(4.74) (see (D.14), Appendix D) that an asymptotic expansion of the initial metric of the form

$$g(f_i, f_j) - b_{ij} = O(r^{-n}) \tag{4.75}$$

(which is observed in BK metrics) will *not* be preserved by the above transformations, except possibly 1) in dimension $n = 3$ or 2) when $k = \bar{k}$ and the conformal factor arises from a conformal isometry of h_k. This is addressed in Appendix D. In particular, it is shown there, in space dimension three and for $\mu_{ri} = 0$, that the mass aspect tensor μ_{ij} of (4.53) transforms as

$$\mu_{AB} \mapsto \bar{\mu}_{AB} = \psi \mu_{AB} \,. \tag{4.76}$$

4.6.4. Gluing in three space dimensions

We consider the mass of the manifold obtained by boundary-gluing of two three-dimensional manifolds (M_a, g_a), $a = 1, 2$. This includes the Horowitz–Myers metrics which are conformally compactifiable, have no boundary, and have negative mass, as well as Kottler metrics which are conformally compactifiable and have totally geodesic boundaries.

Let us denote by V_a the static potential of the asymptotic backgrounds on M_a, $a = 1, 2$. For the spherical components of the boundary at infinity, if any, one only needs to consider the static potential $\sqrt{1+r^2}$, as follows from (4.79) below.

We start with the boundary-gluing of section 4.4. Letting $x = 1/R$ in (4.56), and using the fact that the metric is exactly hyperbolic in $\mathscr{U}_a$ we have

$$\begin{aligned} m_a &:= m(V_a, \partial M_a) = -\lim_{x\to 0} \int_{\{x\}\times\partial M_a} D^j V_a (R^i{}_j - \frac{R}{n}\delta^i_j)\, d\sigma_i \\ &= -\lim_{x\to 0} \int_{\{x\}\times(\partial M_a \setminus \mathscr{U}_a)} D^j V_a (R^i{}_j - \frac{R}{n}\delta^i_j)\, d\sigma_i \,. \end{aligned} \tag{4.77}$$

Let us write r for the radial coordinate as in (4.34) on M_1, so that the static potential entering into the definition of the mass of (M_1, g_1) reads

$$V_1 = \sqrt{r^2 + k}\,. \tag{4.78}$$

Let us write $(\bar{M}, \bar{g})$ for the boundary-glued manifold, $\bar{V}$ for the associated static potential, and $\bar{r}$ for the radial coordinate on $\bar{M}$. Viewing $M_1 \setminus \mathscr{U}_1$ as a subset of $\bar{M}$, using (4.74) with ψ there denoted by ψ_1 here, we can write on $M_1 \setminus \mathscr{U}_1$

$$\bar{V} = \sqrt{\bar{r}^2 + \bar{k}} = \bar{r} + O(\bar{r}^{-1}) = \psi_1 r + O(r^{-1}) = V_1\psi_1 + O(r^{-1})\,. \tag{4.79}$$

Here ψ_1 has been extended to the interior of $\bar{M}_1$ by requiring $\partial_r \psi_1 = 0$.

An identical formula holds on $M_2 \setminus \mathscr{U}_2$, with a conformal factor which we denote by ψ_2.

Assuming in addition to (4.42)-(4.46) that the b-norm of $R^i{}_j - \frac{R}{n}\delta^i_j$ decays as $o(r^{2-n})$ for large r,

$$\begin{aligned} \bar{m} &:= m(\bar{V}, \partial\bar{M}) = -\lim_{x\to 0} \int_{\{x\}\times\partial\bar{M}} D^j \bar{V} (R^i{}_j - \frac{R}{n}\delta^i_j)\, d\sigma_i \\ &= -\sum_{a=1}^{2} \lim_{x\to 0} \int_{\{x\}\times\partial M_a} D^j(\psi_a V_a)(R^i{}_j - \frac{R}{n}\delta^i_j)\, d\sigma_i \,. \end{aligned} \tag{4.80}$$

Comparing with (4.77), we see that the mass of the glued manifold is the sum of mass-type integrals, where the original integrands over ∂M_a are adjusted by the conformal factor relating the metric on the glued boundary to the original one.

The above applies also to the case where the mass aspect tensor is well-defined, giving a simpler formula

$$\bar{m} = -\sum_{a=1}^{2} \int_{\partial M_a} \psi_a \Big((n-1)\mu_{nn} + n \sum_{i=1}^{n-1} \mu_{ii} \Big) d^{n-1}\mu_{h_k}\,. \tag{4.81}$$

It should, however, be pointed out that the gluing-in of an exactly hyperbolic region as in [23] is *not known* to lead to a metric with well defined mass-aspect tensor in the region where the deformation of the metric is carried out, so that in our analysis below we have to use (4.80).

The difference in the mass formulae between the boundary-gluing of section 4.4 and that of [83] is essentially notational, concerning the integration domains in (4.80) and (4.81). Indeed, after the gluing construction presented in section 4.2 of [83] has been done, the boundary manifold there is obtained by removing discs $D(\epsilon_a)$ of coordinate radii ϵ_a from ∂M_a, and connecting the boundaries of the discs with a neck $S^1 \times [0,1]$. (The radii ϵ_a are taken to be one in [83, section 4.2], which is due to a previous rescaling of the coordinates.) For the purpose of the formulae below let us cut the boundary neck $S^1 \times [0,1]$ into two pieces $N_1 := S^1 \times [0,1/2]$ and $N_2 := S^1 \times [1/2,1]$, and let $\Omega_a = (\partial M_a \setminus D(\epsilon_a)) \cup N_a$. In the construction of [83] each Ω_a comes naturally equipped with a constant scalar curvature metric which coincides with the original one on $\partial M_a \setminus D(\epsilon_a)$. The relative conformal factors ψ_a are defined on the Ω_a's with respect to these metrics. We then have

$$\begin{aligned} \bar{m} &:= m(\bar{V}, \partial\bar{M}) \\ &= -\sum_{a=1}^{2} \lim_{x\to 0} \int_{\{x\}\times\Omega_a} D^j(\psi_a V_a)(R^i{}_j - \frac{R}{n}\delta^i_j)\, d\sigma_i \,. \end{aligned} \tag{4.82}$$

Whenever a mass aspect tensor is globally defined on the glued manifold, this last formula coincides with

$$\bar{m} = -\sum_{a=1}^{2} \int_{\Omega_a} \psi_a \Big((n-1)\mu_{nn} + n\sum_{i=1}^{n-1}\mu_{ii}\Big) d^{n-1}\mu_{h_k} \,. \tag{4.83}$$

It should be clear how this generalizes to the boundary-gluing of several three-dimensional manifolds.

4.6.5. Noncompact boundaries

When defining hyperbolic mass, it is usual to assume, and we did, that the conformal boundary at infinity is compact. This is done for convenience: when the boundary manifold is compact, to obtain convergence of the integrals defining mass it suffices to impose decay conditions of the metric g to the asymptotic background b.

Now, the "exotic gluings" construction in [23] creates an open neighborhood, say $\mathscr{O}$, of a subset of the conformal boundary at infinity, such that the metric is conformal to the hyperbolic one in $\mathscr{O}$.

One can then create non-trivial non-compact boundary manifolds by removing closed sets, say Σ, from the boundary at infinity inside $\partial M \cap \mathscr{O}$ and changing the asymptotic background b to a new background $\bar{b}$ on $\partial M \setminus \Sigma$. A simple non-trivial example is provided by taking ∂M to be a two-dimensional torus, Σ to be a finite collection of points $p_i \in \partial M$ (e.g., one point), and replacing the original background with a flat conformal metric h_0

on ∂M by a complete hyperbolic metric with cusps at the (removed) points p_i. Then, instead of measuring the mass of M with respect to the original background with a toroidal boundary, we can define a mass with respect to the new background $\bar{b}$, as in (4.70)-(4.71).

Since the removed set Σ is contained in the set $\mathscr{O}$, where the metric is conformal to the hyperbolic metric, the convergence of the new mass integrals readily follows from the convergence of the original mass: the support of the boundary integrals near infinity is included in a neighborhood of the compact set $\partial M \setminus \overline{\mathscr{O}}$. The arguments presented in section 4.6.4 readily lead to the following formula for the new mass:

$$m(\bar{V}, \partial\bar{M} \setminus \Sigma) = -\lim_{x\to 0} \int_{\{x\}\times(\partial\bar{M}\setminus\Sigma)} D^j(\psi V)(R^i{}_j - \frac{R}{n}\delta^i_j)\, d\sigma_i\,; \tag{4.84}$$

recall that ψ is the conformal factor which relates the original metric h_k to the new one as $h_{\bar{k}} = \psi^{-2}h_k$ and x is a coordinate which vanishes at the conformal boundary at infinity.

4.7. Higher genus solutions with negative mass

In this section, we show existence of classes of three-dimensional ALH manifolds (M, g) with constant scalar curvature, higher-genus conformal boundary at infinity, and negative mass.

4.7.1. Genus two

We start with a construction leading to ALH manifolds with genus at infinity equal to two.

The manifold (M, g) will be obtained by a boundary-gluing of two ALH manifolds, (M_1, g_1) and (M_2, g_2), with *identical toroidal conformal geometries at infinity*. We assume the existence of a coordinate system near the conformal boundary at infinity in which each of the original metrics g_a takes the form

$$g_a = \underbrace{\frac{dr^2}{r^2} + r^2 h_0}_{b} + e_a\,, \qquad r \geq r_0\,, \quad a = 1, 2\,, \tag{4.85}$$

for some $r_0 > 0$, where

$$|e_a|_b + |De_a|_b + |D^2 e_a|_b \leq Cr^{-\sigma} \tag{4.86}$$

with constants $\sigma > 5/2$ and $C > 0$. This guarantees the possibility of performing an "exotic gluing" with a well-defined final mass [23], and is satisfied in particular for the Birmingham-Kottler and Horowitz-Myers metrics, in which cases $\sigma = 3$.

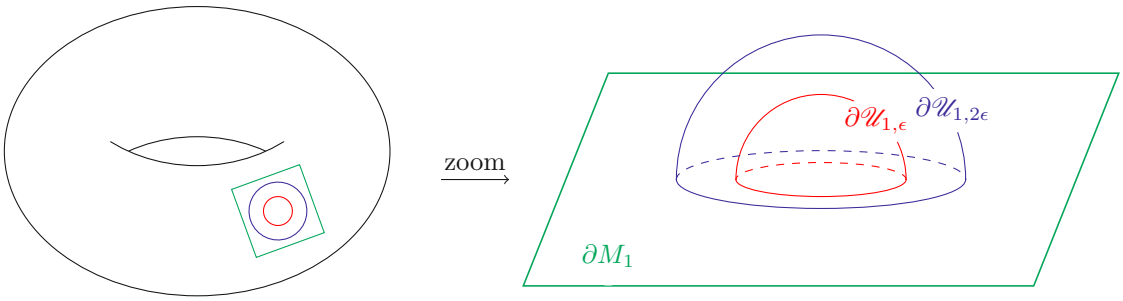

Figure 4.4.: The sets $\mathscr{U}_{1,\epsilon} \subset \mathscr{U}_{1,2\epsilon}$ and their boundaries.

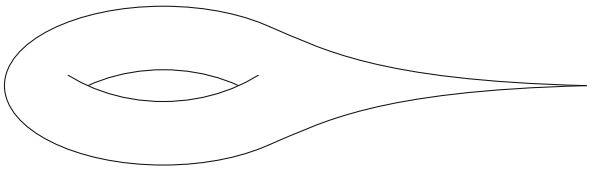

Figure 4.5.: A punctured torus with a hyperbolic metric; the figure is misleading in that the cusp region is actually infinitely long.

We make an appeal to the construction described in Section 4.4, where the hyperbolic metric has been glued in within an ϵ-neighborhood of boundary points $p_a \in \partial M_a$. We use the coordinates of (4.85)-(4.86) with polar coordinates for the boundary metric

$$h_0 = d\rho^2 + \rho^2 d\varphi^2 \tag{4.87}$$

on ∂M_a, with p_a located at the origin of these coordinates. Such coordinates can always be defined, covering a disc $D(\rho_0)$ for some $\rho_0 > 0$. Without loss of generality, we can rescale the metric h_0 on ∂M_a so that the coordinates are defined on the unit disc $D(1)$. (This might rescale the total mass by a positive factor; one then reverts to the original scaling before calculating the mass.)

The metric g_1 is thus the original metric outside the half-ball $\mathscr{U}_{1,2\epsilon}$ of coordinate radius $2\epsilon < 1$, and is exactly hyperbolic inside the half-ball $\mathscr{U}_{1,\epsilon}$ of coordinate radius ϵ (see Figure 4.4); similarly for g_2. For reasons that will become clear in the proof, we need to consider a family of boundary gluings indexed by a parameter $i \to \infty$.

As notation suggests, the parameter i will be taken in $\mathbb{N}$; we will indicate how to transition to a continuous parameter i in Remark 4.12 below.

For $i \geq 8/\epsilon$ we choose both hyperbolic hyperplanes $\mathfrak{h}_{1,i}$ and $\mathfrak{h}_{2,i}$ of section 4.4 to be half-spheres of radius $1/i$ centered at the origin of the coordinates (4.87). We choose any

pair $(\Lambda_1 := \Lambda_{\mathfrak{h}_{1,i},+}, \Lambda_2 := \Lambda_{\mathfrak{h}_{2,i},-})$ as in section 4.4 to obtain the boundary-glued manifold $M := M_{\Lambda_1,\Lambda_2}$.

Recall that, given a flat torus $(\mathbb{T}^2, h_0)$ and a point $p \in \mathbb{T}^2$, there exists on $\mathbb{T}^2 \setminus \{p\}$ a smooth function ω such that the metric $e^\omega h_0$ is complete, has constant Gauss curvature equal to -1, with $(\mathbb{T}^2, e^\omega h_0)$ having finite total area; see Figure 4.5 and Appendix B, compare [100, Proposition 2.3].

We claim:

Theorem 4.3. *Consider two three-dimensional ALH manifolds (M_a, g_a), $a = 1, 2$, with constant scalar curvature and with a metric of the form (4.85)-(4.86) with the same flat metric h_0. Let $p \in \partial M_1$ and let $e^\omega h_0$ be the unique constant negative curvature metric with a cusp at p. The mass of the Maskit-doubled metric as described above converges, as ϵ tends to zero and i tends to infinity, to the finite limit*

$$-\sum_{a=1}^{2} \lim_{r\to\infty} \int_{\{r\}\times\mathbb{T}^2} D^j(e^{-\omega/2}r)(R^i{}_j - \frac{R}{n}\delta^i_j)\, d\sigma_i\,. \tag{4.88}$$

In this sum R_{ij} is the Ricci tensor of g_1 when $a = 1$ and of g_2 when $a = 2$.

This leads us to existence of negative-mass solutions without boundary:

Corollary 4.4. *There exist three-dimensional conformally compactifiable ALH manifolds without boundary at finite distance, with constant scalar curvature, genus two infinity, and negative mass.*

Proof of Corollary 4.3: We apply Theorem 4.1 to two identical copies of a Horowitz-Myers instanton. Keeping in mind that $m_c > 0$, it follows from (4.88) and (4.81) that m approaches

$$-\infty < -2m_c \int_{\mathbb{T}^2} e^{-\omega/2} d\mu_{h_0} < 0 \tag{4.89}$$

when ϵ tends to zero and i tends to infinity, and hence is negative for sufficiently small ϵ and sufficiently large i. □

Remark 4.5. In the case of the square torus with area equal one, discussed in Appendix B, the function ω in (4.89) satisfies (cf. (B.5))

$$e^{-\omega/2} \leq \frac{\Gamma(1/4)^2}{4\pi^{3/2}} \approx 0.59\,, \tag{4.90}$$

which leads to a rough lower estimate of the mass m of the manifolds obtained by gluing two identical copies of the Horowitz-Myers instanton manifold, for small ϵ and large i,

$$-1.18\, m_c < m < 0\,. \tag{4.91}$$

An upper bound can be obtained by numerically integrating the inverse of the right-hand side of (B.3), leading to

$$-1.18\, m_c < m < -0.68\, m_c\,. \tag{4.92}$$

(The integral of the inverse of the left-hand side of (B.3) gives a worse lower bound $\approx -4.02\, m_c$.)

Proof of Theorem 4.3: By construction, the boundary ∂M of the new manifold is a doubling of

$$\hat{M}_i := \partial M_1 \setminus D(1/i)\,. \tag{4.93}$$

We will often view both $\hat{M}_i$ and its double as subsets of ∂M.

Consider the conformal class of metrics on ∂M induced by g. This conformal class depends upon i but is independent of ϵ, keeping in mind that $\epsilon \geq 8/i$. In this class there exists a unique metric h_{-1} with constant scalar curvature equal to minus two which can be constructed as follows: Let $\hat{h}_i$ be any representative of the conformal class of metrics on ∂M_1 induced by g which is

1. invariant under reflection across $\hat{M}_i$, so that the coordinate circle

$$S_{1/i} = \hat{M}_i \tag{4.94}$$

of coordinate radius $1/i$ is a totally geodesic boundary for $(\hat{M}_i, \hat{h}_i)$, and which is

2. invariant under rotations near $S_{1/i}$.

While any metric $\hat{h}_i$ as in 1. and 2. is adequate, a useful example is provided by the metric which on ∂M_1 equals $\chi^2 h_0$, where $\chi \geq 1/2$ is any smooth function on $\partial M_1 \setminus \{p\}$ which equals to $1/\rho$ on $D(1)\setminus\{0\}$, where ρ is the coordinate radius in the local coordinates on ∂M_1. This can be accompanied by the introduction of a new coordinate

$$\hat{\rho} = \frac{\log(\rho)}{\log(i)} + 1\,, \tag{4.95}$$

so that the flat metric

$$h_0 = d\rho^2 + \rho^2 d\varphi^2\,, \qquad \rho \in [1/i, 1] \tag{4.96}$$

becomes

$$h_0 = \rho^2(\frac{d\rho^2}{\rho^2} + d\varphi^2) = \rho^2(\log^2(i) d\hat{\rho}^2 + d\varphi^2)\,, \qquad \hat{\rho} \in [0, 1]\,, \tag{4.97}$$

thus $\hat{h}_i = \log^2(i) d\hat{\rho}^2 + d\varphi^2$ on $[1, i] \times S^1$.

In this coordinate system the *reflection across* $\hat{M}_i$ is the map $(\hat{\rho}, \varphi) \mapsto (-\hat{\rho}, \varphi)$, after extending the range of $\hat{\rho}$ from $[0, 1]$ to $[-1, 1]$.

Given a function f defined on $\overline{D(1) \setminus D(1/i)}$ in the original coordinates (ρ, φ), the *mirror-symmetric doubling* of f is defined as the function

$$[-1,1] \times S^1 \ni (\hat{\rho}, \varphi) \mapsto \hat{f}(\hat{\rho}, \varphi) = \begin{cases} f(e^{\log(i)(\hat{\rho}-1)}, \varphi) & \hat{\rho} \geq 0; \\ f(e^{\log(i)(-\hat{\rho}-1)}, \varphi) & \hat{\rho} < 0. \end{cases} \tag{4.98}$$

The mirror-symmetric doubling of a tensor field is obtained by transforming the tensor field to the coordinates $(\hat{\rho}, \varphi)$ and mirror-doubling all its coordinate-components. For example, after doubling of $\hat{M}_i$, the tensor field $\hat{h}_i = \log^2(i) d\hat{\rho}^2 + d\varphi^2$ just defined above on $[0,1] \times S^1$ maintains the same form $\log^2(i) d\hat{\rho}^2 + d\varphi^2$ on $[-1,1] \times S^1$ after doubling.

Another example, which plays an important role in our proof below, is provided by the daunting-looking metric (cf., e.g., [60])

$$e^{\omega_{*,i}} h_0 := \Big(\frac{\pi}{\log(i^2) \sin(\pi \frac{\log \rho}{\log(i^2)}) \rho} \Big)^2 (d\rho^2 + \rho^2 d\varphi^2) \,, \qquad \rho \in (1/i^2, 1) \,, \tag{4.99}$$

which has constant negative scalar curvature equal to -2. The conformal factor $e^{\omega_{*,i}}$ tends to infinity at $\rho = 1/i^2$ and at $\rho = 1$. In the coordinates $(\hat{\rho}, \varphi)$ the metric (4.99) reads

$$e^{\omega_{*,i}} h_0 = \Big(\frac{\pi}{2 \cos(\pi \hat{\rho}/2)} \Big)^2 (d\hat{\rho}^2 + \frac{1}{\log^2(i)} d\varphi^2) \,, \qquad \hat{\rho} \in (-1, 1) \,, \tag{4.100}$$

which is manifestly mirror-invariant. Note that the circle $\hat{\rho} = 0$ is a closed geodesic minimizing length, of length $\pi^2 / \log(i)$.

Let $u_i : \partial M \to \mathbb{R}$ be the unique solution of the two-dimensional Yamabe equation

$$\Delta_{\hat{h}_i} u_i = -R e^{u_i} + \hat{R}_i \,, \tag{4.101}$$

with $R = -2$, and where $\hat{R}_i$ is the scalar curvature of the metric $\hat{h}_i$, so that the metric $e^{u_i} \hat{h}_i$ has scalar curvature R. It is important in what follows that the function u_i is independent of ϵ.

(As uniqueness is likewise important in our analysis, let us provide an argument: let $\tilde{u}_i$ and $\hat{u}_i$ be two solutions, rename the metric $e^{\hat{u}_i} \hat{h}_i$ to $\hat{h}_i$, then from $\tilde{u}_i$ one obtains a solution of (4.101) with $R = \hat{R} = -2$. Multiplying the resulting equation by u_i and integrating over ∂M one obtains

$$\int |du_i|^2 d\mu_{\hat{h}_i} = 2 \int (1 - e^{u_i}) u_i d\mu_{\hat{h}_i} \,. \tag{4.102}$$

Since the integrand of the right-hand side is negative except at $u_i = 0$, we find $u_i \equiv 0$, hence $\tilde{u}_i \equiv \hat{u}_i$.)

Uniqueness implies that u_i is invariant under reflection across $\hat{M}_i$. Hence u_i has vanishing normal derivative on $S_{1/i}$.

As $\hat{h}_i$ is conformal to h_0 on $\hat{M}_i$, there exists a function $\hat{u}_i$ so that we have

$$\hat{h}_i = e^{\hat{u}_i} h_0 \tag{4.103}$$

on $\hat{M}_i$. Then the metric

$$e^{u_i+\hat{u}_i} h_0 \tag{4.104}$$

defined on $\hat{M}_i$, has scalar curvature equal to minus two. The mirror-symmetric doubling of $\hat{h}_i$ across $S_{1/i}$ coincides with the metric h_{-1} on ∂M_1.

Now, by construction, $\hat{u}_i$ is rotation-invariant near $S_{1/i}$. The fact that $S_{1/i}$ is totally geodesic is equivalent to the vanishing of the radial derivative of $e^{\hat{u}_i/2}\rho$ on $S_{1/i}$:

$$0 = \partial_\rho (e^{\hat{u}_i/2}\rho)|_{S_{1/i}} \qquad \Longrightarrow \qquad \partial_\rho \hat{u}_i|_{S_{1/i}} = -2i\,. \tag{4.105}$$

From what has been said we have

$$\partial_\rho u_i|_{S_{1/i}} = 0\,. \tag{4.106}$$

Since h_0 is flat, we conclude that the function

$$\omega_i := u_i + \hat{u}_i \tag{4.107}$$

satisfies on $\hat{M}_i$ the equation

$$\Delta_{h_0}\omega_i = 2e^{\omega_i}\,, \tag{4.108}$$

with Neumann boundary data at the coordinate circle $S_{1/i}$ of radius $1/i$ centered at the origin:

$$\partial_\rho \omega_i|_{S_{1/i}} = -2i\,. \tag{4.109}$$

Now, while the function ω_i depends only upon i, the metric on M depends upon both ϵ and i. This has the unfortunate consequence that the sign of the mass of M is not clear. In what follows we will determine this sign for i large and ϵ small. For this, we need to understand what happens with the mass integrand (4.80) when i tends to infinity and ϵ tends to zero. The idea of the argument is to show that the sequence of functions ω_i, or at least a subsequence thereof, converges to a limit, with sufficient control of the limit to guarantee control of the mass. The needed convergence result is perhaps contained in [101], but it is not completely apparent to us that this is the case, so we provide a direct argument, different from the one in [101].

The maximum principle shows that ω_i has no interior maximum on the compact manifold with boundary $\partial M_1 \setminus D(a)$ for $a \in [1/i, 1]$, where $D(a)$ denotes an open coordinate disc of radius a lying on the boundary ∂M_1 and centered at p.

Integrating (4.108) over $\hat{M}_i$ and using (4.109) one finds

$$\int_{\hat{M}_i} e^{\omega_i} d\mu_{h_0} = 2\pi \tag{4.110}$$

which follows from Stokes' theorem.

We continue the proof of Theorem 4.3 with the (well known, cf. e.g. [60]) observation, that solutions of the equation

$$\Delta\omega = 2e^{\omega} \tag{4.111}$$

satisfy a comparison principle, which we formulate in the simplest form sufficient for our purposes: If both ω and $\hat{\omega}$ satisfy (4.111) in a bounded domain Ω with boundary, and if $\hat{\omega} > \omega$ near the boundary, then $\hat{\omega} > \omega$ on Ω. (This comparison is particularly useful with functions $\hat{\omega}$ which tend to infinity when $\partial\Omega$ is approached.) Indeed, if ω is continuous on the closure $\bar{\Omega}$ of Ω, the function $\omega - \hat{\omega}$ is then negative near $\partial\Omega$, and satisfies the equation

$$\Delta_{h_0}(\omega - \hat{\omega}) = 2e^{\omega} - 2e^{\hat{\omega}}\,. \tag{4.112}$$

If $\omega > \hat{\omega}$ somewhere, then $\omega - \hat{\omega}$ would have a positive maximum at some point $q \in \Omega$ away from the boundary. Since the function $x \mapsto 2e^x$ is increasing, the right-hand side of (4.112) would be positive at q. But the left-hand side is nonpositive at a maximum, a contradiction. We rephrase this loosely as

$$\hat{\omega} > \omega \text{ on } \partial\Omega \quad \Longrightarrow \quad \hat{\omega} > \omega \text{ on } \Omega. \tag{4.113}$$

For $0 < a < b$ let

$$\Gamma(a, b) := D(b) \setminus D(a)\,.$$

The comparison principle allows us to prove:

Lemma 4.6. *On $\Gamma(1/i, 1)$ it holds that*

$$e^{w_i} \leq e^{\omega_{*,i}} := \Big(\frac{\pi}{\log(i^2)\sin(\pi\frac{\log\rho}{\log(i^2)})\rho}\Big)^2. \tag{4.114}$$

Remark 4.7. On the circle $\rho = 1/i$ we have

$$e^{\omega_{*,i}} = \frac{\pi^2 i^2}{4\log^2(i)}, \tag{4.115}$$

which is unbounded in i, but the metric length ℓ_i of $S_{1/i}$ equals

$$\ell_i = \frac{1}{i}\int_{\varphi\in[0,2\pi]} (e^{\omega_i/2})_{|\rho=1/i} d\varphi \leq \frac{1}{i}\int_{\varphi\in[0,2\pi]} (e^{\omega_{*,i}/2})_{|\rho=1/i} d\varphi = \frac{\pi^2}{\log i}, \tag{4.116}$$

so that ℓ_i approaches zero as i tends to infinity.

Proof of Lemma 4.6: The metric (compare (4.99))

$$e^{\omega_{*,\sqrt{t}}} h_0 = \Big(\frac{\pi}{|\log t|}\csc(\pi\frac{\log|z|}{\log|t|})\Big)^2 \frac{|dz|^2}{|z|^2} \tag{4.117}$$

has constant negative scalar curvature equal to -2. Furthermore, the circle $S_{1/i}$ is minimal when $t = i^2$:

$$\partial_\rho(\rho e^{\frac{\omega_{*,i}}{2}})|_{\rho=1/i} = 0\,. \tag{4.118}$$

The conformal factor $e^{\omega_{*,i}}$ tends to infinity at $\rho = 1/i^2$ and at $\rho = 1$.

The change of the complex variable $z \mapsto w = -1/(i^2\bar{z})$, where $\bar{z}$ is the complex conjugate of z, reproduces the metric on $w \in \Gamma(1/i^2, 1)$ and exchanges the regions on both sides of the geodesic $|z| = |w| = 1/i$. Our doubled metric on ∂M is likewise symmetric relatively to this geodesic. The conformal factor e^{ω_i}, extended to $\rho \in (1/i^2, 1/i)$ using the map just described, provides a smooth solution of the Yamabe equation (4.111) on $\Gamma(1/i^2, 1)$ (compare the discussion around (4.98)). It takes finite values both at $\rho = 1/i^2$ and at $\rho = 1$. The result follows from the comparison principle. □

Corollary 4.8. *For any $\rho_1 \in (0, 1)$, there exists a constant $\hat{c} = \hat{c}(\rho_1)$ such that*

$$\omega_i \leq \hat{c} \tag{4.119}$$

on $\hat{M}_i \setminus D(\rho_1)$, independently of i.

Proof. The inequality

$$e^{w_i} \leq e^{\omega_{*,i}} = \Big(\frac{\pi}{\log(i^2)\sin(\pi\frac{\log\rho_1}{\log(i^2)})\rho_1}\Big)^2 \longrightarrow_{i\to+\infty} \frac{1}{\rho_1^2\log^2(\rho_1)}\,, \tag{4.120}$$

shows that the ω_i's are bounded by a constant $\hat{c}(\rho_1)$ independently of i on $S(\rho_1)$ for $\rho_1 \in (0, 1)$. The result follows from the maximum principle. □

The corollary gives an estimation of the conformal factors from above. To prove convergence of the sequence ω_i, away from the puncture, we also need to bound the sequence of conformal factors away from zero. The next lemma provides a first step towards this. At its heart lies the inequality (4.123), which shows that the area does not concentrate near the minimal geodesic $S_{1/i}$. The parameter $\varepsilon > 0$ below should not be confused with the parameter ϵ introduced by the exotic gluing of M_1 with M_2:

Lemma 4.9. *For all $\varepsilon > 0$ sufficiently small and all i sufficiently large we have the bounds*

$$\inf_{\partial M_1\setminus D(\varepsilon/2)}(\omega_i - \log 2) \leq \log\frac{\pi}{|\partial M_1 \setminus D(\varepsilon/2)|_{h_0}} \leq \sup_{\partial M_1\setminus D(\varepsilon/2)}\omega_i\,, \tag{4.121}$$

where $|U|_{h_0}$ denotes the h_0 area of a set U, and note that the middle term is independent of i.

Proof. We have

$$\int_{\Gamma(a,b)} e^{\omega_{*,i}}d\mu_{h_0} = -\frac{2\pi^2\cot\Big(\frac{\pi\log(\rho)}{\log(i^2)}\Big)}{\log(i^2)}\Big|_a^b\,, \tag{4.122}$$

and note that

$$\int_{\Gamma(1/i,\varepsilon/2)} e^{\omega_{*,i}} d\mu_{h_0} = \frac{2\pi^2 \cot\left(\frac{\pi \log(2/\varepsilon)}{\log(i^2)}\right)}{\log(i^2)} \to_{i\to\infty} \frac{2\pi}{\log(2/\varepsilon)} \to_{\varepsilon\to 0} 0\,. \tag{4.123}$$

Equation (4.110) gives

$$2\pi \;=\; \int_{\hat{M}_i} e^{\omega_i} d\mu_{h_0} = \int_{\partial M_1 \setminus D(\varepsilon/2)} e^{\omega_i} d\mu_{h_0} + \int_{\Gamma(1/i,\varepsilon/2)} e^{\omega_i} d\mu_{h_0}\,. \tag{4.124}$$

The estimate (4.114) shows that

$$\int_{\Gamma(1/i,\varepsilon/2)} e^{\omega_i} d\mu_{h_0} \;\leq\; \int_{\Gamma(1/i,\varepsilon/2)} e^{\omega_{*,i}} d\mu_{h_0}\,. \tag{4.125}$$

Equation (4.123) shows that there exists ε_0 such that for all $2/i < \varepsilon \leq \varepsilon_0$ the last term in (4.124) is in $(0,\pi)$, which implies

$$\pi \leq \int_{\partial M_1 \setminus D(\varepsilon/2)} e^{\omega_i} d\mu_{h_0} < 2\pi\,. \tag{4.126}$$

The conclusion readily follows using

$$\int_{\partial M_1 \setminus D(\varepsilon/2)} e^{\inf \omega_i} d\mu_{h_0} \leq \int_{\partial M_1 \setminus D(\varepsilon/2)} e^{\omega_i} d\mu_{h_0} \leq \int_{\partial M_1 \setminus D(\varepsilon/2)} e^{\sup \omega_i} d\mu_{h_0}\,. \tag{4.127}$$

□

We continue with:

Lemma 4.10. *There exists a smooth function*

$$\omega_\infty : \partial M_1 \setminus \{p\} \to \mathbb{R} \tag{4.128}$$

such that a subsequence of $\{\omega_{i_j}\}_{j\in\mathbb{N}}$ converges uniformly, together with any number of derivatives, to ω_∞ on every compact subset of $\partial M_1 \setminus \{p\}$.

Proof. Let K be any compact subset of $\partial M_1 \setminus \{p\}$, there exists $\rho_K > 0$ such that $K \subset \partial M_1 \setminus D(\rho_K)$. It thus suffices to prove the result with $K = \partial M_1 \setminus D(\rho_K)$, which will be assumed from now on.

Let $K_1 = \partial M_1 \setminus D(\rho_K/2)$. Choosing $\varepsilon < \rho_K/4$ in Lemma 4.9 ensures that (4.121) holds on K_1 for all $i \geq i_1$ for some $i_1 < \infty$. Let $i \geq i_1$, by Corollary 4.8 there exists a constant c_1, independent of i, such that

$$v_i := -\omega_i \geq c_1 \tag{4.129}$$

on K_1. Define

$$\hat{v}_i := v_i - c_1 + 1\,. \tag{4.130}$$

It holds that $\hat{v}_i \geq 1$ on K_1. Moreover, $\hat{v}_i$ satisfies the equation[a]

$$\Delta_{h_0} \hat{v}_i = \psi_i \hat{v}_i \,, \tag{4.131}$$

where

$$0 \geq \psi_i := -2\frac{e^{-v_i}}{\hat{v}_i} \geq -2e^{-c_1} \,. \tag{4.132}$$

By Harnack's inequality there exists a constant $C_1 = C_1(K, K_1) > 0$ such that on K we have

$$\sup_K \hat{v}_i \leq C_1 \inf_{K_1} \hat{v}_i \,. \tag{4.133}$$

This, together with the definition of $\hat{v}_i$, shows that

$$\sup_K v_i \leq C_1 \inf_{K_1} v_i + d_1 = C_1(-\sup_{K_1} \omega_i) + d_1 \,, \tag{4.134}$$

for some constant d_1. Equation (4.121) gives

$$-\sup_{K_1} \omega_i \leq -\ln \frac{\pi}{|\partial M_1 \setminus D(\varepsilon/2)|_{h_0}} =: c_2 \,, \tag{4.135}$$

From (4.134) we obtain

$$\sup_K v_i \leq C_1 c_2 + d_1 \quad \Longrightarrow \quad \inf_K \omega_i = -\sup_K v_i \geq -(C_1 c_2 + d_1) \,. \tag{4.136}$$

This, together with (4.129), shows that that for every compact subset K of $\partial M_1 \setminus \{p\}$ there exists a constant $\hat{C}_K$ such that

$$-\hat{C}_K \leq \omega_i \leq \hat{C}_K \,. \tag{4.137}$$

Elliptic estimates, together with a standard diagonalisation argument, show that there exists a subsequence ω_{i_j} which converges uniformly on every compact subset of $\partial M_1 \setminus \{p\}$ to a solution ω_∞ of (4.108) on $\partial M_1 \setminus \{p\}$. Convergence of derivatives follows again from elliptic estimates. □

We return to the proof of Theorem 4.3. Equation (4.110) shows that we can use [102] to conclude that there exists $\alpha > -2$ such that for small ρ we have

$$\omega_\infty = \alpha \log \rho + O(1) \qquad \Longrightarrow \qquad e^{\omega_\infty} \sim \rho^\alpha \,, \tag{4.138}$$

or

$$\omega_\infty = -2\log(-\rho \log \rho) + O(1) \qquad \Longrightarrow \qquad e^{\omega_\infty} \sim \rho^{-2} \log^{-2} \rho \,. \tag{4.139}$$

Now, we claim that the case $\alpha \geq 0$ cannot occur in our context. Indeed, if (4.138) holds,

[a] We are grateful to Yanyan Li for providing the argument leading to (4.134).

integrating (4.111) over $\mathbb{T}^2 \setminus D(p,\delta)$ one finds, for i large enough,

$$0 < 2\int_{\mathbb{T}^2\setminus D(p,\delta)} e^{\omega_i}\, d\mu_{h_0} = \int_{\mathbb{T}^2\setminus D(p,\delta)} \Delta\omega_i\, d\mu_{h_0} = -\oint_{S_\delta} \partial_\rho \omega_i\, d\varphi \to_{i\to\infty} -2\pi\alpha + O(\delta)\,. \tag{4.140}$$

Choosing δ sufficiently small, we conclude that

$$\alpha \in (-2, 0)\,. \tag{4.141}$$

We are ready now to analyse the mass of M. By construction, M is the union of $M_1 \setminus \mathscr{U}_{1,1/i}$ and $M_2 \setminus \mathscr{U}_{1,1/i}$, identified along the boundary $\mathfrak{h}_{1,i}$. Since the metric is exactly hyperbolic in $\mathscr{U}_{1,\epsilon}$, the mass integrands vanish in $\mathscr{U}_{1,\epsilon} \setminus \mathscr{U}_{1,1/i}$. Let $m_{i,\epsilon}$ denote the mass of either summand in (4.80). In space-dimension $n = 3$ we have

$$\begin{aligned} m_{i,\epsilon} &= -\lim_{x\to 0}\int_{\{x\}\times\partial M_1} D^j(\psi_i V_1)(R^k{}_j - \frac{R}{3}\delta^k_j)\, d\sigma_k \\ &= -\lim_{x\to 0}\int_{\{x\}\times(\partial M_1\setminus D(\epsilon))} D^j(\psi_i V_1)(R^k{}_j - \frac{R}{3}\delta^k_j)\, d\sigma_k\,, \end{aligned} \tag{4.142}$$

where

$$\psi_i = e^{-\omega_i/2}\,. \tag{4.143}$$

We will need to estimate the derivatives of the functions ψ_i. As a step towards this, for $y \in \overline{D(4)\setminus D(1/2)}$ we set

$$f_{i,\epsilon}(y) = \begin{cases} \omega_i(\epsilon y) - \alpha\log(\epsilon|y|), & \text{under (4.138);} \\ \omega_i(\epsilon y) + 2\log(-\epsilon|y|\log(\epsilon|y|)), & \text{under (4.139).} \end{cases} \tag{4.144}$$

Each of the functions $f_{i,\epsilon}$ satisfies on $D(4)\setminus\overline{D(1/2)}$ the equation

$$\Delta_{h_0} f_{i,\epsilon} = \begin{cases} 2\epsilon^{2+\alpha}|y|^\alpha e^{f_{i,\epsilon}}, & \text{under (4.138);} \\ \dfrac{2e^{f_{i,\epsilon}}}{|y|^2(\log(\epsilon|y|))^2} - \dfrac{2}{|y|^2(\log(\epsilon|y|))^2}, & \text{under (4.139).} \end{cases} \tag{4.145}$$

For every ϵ there exists $i_0(\epsilon)$ such that the functions $f_{i,\epsilon}$ are bounded uniformly in ϵ and i for $i \geq i_0$. This leads to an estimate on the derivatives of $f_{i,\epsilon}$ on $\overline{D(2)\setminus D(1)}$ (see [103, Section 3.4]):

$$|\partial f_{i,\epsilon}| + |\partial\partial f_{i,\epsilon}| \leq C\,, \tag{4.146}$$

for some constant C independent of ϵ and of i provided that $i \geq i_0(\epsilon)$.

In view of (4.142)-(4.143), we will need estimates for $e^{-\omega_i/2}$. From (4.146) one obtains on $\overline{D(2\epsilon)\setminus D(\epsilon)}$, for $i \geq i_0(\epsilon)$,

$$|\partial_A e^{-\omega_i/2}| \leq C\epsilon^{-1}e^{-\omega_i/2}\,, \qquad |\partial_A\partial_B e^{-\omega_i/2}| \leq C\epsilon^{-2}e^{-\omega_i/2}\,, \tag{4.147}$$

for some possibly different constant C which is independent of ϵ and i when $i \geq i(\epsilon)$.

Directly from [102], or replacing v_i by v_∞ in the argument just given, one finds

$$|\partial_A e^{-\omega_\infty/2}| \leq C\rho^{-1}e^{-\omega_\infty/2}\,, \qquad |\partial_A\partial_B e^{-\omega_\infty/2}| \leq C\rho^{-2}e^{-\omega_\infty/2}\,, \tag{4.148}$$

for possibly yet another constant C.

Equation (4.142) can be rewritten as

$$\begin{aligned} m_{i,\epsilon} \;=\; & \underbrace{-2\int_{\partial M_1\setminus D(2\epsilon)} D^j(\psi_i V_1)(R^k{}_j - \frac{R}{n}\delta^k_j)\,d\sigma_k}_{=:\hat{m}_{i,\epsilon}} \\ & \underbrace{-2\lim_{x\to 0}\int_{\{x\}\times\overline{(D(2\epsilon)\setminus D(\epsilon/2))}} D^j(\psi_i V_1)(R^k{}_j - \frac{R}{n}\delta^k_j)\,d\sigma_k}_{=:(*)}\,. \end{aligned} \tag{4.149}$$

We claim that the second line can be made arbitrarily small by choosing i sufficiently large and ϵ sufficiently small. For this, we apply the divergence theorem on the set

$$\Omega_\epsilon := \{0 \leq x \leq \epsilon/100\} \times (\overline{D(2\epsilon)\setminus D(\epsilon/2)})\,.$$

Letting

$$\mathbb{X}^k := (R^k{}_j - \frac{R}{n}\delta^k_j)D^j(\psi_i V_1)\,, \tag{4.150}$$

where ψ_i has been extended away from ∂M_1 by requiring $\partial_r\psi_i = 0$, we have

$$\int_{\Omega_\epsilon} D_k\mathbb{X}^k d\mu_g = (*) + \underbrace{\int_{\Omega_\epsilon\cap\{x=\epsilon/100\}}\mathbb{X}^k d\sigma_k}_{=:a} + \underbrace{\int_{[0,\epsilon/100]\times S_{2\epsilon}}\mathbb{X}^k d\sigma_k}_{=:b} + \underbrace{\int_{[0,\epsilon/100]\times S_{\epsilon/2}}\mathbb{X}^k d\sigma_k}_{=:c}\,. \tag{4.151}$$

On $[0,\epsilon/100]\times S_{\epsilon/2}$ the metric is exactly hyperbolic, thus $c = 0$.

We will do the calculation that follows in general dimensions $n \geq 3$. We will assume (4.86) except that we require now

$$\sigma > n - \frac{1}{2}\,. \tag{4.152}$$

Following [63] we define s via the inequality

$$\sigma > (n-1)/2 + s \text{ for some } s \in (n/2, (n+1)/2) \tag{4.153}$$

(actually $s = n/2$ is also allowed in [63] but we need $s > n/2$ in our calculations below). We then have the following estimates in Ω_ϵ ([23], see also [63, Remark 2.1]):

$$|g-b|_b + |Db|_b + |D^2 b|_b = O(r^{-\sigma}) + o(\epsilon^{\sigma-s}r^{-s})\,; \tag{4.154}$$

recall that D is the covariant derivative of g and $r = 1/x$. Let $\bar{V} = \psi_i r \equiv \psi_i V_1$. Then $d\bar{V} = \psi_i dr + r\partial_A \psi_i dx^A$ so that $|d\bar{V}|_b = \sqrt{r^2\psi_i^2 + |d\psi_i|^2_{h_0}}$. We thus have

$$|d\bar{V}|_b \leq \psi_i r + |d\psi_i|_{h_0}\,, \tag{4.155}$$

and

$$|R^i{}_j - \frac{R}{n}\delta^i_j|_b = \begin{cases} 0, & \text{in the hyperbolic region;} \\ O(r^{-\sigma}) + o(\varepsilon^{\sigma-s}r^{-s}), & \text{in the gluing region;} \\ O(r^{-\sigma}), & \text{elsewhere.} \end{cases} \tag{4.156}$$

We are ready now to consider the integral b in (4.151). There we are in the last case of (4.156) so that, setting $x = 1/r$, it holds

$$b = \int_{[0,\epsilon/100]\times S_{2\epsilon}} O(x^\sigma)(O(x^{-1})\psi_i + |d\psi_i|_{h_0})x^{1-n}\,dx\,d^{n-2}\mu\,, \tag{4.157}$$

where $d^{n-2}\mu$ is the measure induced by h_0 on $S_{2\epsilon}$. Convergence of the integral in x requires $\sigma > n-1$ (which is satisfied in view of (4.152)), and after integration one obtains

$$b = \int_{S_{2\epsilon}} O(\epsilon^{\sigma-n+1})(\psi_i + \epsilon|d\psi_i|_{h_0})d^{n-2}\mu\,. \tag{4.158}$$

Consider, next, the integral a in (4.151). At $r = 100/\epsilon$ we find, after taking into account the measure induced by g,

$$a = \int_{D(2\epsilon)\setminus D(\epsilon/2)} (O(\epsilon^{\sigma-n})\psi_i + O(\epsilon^{\sigma-n+1})|d\psi_i|_{h_0})d\mu_{h_0}\,. \tag{4.159}$$

We pass now to the analysis of the integral over Ω_ϵ. A calculation shows that

$$\mathring{D}\mathring{D}\bar{V} = \bar{V}b + r\partial_A\partial_B\psi_i\,dx^A dx^B \tag{4.160}$$

(recall that $\mathring{D}$ is the covariant derivative of the metric $b = dr^2/r^2 + r^2 h_0$), so that

$$|\mathring{D}\mathring{D}\bar{V} - \bar{V}b|_b = \frac{\sqrt{h_0^{AB}h_0^{CD}\partial_A\partial_C\psi_i\partial_B\partial_D\psi_i}}{r} \equiv \frac{|\partial^2\psi_i|_{h_0}}{r}\,. \tag{4.161}$$

Thus, with the error terms for tensors in b-norm unless explicitly indicated otherwise,

$$\begin{aligned} D_kD_j\bar{V} &= \mathring{D}_k\mathring{D}_j\bar{V} + (O(r^{-\sigma}) + o(\varepsilon^{\sigma-s}r^{-s}))D\bar{V} \\ &= \bar{V}b_{kj} + O(|\partial^2\psi_i|_{h_0}r^{-1}) + (O(r^{-\sigma}) + o(\varepsilon^{\sigma-s}r^{-s}))D\bar{V} \\ &= \bar{V}(g_{kj} + O(r^{-\sigma}) + o(\varepsilon^{\sigma-s}r^{-s})) + O(|\partial^2\psi_i|_{h_0}r^{-1}) \\ &\quad +(O(r^{-\sigma}) + o(\varepsilon^{\sigma-s}r^{-s}))(\psi_i r + |d\psi_i|_{h_0}) \\ &= \bar{V}g_{kj} + O(|\partial^2\psi_i|_{h_0})r^{-1} + \psi_i(O(r^{1-\sigma}) + o(\varepsilon^{\sigma-s}r^{1-s})) \\ &\quad +|d\psi_i|_{h_0}(O(r^{-\sigma}) + o(\varepsilon^{\sigma-s}r^{-s}))\,. \end{aligned} \tag{4.162}$$

Next, the curvature scalar R is constant, which implies that $D_iR^i{}_j = 0$ by the (twice contracted) second Bianchi identity. We thus find

$$\begin{aligned} D_k\mathbb{X}^k &= \underbrace{(R^k{}_j - \frac{R}{n}\delta^k_j)}_{O(r^{-\sigma})+o(\varepsilon^{\sigma-s}r^{-s})} D_kD^j\bar{V} \\ &= (O(r^{-\sigma}) + o(\varepsilon^{\sigma-s}r^{-s}))(O(r^{1-\sigma}) + o(\varepsilon^{\sigma-s}r^{-s+1}))\psi_i \\ &\quad +(O(r^{-\sigma}) + o(\varepsilon^{\sigma-s}r^{-s}))(O(r^{-\sigma}) + o(\varepsilon^{\sigma-s}r^{-s}))|d\psi_i|_{h_0} \\ &\quad +(O(r^{-\sigma-1}) + o(\epsilon^{\sigma-s}r^{-s-1}))|\partial^2\psi_i|_{h_0} \\ &= (O(r^{-2\sigma+1}) + o(\varepsilon^{\sigma-s}r^{-s-\sigma+1}) + o(\varepsilon^{2\sigma-2s}r^{-2s+1}))\psi_i \\ &\quad +(O(r^{-2\sigma}) + o(\varepsilon^{\sigma-s}r^{-s-\sigma}) + o(\varepsilon^{2\sigma-2s}r^{-2s}))|d\psi_i|_{h_0} \\ &\quad +(O(r^{-\sigma-1}) + o(\epsilon^{\sigma-s}r^{-s-1}))|\partial^2\psi_i|_{h_0}\,. \end{aligned} \tag{4.163}$$

The requirement of convergence of the integral in r together with (4.153) leads to the restriction $n < 5$. Assuming this, we find

$$\int_{\Omega_\epsilon} D_k\mathbb{X}^k d\mu_g = \int_{D(2\epsilon)\setminus D(\epsilon/2)} (O(\epsilon^{2\sigma-n})\psi_i + O(\epsilon^{2\sigma-n+1})|d\psi_i|_{h_0} + O(\epsilon^{\sigma-n+2})|\partial^2\psi_i|_{h_0})d\mu_{h_0}\,. \tag{4.164}$$

Collecting terms in (4.151) leads to the following form of (4.149)

$$\begin{aligned} m_{i,\epsilon} &= \hat{m}_{i,\epsilon} + \int_{S_{2\epsilon}} O(\epsilon^{\sigma-n+1})(\psi_i + \epsilon|d\psi_i|_{h_0})d^{n-2}\mu \\ &\quad + \int_{D(2\epsilon)\setminus D(\epsilon/2)} (O(\epsilon^{\sigma-n})\psi_i + O(\epsilon^{\sigma-n+1})|d\psi_i|_{h_0} + O(\epsilon^{\sigma-n+2})|\partial^2\psi_i|_{h_0})d\mu_{h_0}\,. \end{aligned} \tag{4.165}$$

Let $\eta > 0$ and $\psi_\infty = e^{-\omega_\infty/2}$. If $n = 3$ (thus $\sigma > 5/2$), by (4.138)-(4.139), (4.141) and

(4.148) we can choose ϵ small enough so that

$$\int_{S_{2\epsilon}} O(\epsilon^{\sigma-n+1})(\psi_i + \epsilon|d\psi_i|_{h_0})d^{n-2}\mu$$
$$+ \int_{D(2\epsilon)\setminus D(\epsilon/2)} (O(\epsilon^{\sigma-n})\psi_\infty + O(\epsilon^{\sigma-n+1})|d\psi_\infty|_{h_0} + O(\epsilon^{\sigma-n+2})|\partial^2\psi_\infty|_{h_0})d\mu_{h_0} < \eta/2\,. \tag{4.166}$$

The function ψ_i tends uniformly on $\overline{D(2\epsilon)\setminus D(\epsilon/2)}$ to ψ_∞ when i tends to infinity. This, together with (4.147), shows that we can choose i large enough so that

$$\int_{S_{2\epsilon}} O(\epsilon^{\sigma-n+1})(|\psi_\infty - \psi_i| + \epsilon|d\psi_\infty - d\psi_i|_{h_0})d^{n-2}\mu$$
$$+ \int_{D(2\epsilon)\setminus D(\epsilon/2)} \Big(O(\epsilon^{\sigma-n})|\psi_\infty - \psi_i| + O(\epsilon^{\sigma-n+1})|d(\psi_\infty - \psi_i)|_{h_0}$$
$$+ O(\epsilon^{\sigma-n+2})|\partial^2(\psi_\infty - \psi_i)|_{h_0}\Big)d\mu_{h_0} < \eta/2\,. \tag{4.167}$$

We conclude that the integral over the annulus $\overline{D(2\epsilon)\setminus D(\epsilon/2)}$ tends to zero as ϵ tends to zero and i tends to infinity.

The above analysis of the mass can be summarised as follows:

Proposition 4.11. *Suppose that for every $\eta > 0$ we can find i large enough so that* (4.166)-(4.167) *hold. Then, when ϵ tends to zero and i tends to infinity the mass of each summand of (M, g) tends to*

$$-\lim_{x\to 0}\int_{\{x\}\times\partial M_1} D^j(\psi_\infty V_1)(R^k{}_j - \frac{R}{n}\delta^k_j)\,d\sigma_k\,, \tag{4.168}$$

where the limit exists and is finite.

By Remark 4.7 and Deligne-Mumford compactness (cf., e.g., [104, Proposition A.2, Appendix A.1]) the metric $e^{\omega_\infty}h_0$ is the hyperbolic metric on the punctured torus. This finishes the proof or Theorem 4.3. □

Remark 4.12. For further reference, we comment on the possibility that the discrete family of circles $S_{1/i}$ across which the doubling has been done is replaced by a continuous family S_a, with $a \in (0, a_0)$ for some $a_0 > 0$, with associated family of solutions ω_a. The only place in our arguments above where the discrete character of the parameter a matters is the extraction of a diagonal subsequence so that the solutions converge to a limiting function. For this we take any sequence a_i converging to zero, so that the resulting sequence ω_{a_i} has a subsequence $\omega_{a_{i_j}}$ converging to a limiting function, say $\omega_{\{a_{i_j}\}}$, on compact subsets of $\mathbb{T}^2\setminus\{p\}$. By what has been said the metric $e^{\omega_{\{a_{i_j}\}}}h_0$ is the unique hyperbolic metric on $\mathbb{T}^2\setminus\{p\}$ with puncture at p, hence is independent both

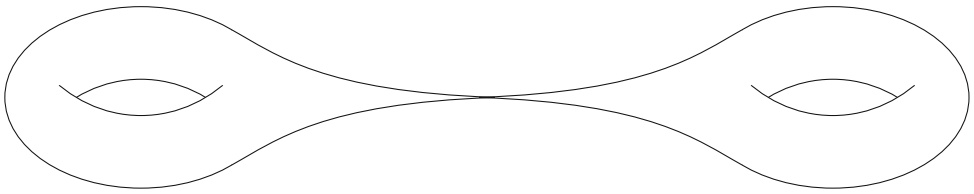

Figure 4.6.: Two punctured tori, connected by a thin neck. In the limit $i \to \infty$ the necks become longer and longer with circumferences shrinking to zero.

of the sequence a_{i_j} and of the sequence a_i. Setting $\omega_\infty := \omega_{\{a_{i_j}\}}$, it is then standard to show that ω_a converges to ω_∞ on any compact subset of $\mathbb{T}^2 \setminus \{p\}$ as a tends to zero, and depends continuously on a on any compact subset of $\mathbb{T}^2 \setminus \{p\}$ in C^∞, with the length of the minimizing geodesic in the middle of the connecting neck depending continuously upon a, and with the mass of (M, g) depending continuously upon a.

It is of interest to enquire about the shape of the glued boundary-manifold. From what has been said the metric on the conformal boundary converges (uniformly on compact sets away from the puncture) to the cusp metric on each of the two copies of the punctured torus (cf. Figure 4.5), with asymptotic behavior near the puncture approximated by (compare [105])

$$\frac{1}{\rho^2 \log^2(\rho)}(dx^2 + dy^2) = \frac{1}{\rho^2 \log^2(\rho)}(d\rho^2 + \rho^2 d\varphi^2)\,. \tag{4.169}$$

Since

$$\int \frac{1}{\rho \log \rho} d\rho = \log(-\log \rho) \to_{\rho \to 0} \infty\,, \tag{4.170}$$

the connecting necks become longer and longer, with a circumference $\approx 2\pi/|\log \rho| = 2\pi/\log i$ tending to zero when $i \to \infty$, see Figure 4.6.

4.7.2. Higher genus

It should be clear that one can iterate the construction of the last section to obtain three-dimensional conformally compact ALH manifolds without boundary, with constant scalar curvature, negative mass, and a conformal infinity of arbitrary genus. One possible way of doing this proceeds as follows: Let (M_1, g_1) be a three-dimensional ALH metric with constant scalar curvature and toroidal boundary at infinity. Let $N \in \mathbb{N}$ and let $\{p_i\}_{i=1}^N$ be a collection of points lying on the conformal boundary ∂M_1 of M_1. Let $\mathscr{U}_i$ be any pairwise-disjoint family of coordinate half-balls of coordinate radius ϵ_i centered at the points p_i. Let (M_2, g_2) be another ALH manifold with the same asymptotic behaviour and identical conformal geometry at infinity; e.g., an identical copy of (M_1, g_1). The manifold (M, g) is taken to be a boundary-gluing of (M_1, g_1) with (M_2, g_2), where each $\mathscr{U}_i \subset M_1$ is glued with its partner in M_2 in a symmetric way; Figure 4.8 illustrates what

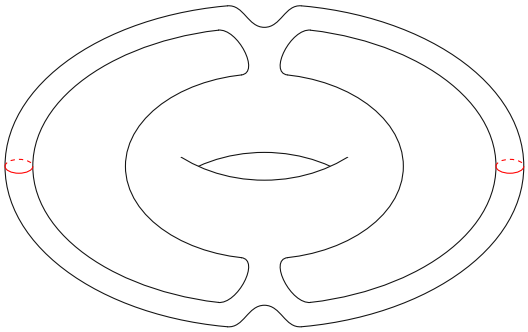

Figure 4.7.: The symmetry ψ is a reflection across the vertical plane passing through the center of the figure. The gluing is done at the discs, whose boundaries become closed geodesics on the boundary, indicated in red in the figure. The construction is symmetric under the reflection across the horizontal plane passing through the center of the figure.

happens at the conformal boundary at infinity. Solving the Yamabe equation on ∂M, for $j \in \mathbb{N}$ one obtains a function ω_j on

$$\hat{M}_j := \partial M_1 \setminus \left(\cup_{i=1}^{N} D(p_i, 1/j) \right) \tag{4.171}$$

such that the constant-Gauss-curvature representative of the conformal metric on ∂M equals

$$e^{\omega_j} h_0 \,. \tag{4.172}$$

This leads to the integral identity

$$\int_{\hat{M}_j} e^{\omega_j} d\mu_{h_0} = 2N\pi \,. \tag{4.173}$$

The analysis of Section 4.7.1 applies near each of the punctures p_i. Letting $m(\epsilon_1, \cdots, \epsilon_N, j)$ denote the mass of (M, g) we conclude that if we started with a Horowitz-Myers metric we will have

$$m(\epsilon_1, \cdots, \epsilon_N, j) < 0 \tag{4.174}$$

for all j larger than j_0, for some j_0 that depends upon $\max \epsilon_i$.

From (4.173) we find

$$|\partial M|_{h_{-1}} = 2 \int_{\hat{M}_j} e^{\omega_j} d\mu_{h_0} = 4N\pi \,. \tag{4.175}$$

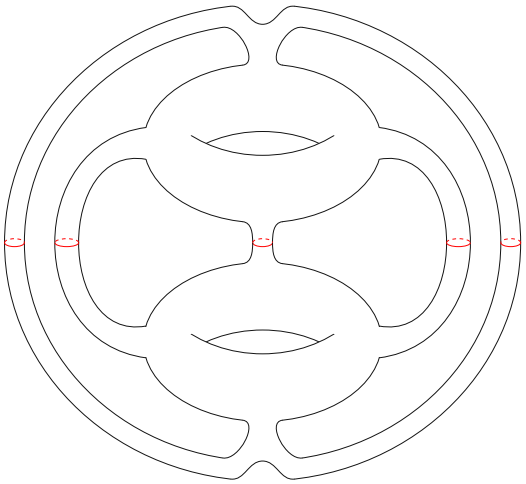

Figure 4.8.: The gluing is done at the discs, whose boundaries become closed geodesics on the boundary, indicated in red in the figure. The construction is symmetric under the reflection across the horizontal plane passing through the center of the figure.

Equivalently, since the scalar curvature $R_{h_{-1}}$ of the metric h_{-1} equals -2 we have

$$4\pi\chi(\partial M) = \int_{\partial M} R_{h_{-1}} d\mu_{h_{-1}} = -4 \int_{\hat{M}_j} e^{\omega_j} d\mu_{h_0} = -8N\pi\,, \tag{4.176}$$

which shows that $\chi(\partial M) = -2N$, and thus ∂M has genus $N+1$.

A variation of the above is the following: Let $\psi : \partial M_1 \to \partial M_1$ be an isometry of (M_1, h_0) such that $\psi \circ \psi$ is the identity map. Let N be even, say $N = 2\hat{N}$, and suppose that the collection $\{p_i\}_{i=1}^{N}$ of N distinct points on ∂M_1 takes the form $\{q_i, \psi(q_i)\}_{i=1}^{\hat{N}}$. We can then pairwise glue, as above, neighborhoods of the points q_i with neighborhoods of their ψ-symmetric partners $\psi(q_i)$. Thus ∂M is obtained by adding to ∂M_1 a family of $\hat{N}$ necks connecting the points q_i and $\psi(q_i)$; see Figure 4.7.

Let M_1 be the Horowitz-Myers instanton. If we choose ψ and the necks in a way compatible with the constructions described in Section 4.7.1, one obtains a family of ALH manifolds with constant scalar curvature, with conformal infinity of genus $\hat{N}+1$, with masses $m(\epsilon_1, \cdots, \epsilon_{\hat{N}}, j)$ which are negative for j large enough.

4.8. A lower bound on mass?

It has been conjectured [20, 62] that the Horowitz–Myers instantons have the lowest mass within the class of ALH manifolds without boundary and with the same conformal metric at their toroidal infinity. If it were true, that the mass for conformally compact three-dimensional manifolds with constant scalar curvature and toroidal infinity can be arbitrarily negative at fixed conformal class at infinity, then our construction would

provide higher-genus constant-scalar-curvature metrics which have arbitrarily negative mass at fixed conformal class at infinity.

As such, one can envision a construction that cuts a metric with conformal infinity of higher genus into pieces, producing a finite number of ALH metrics with toroidal infinity which would assemble together to the original one by a boundary-gluing in the spirit of this work. The validity of the Horowitz–Myers conjecture would then provide a lower bound for the mass of each summand. It is thus tempting to formulate the following conjecture

Conjecture 4.13. *Let (M, g) be an n-dimensional conformally compact ALH manifold, without boundary with well defined mass m and with scalar curvature satisfying $R \geq -n(n-1)$. There exists a constant m_0, which depends only upon the conformal class of the metric at infinity and which is negative if this conformal class is not that of the round sphere, such that*

$$m \geq m_0 \,. \tag{4.177}$$

It is also tempting to conjecture existence of unique static metrics as above which saturate the inequality if m_0 is optimal.

5. Conclusions

In this thesis, we have investigated aspects of general relativity with negative cosmological constant in three and four spacetime dimensions. In chapter 3, we focused on a particular solution to Einstein gravity with negative cosmological constant, the BTZ black hole, and showed that it can be visualized using projection diagrams [24], introduced in this thesis in chapter 2. Indeed, the diagrams provided in [35] are precisely such projection diagrams. We argued why slices of the BTZ black hole do not provide a meaningful representation of the causal structure of the three-dimensional spacetime.

Projection diagrams were also used to visualize the causal structure of a different class of spacetimes, so-called warped flat spacetimes [1]. It was shown that the quotients of warped flat space studied in [22] do not describe black hole solutions, contrary to claims made in that paper. As projection diagrams do not rely on the existence of a conformal completion, we do not conformally complete warped flat spacetimes to study their causal structure. Preliminary calculations based on the asymptotic behavior of geodesics strongly suggest that the asymptotic boundary is null and that a conformal completion does not exist. It would be of interest to prove non-existence of the conformal completion of warped flat spacetimes and prompt a similar study for warped dS_3 and warped AdS_3 spacetimes. Quotients of warped AdS_3 and warped flat space appear in the near horizon region of extremal Kerr (dS) black holes and boundary conditions encompassing these spacetimes have been studied extensively for AdS/CFT applications. We expect that clarifying these issues will shed further light on the geometry of extremal black holes and prove useful for the study of boundary conditions and asymptotic symmetries.

At the end of chapter 3, we discussed how a microstate counting of the $(2+1)$-dimensional BTZ black hole can be performed based on the asymptotic symmetry analysis of Brown and Henneaux [21] and the assumption that the phase space of quantum gravity falls into representations of this algebra [13]. For this microstate counting to work, the energy of asymptotically AdS_3 spacetimes has to be bounded from below. Results supporting this statement were provided in [50], where positivity of energy is studied using coadjoint orbits. While in higher dimensions many positive energy theorems are available in the mathematical general relativity literature, we do not know of any literature (aside from [50]) covering the case of spacetime dimension three with negative cosmological constant. It would be of interest to formulate a theorem for the case of $(2+1)$ dimensions similar to the ones available in higher dimensions. I plan to focus on this question in the near future.

The status of positive energy theorems for general relativity in *space* dimension greater or equal to three was reviewed in chapter 4 with a particular focus on the Horowitz–Myers conjecture and its connection to the AdS/CFT correspondence. We provide the results of [2], where a formula for the energy of asymptotically locally hyperbolic (ALH) manifolds

obtained by a gluing at infinity of two ALH manifolds was derived. As an application, we showed that there exist three-dimensional conformally compact ALH manifolds without black hole boundary with connected conformal infinity of higher genus, constant negative scalar curvature and negative mass. Such spaces were not known to exist previously. Recall that the mass is normalized with respect to locally hyperbolic space, which then per definition has mass zero. While this does not provide a lower bound on the energy of ALH manifolds with higher genus conformal infinity, it shows that in space dimension three the lower bound is not provided by locally hyperbolic space. Employing a putative AdS/CFT correspondence, proofing (or falsifying) the existence of a lower bound on the energy of ALH spaces, would put constraints on conformal field theories on higher genus surfaces. It would be of interest to use the gluing construction of [23] and the results from [2] to construct ALH spaces of a given topology and mass, which could be used to put further constraints on table 4.1. A particular example, currently in progress, is the construction of three-dimensional conformally compact ALH manifolds with toroidal black hole boundary, connected conformal infinity of higher genus, constant negative scalar curvature and negative mass.

I hope to have convinced the reader that the study of general relativity on negatively curved spacetimes is a fruitful endeavor with many mysteries to be unraveled — amongst them the positivity of energy and its implications on the AdS/CFT correspondence.

A. Warped Spacetimes as pseudo-Riemannian submersions

In this appendix the origin of the terminology warped AdS_3, warped dS_3 and warped flat space is explained. According to [106] AdS_3 can be written "as a kind of Hopf fibration" over AdS_2. As already discussed in the main text in subsection 3.5.2 the suitable mathematical terminology is pseudo-Riemannian submersion.

Definition A.1. ***Submersion***
If $\pi : M \to B$ is a smooth map, we have the push-forward $\pi_* : TM \to TB$. If π_* is surjective at every point, we say that π is a (smooth) submersion.

Definition A.2. ***Riemannian Submersion***
Let (M, g) and (B, h) be Riemannian manifolds. A Riemannian submersion $\pi : M \to B$ is a surjective submersion from one Riemannian manifold to another satisfying that the push-forward $\pi_* : TM \to TB$ preserves the length of horizontal vectors: $\pi_* : \ker(\pi_*)^\perp \to TB$ is an isometry.

The definition of a Riemannian submersion can be extended to pseudo-Riemannian manifolds. In the examples below, we have that (M, g) is warped AdS_3, warped dS_3 and warped flat space, while (B, h) is AdS_2, dS_2 and $\mathbb{R}^{1,1}$.

Warped AdS_3 Space

We start with warped AdS_3 space (M, g) with metric

$$g = \frac{1}{\nu^2 + 3\epsilon}\left(-\cosh^2\sigma d\tau^2 + d\sigma^2 + \frac{4\nu^2}{\nu^2 + 3\epsilon}(dy + \sinh\sigma d\tau)^2\right). \tag{A.1}$$

The first two terms in the bracket comprise AdS_2 space (B, h) with metric

$$h = \frac{1}{\nu^2 + 3\epsilon}\left(-\cosh^2\sigma d\tau^2 + d\sigma^2\right) \tag{A.2}$$

and curvature $R = -6\epsilon + 2\nu^2$. We now check explicitly whether $\pi : M \to B$, $(y, \sigma, \tau) \mapsto (\sigma, \tau)$ is a pseudo-Riemannian submersion. We have

$$\ker(\pi_*) = \mathrm{span}\{\partial_y\} \tag{A.3}$$

and

$$\ker(\pi_*)^\perp = \{v | g(\partial_y, v) = 0\} = \mathrm{span}\{\partial_\sigma, -\sinh\sigma\partial_y + \partial_\tau\}\,. \tag{A.4}$$

Now, π is a pseudo-Riemannian submersion if $\pi_* : \ker(\pi_*)^\perp \to TB$ is an isometry. Since

$$g(\partial_\sigma, \partial_\sigma) = \frac{1}{\nu^2 + 3\epsilon} = h(\partial_\sigma, \partial_\sigma)\,, \tag{A.5}$$

$$g(-\sinh\sigma\partial_y + \partial_\tau, -\sinh\sigma\partial_y + \partial_\tau) = -\frac{1}{\nu^2 + 3\epsilon}\cosh^2\sigma = h(\partial_\tau, \partial_\tau)\,, \tag{A.6}$$

$$g(-\sinh\sigma\partial_y + \partial_\tau, \partial_\sigma) = 0 = h(\partial_\tau, \partial_\sigma)\,. \tag{A.7}$$

the map $\pi : \mathrm{WAdS}_3 \to \mathrm{AdS}_2$, $(y, \sigma, \tau) \mapsto (\sigma, \tau)$ is a pseudo-Riemannian submersion.

Warped dS_3 Space

Warped dS space (M, g) is given by

$$g = \frac{1}{3 - \nu^2}\left(-d\sigma^2 + \sinh^2(\sigma)d\tau^2 + \frac{4\nu^2}{\nu^2 - 3}(dy + \cosh(\sigma)d\tau)^2\right). \tag{A.8}$$

The relation to the coordinates in the main text (3.131) is given by

$$r = \cosh(\sigma)\,. \tag{A.9}$$

The first two terms in the bracket comprise dS_2 space (B, h) with metric

$$h = \frac{1}{3 - \nu^2}\left(-d\sigma^2 + \sinh^2(\sigma)d\tau^2\right). \tag{A.10}$$

and curvature $R = 6 - 2\nu^2$. The map $\pi : M \to B$, $(y, \sigma, \tau) \mapsto (\sigma, \tau)$ is a pseudo-Riemannian submersion since

$$\ker(\pi_*) = \mathrm{span}\{\partial_y\} \tag{A.11}$$

and

$$\ker(\pi_*)^\perp = \{v | g(\partial_y, v) = 0\} = \mathrm{span}\{\partial_\sigma, -\cosh\sigma\partial_y + \partial_\tau\} \tag{A.12}$$

yields

$$g(\partial_\sigma, \partial_\sigma) = -\frac{1}{3 - \nu^2} = h(\partial_\sigma, \partial_\sigma)\,, \tag{A.13}$$

$$g(-\cosh\sigma\partial_y + \partial_\tau, -\cosh\sigma\partial_y + \partial_\tau) = \frac{1}{3 - \nu^2}\sinh^2(\sigma) = h(\partial_\tau, \partial_\tau)\,, \tag{A.14}$$

$$g(-\cosh\sigma\partial_y + \partial_\tau, \partial_\sigma) = 0 = h(\partial_\tau, \partial_\sigma)\,. \tag{A.15}$$

Warped Flat Space

Warped flat space (M, g) reads

$$g = -d\tau^2 + dx^2 + 12(dy + xd\tau)^2 \tag{A.16}$$

and $B = R^{1,1}$

$$h = -d\tau^2 + dx^2 \,. \tag{A.17}$$

The map $\pi : M \to B, (\tau, x, y) \mapsto (\tau, x)$ is a Riemannian submersion since

$$\ker(\pi_*) = \mathrm{span}\{\partial_y\} \tag{A.18}$$

and

$$\ker(\pi_*)^\perp = \mathrm{span}\{\partial_\tau - x\partial_y, \partial_x\} \,, \tag{A.19}$$

which yields

$$g(\partial_\tau - x\partial_y, \partial_\tau - x\partial_y) = -1 = h(\partial_\tau, \partial_\tau) \,, \tag{A.20}$$

$$g(\partial_\tau - x\partial_y, \partial_x) = 0 = h(\partial_\tau, \partial_x) \,, \tag{A.21}$$

$$g(\partial_x, \partial_x) = 1 = h(\partial_x, \partial_x) \,. \tag{A.22}$$

B. A punctured torus

This appendix is from [2] (co-authored with Piotr Chruściel and Erwann Delay)

In this appendix, we review some inequalities for the simplest hyperbolic one-punctured torus which are used in the main text to provide a rough upper and lower bound on the mass. Recall that the model for the cusp (at $t = -\infty$ or $\rho = 0$) is :

$$dt^2 + e^{2t}d\varphi^2 = \frac{1}{\rho^2 \log^2(\rho)}(d\rho^2 + \rho^2 d\varphi^2), \tag{B.1}$$

with $e^{-t} = -\log(\rho)$. Here the Gauss curvature is -1, thus the Ricci scalar equals -2. The simplest hyperbolic one-punctured torus, also called "the hyperbolic torus with one cusp", is $(\mathbb{R}^2\backslash\mathbb{Z}^2)/\mathbb{Z}^2$ with a hyperbolic metric. Let us use the notation of [107] (keeping in mind a different scaling of the hyperbolic metric there) in order to compare the hyperbolic metric and the flat metric on this torus. For a domain D in $\mathbb{C}$, the complete hyperbolic metric on D with Gauss curvature equal to -1, as obtained using the Riemann mapping theorem applied to the universal covering space, is denoted by $4\rho_D^2(z)|dz|^2$. If $D \subset D'$ then by the comparison principle (4.113), also known as the Nevanlinna principle, we have $\rho_D \geq \rho_{D'}$. Let us set

$$D_0 = \hat{\mathbb{C}}\backslash\{0,1,\infty\}\ ,\ \ \mathbb{D}^* = B(0,1)\backslash\{0\}\ ,\ \ \mathbb{Z}[i] = \{m+in\ , m,n \in \mathbb{Z}\} = \mathbb{Z}^2\ ,\ \ \tilde{D} = \mathbb{C}\backslash\mathbb{Z}[i]\,. \tag{B.2}$$

Because $\mathbb{D}^* \subset \tilde{D} \subset D_0$, by the inequality of [108] (see, e.g. [107], inequality (1.2)) we have

$$\frac{1}{|z|(|\log(|z|)| + C_1)} \leq 2\rho_{D_0}(z) \leq 2\rho_{\tilde{D}}(z) \leq 2\rho_{\mathbb{D}^*}(z) = \frac{1}{|z||\log(|z|)|}\,, \tag{B.3}$$

where $C_1 = \Gamma(1/4)^4/4\pi^2 \sim 4.37688$.

Let $p : \mathbb{C} \longrightarrow T_0 = \mathbb{C}/\mathbb{Z}[i]$ be the canonical projection and denote by $[z] = p(z)$ the equivalence class of z. Let $D = T_0\backslash\{[0]\}$, then D is proper subdomain of T_0 and $p^{-1}(D) = \tilde{D}$. On D, $\rho_D([z]) = \rho_{\tilde{D}}(z)$ is well defined. This defines the "hyperbolic density" ρ_{X_0} on $X_0 = \tilde{D}/\mathbb{Z}[i]$, which is the simplest one-punctured hyperbolic torus.

Because of the symmetries of $\tilde{D}$, the inequalities (B.3) on $\{z = x + iy,\ \ x, y \in [-1/2, 1/2]\}\backslash\{0\}$ provide an estimate of ρ_{X_0} throughout X_0.

It follows from (B.3) that near the origin we have

$$2\rho_{\tilde{D}} = \frac{1}{|z||\log(|z|)|}\left(1 + O(\frac{1}{|\log(|z|)|})\right). \tag{B.4}$$

Note also that by [107] the minimum of ρ_{X_0} is attained at $\frac{1+i}{2}$ and is given by his formula (1.3):

$$\inf 2\rho_{X_0} = \frac{4\pi^{3/2}}{\Gamma(1/4)^2} \approx 1.695\,. \tag{B.5}$$

C. Static KIDs

This appendix is from [2] (co-authored with Piotr Chruściel and Erwann Delay)

In this appendix, we find all static potentials or equivalently static Killing Initial Data (KIDs), introduced in section 2.3, for the Birmingham–Kottler metric and the Horowitz–Myers metric in $(n+1)$-dimensions. We start by computing the KIDs for the Birmingham–Kottler metric (C.1). We find that for $m_c \neq 0$ and $n \neq 2$ the solution to the KID equations is given by (C.44). Otherwise, the solution to the KID equations takes the form (C.26). For $m_c = 0$ and $n \neq 2$ β is of the form (C.35) or (C.36) and Ω is a solution to the differential equations (C.37). In the case $n = 2$, the function β is of the form (C.46) or (C.47) and Ω takes the form (C.49). Next, we consider the Horowitz–Myers metric (C.50), which for $m_c = 0$ is of Birmingham–Kottler type. For $m_c \neq 0$ we have that the solution to the KID equation is given by (C.75).

Birmingham–Kottler

The Birmingham–Kottler metric in $(n+1)$-dimensions, $n \geq 2$, which we denote by $\tilde{g}$, reads

$$\tilde{g} = -f(r)dt^2 + \frac{1}{f(r)}dr^2 + r^2 \mathring{h}_{AB} dx^A dx^B \,, \tag{C.1}$$

where $\mathring{h}_{AB} = \mathring{h}_{AB}(x^C)$ where $A, B = 1, ...n-1$, and with

$$f(r) = r^2 + k - \frac{2m_c}{r^{n-2}} \tag{C.2}$$

and

$$R(\mathring{h}) = k(n-1)(n-2) \,, \quad k \in \{0, \pm 1\} \,. \tag{C.3}$$

For $n = 2$, $R(\mathring{h})$ vanishes and thus we set $k = 0$ without loss of generality and obtain

$$f(r) = r^2 - 2m_c \,. \tag{C.4}$$

The metric (C.1) fulfills the Einstein equations with negative cosmological constant

$$\Lambda = -\frac{n(n-1)}{2} \,. \tag{C.5}$$

Using this normalisation of Λ, the Einstein equations read

$$R_{ab}(\tilde{g}) = -n\tilde{g}_{ab}\,, \qquad R(\tilde{g}) = -n(n+1)\,, \tag{C.6}$$

where a, b run from $1, ..., n+1$. To compute the KIDs we need the Ricci scalar and the Ricci tensor of the spatial part of $\tilde{g}$, which we denote as g in what follows. These can be obtained from the Gauss-Codazzi equation [6]

$$R_{abcd}(g) = R^{\parallel}_{abcd}(\tilde{g}) - K_{ac}K_{bd} + K_{bc}K_{ad}\,. \tag{C.7}$$

where K_{ab} is the extrinsic curvature of the level sets of t (zero in our case)

$$K_{ab} = g_a{}^c \tilde{D}_c \tilde{n}_b\,, \tag{C.8}$$

with $\tilde{n}_a$ being the normal one-form with the normalization chosen such that $\tilde{n}^a\tilde{n}_a = -1$. The superscript "$\parallel$" means that the respective tensor is projected to the submanifold, e.g. $R^{\parallel}_{abcd}(\tilde{g}) = g_a{}^e g_b{}^f g_c{}^g g_d{}^h R_{efgh}(\tilde{g})$. Contracting with g^{ac} we obtain

$$R_{ab}(g) = R^{\parallel}_{ab}(\tilde{g}) + \left(R_{cadb}(\tilde{g})\tilde{n}^c\tilde{n}^d\right)^{\parallel} - KK_{ab} + K_{ac}K^c{}_b \tag{C.9}$$

with [7, p. 518]

$$\left(R_{cadb}(\tilde{g})\tilde{n}^c\tilde{n}^d\right)^{\parallel} = -\mathcal{L}_{\tilde{n}}K_{ab} + K_{ac}K^c{}_b + D_{(a}a_{b)} + a_a a_b\,, \tag{C.10}$$

where $a_a = \tilde{n}^b\tilde{D}_b\tilde{n}_a$, D_a denotes the covariant derivative of the metric g, such that

$$R_{ab}(g) = R^{\parallel}_{ab}(\tilde{g}) - \mathcal{L}_{\tilde{n}}K_{ab} + 2K_{ac}K^c{}_b - KK_{ab} + D_{(a}a_{b)} + a_a a_b\,. \tag{C.11}$$

The normal one-form to $t = \text{const.}$ surfaces reads

$$\tilde{n} = \sqrt{f}dt \tag{C.12}$$

such that $\tilde{n}_a\tilde{g}^{ab}\tilde{n}_b = -1$. Finally,

$$\tilde{g}_{ab} = g_{ab} - \tilde{n}_a\tilde{n}_b \tag{C.13}$$

yielding that in coordinates t, r, x^A, the tensor field g reads

$$g_{ab} = \begin{pmatrix} 0 & 0 & 0 \\ 0 & 1/f(r) & 0 \\ 0 & 0 & r^2\mathring{h}_{AB} \end{pmatrix}, \qquad g^a{}_b = \begin{pmatrix} 0 & 0 & 0 \\ 0 & 1 & 0 \\ 0 & 0 & 1_{AB} \end{pmatrix} \tag{C.14}$$

The only-nonvanishing Christoffel symbols (up to symmetries) are

$$\tilde{\Gamma}^{t}{}_{tr} = \frac{\partial_r f}{2f}\,, \quad \tilde{\Gamma}^{r}{}_{rr} = -\frac{\partial_r f}{2f}\,, \quad \tilde{\Gamma}^{r}{}_{tt} = -\frac{f\partial_r f}{2}\,, \quad \tilde{\Gamma}^{r}{}_{AB} = -r\mathring{h}_{AB} f(r)\,, \tag{C.15}$$

$$\tilde{\Gamma}^{C}{}_{rA} = \frac{\delta^{C}{}_{A}}{r}\,, \quad \tilde{\Gamma}^{C}{}_{AB} = \frac{1}{2}\mathring{h}^{CD}\Big(\partial_A \mathring{h}_{BD} + \partial_B \mathring{h}_{AD} - \partial_D \mathring{h}_{AB}\Big)\,. \tag{C.16}$$

As already mentioned, in our case all components of K_{ab} vanish, so that the expression of the Ricci tensor of the constant t submanifold (C.11) simplifies to

$$R_{ab}(g) = R^{\parallel}_{ab}(\tilde{g}) + D_{(a}a_{b)} + a_a a_b\,. \tag{C.17}$$

with $a = a_r dr$ given by

$$a_r = \tilde{n}^t \tilde{D}_t \tilde{n}_r = \frac{1}{2f}\partial_r f \tag{C.18}$$

and

$$D_r a_r = -\frac{1}{4f^2}(\partial_r f)^2 + \frac{1}{2f}\partial_r\partial_r f\,, \qquad D_A a_B = \frac{\partial_r f}{2} r\mathring{h}_{AB}\,. \tag{C.19}$$

The only non-vanishing components of the Ricci tensor of the metric induced on the submanifolds of constant t are

$$R_{rr} = -\frac{n}{f} + \frac{1}{2f}\partial_r\partial_r f\,, \qquad R_{AB} = \left(-nr^2 + \frac{\partial_r f}{2} r\right)\mathring{h}_{AB} \tag{C.20}$$

and thus

$$R = R_{rr}g^{rr} + R_{AB}g^{AB} = -n(n-1)\,, \tag{C.21}$$

where we have used the explicit form of $f(r)$. Now we consider the KID equation

$$A_{ij} := D_i D_j V - V\left(R_{ij} - \frac{R}{n-1}g_{ij}\right) = D_i D_j V - V(R_{ij} + n g_{ij}) = 0 \tag{C.22}$$

where $i, j \in 1, ...n-1$. We have that

$$A_{rr} = \partial_r\partial_r V + \frac{1}{2f}\partial_r f\partial_r V - \frac{V}{2f}\partial_r\partial_r f = 0\,, \tag{C.23}$$

$$A_{rA} = \partial_r\partial_A V - \frac{\delta_A{}^C}{r}\partial_C V = \partial_r\partial_A V - \frac{1}{r}\partial_A V = 0\,, \tag{C.24}$$

$$A_{AB} = \partial_A\partial_B V - \Gamma^{C}{}_{AB}\partial_C V + r\mathring{h}_{AB} f\partial_r V - \frac{V\partial_r f}{2} r\mathring{h}_{AB} = 0\,. \tag{C.25}$$

Integrating the second equation in r we have that

$$\boxed{V(r, x^1, ..., x^{n-1}) = \beta(r) + r\Omega(x^1, ...x^{n-1})\,,} \tag{C.26}$$

for some functions β and Ω. Plugging (C.26) into A_{rr} we find

$$\Omega(x^1, ...x^{n-1})\frac{(\partial_r f - r\partial_r\partial_r f)}{f} + \frac{\partial_r f\partial_r\beta - \beta\partial_r\partial_r f + 2f\partial_r\partial_r\beta}{f} = 0\,. \tag{C.27}$$

Thus, the differential equation can only be fulfilled if *either* $\Omega(x^1, ...x^{n-1})$ is constant, which can then be taken to be zero without loss of generality, *or* if

$$\partial_r f - r\partial_r\partial_r f \equiv 2m_c(n-2)nr^{1-n} = 0\,, \tag{C.28}$$

which can only be fulfilled if $m_c = 0$ or $n = 2$.

The remaining part of (C.27) reads

$$\partial_r f\partial_r\beta - \beta\partial_r\partial_r f + 2f\partial_r\partial_r\beta = 0\,. \tag{C.29}$$

Changing the dependent variable β to

$$\beta(r) = \sqrt{f(r)}\beta_2(r) \tag{C.30}$$

we can solve the differential equation

$$3\partial_r f\partial_r\beta_2 + 2f\partial_r\partial_r\beta_2 = 0 \tag{C.31}$$

explicitly

$$\beta_2(r) = \tilde{c} - \hat{c}\int \frac{dr}{f(r)^{\frac{3}{2}}}\,, \tag{C.32}$$

which yields

$$\beta(r) = \tilde{c}\sqrt{f(r)} - \hat{c}\sqrt{f(r)}\int \frac{dr}{f(r)^{\frac{3}{2}}}\,. \tag{C.33}$$

C.0.1. $m_c = 0$, $n \neq 2$

In the case $m_c = 0$ the function f reduces to

$$f(r) = r^2 + k\,, \tag{C.34}$$

and (C.33) readily integrates to

$$\boxed{\beta(r) = -\frac{\hat{c}r}{k} + \tilde{c}\sqrt{r^2+k}} \tag{C.35}$$

if $k \neq 0$, and to

$$\boxed{\beta(r) = \frac{\hat{c}}{2r} + \tilde{c}r} \tag{C.36}$$

if $k = 0$. The differential equations (C.25) reduce to

$$\boxed{D_A D_B \Omega \equiv \partial_A \partial_B \Omega - \Gamma^C_{AB} \partial_C \Omega = \mathring{h}_{AB}(\hat{c} - k\Omega)\,.} \tag{C.37}$$

This is an overdetermined system of equations, and all triples $(M, \mathring{h}, \Omega)$ satisfying (C.37), where $\Omega \not\equiv 0$ and $(M, \mathring{h})$ is a complete Riemannian manifold, were classified in [109]. In the special case

$$\mathring{h}_{AB} dx^A dx^B = d\psi^2 + \left(d\theta^1\right)^2 + ... + \left(d\theta^{n-2}\right)^2 \tag{C.38}$$

the constant k is zero and all Christoffel symbols of the boundary metric $\mathring{h}$ vanish, so that (C.37) becomes

$$\partial_A \partial_B \Omega = \hat{c}\, \delta_{AB}\,. \tag{C.39}$$

We find

$$\boxed{V(r) = \tilde{c} r + \frac{\hat{c}}{2r} + r\left(c\psi + \hat{c}\frac{\psi^2}{2}\right) + r\sum_{I=1}^{n-2} c_I \theta^I + \hat{c}\frac{|\theta|^2}{2}\,,} \tag{C.40}$$

where c and c_I are constants.

$m_c \neq 0$, $n \neq 2$

In the generic case $m_c \neq 0$ the function $\Omega(x^1, ...x^{n-1}) = 0$ and the function V reduces to

$$V(r, x^1, ...x^{n-1}) = \beta(r) = \tilde{c}\sqrt{f(r)} - \hat{c}\sqrt{f(r)} \int \frac{dr}{f(r)^{\frac{3}{2}}}\,. \tag{C.41}$$

The final set of equations that needs to be solved is (C.25), which in this case reduces to

$$A_{AB} = r\mathring{h}_{AB} f \partial_r V - \frac{V \partial_r f}{2} r \mathring{h}_{AB} = 0\,. \tag{C.42}$$

Contracting with $\mathring{h}^{AB}$ yields

$$r f \partial_r V - \frac{V \partial_r f}{2} r = 0 \tag{C.43}$$

which implies that $\hat{c} = 0$ and thus

$$\boxed{V(r, x^1, ..., x^{n-1}) = \tilde{c}\sqrt{f(r)}\,.} \tag{C.44}$$

$n = 2$

As already discussed, in the case $n = 2$ the function $f(r)$ reduces to

$$f(r) = r^2 - 2m_c\,, \tag{C.45}$$

which has the same functional form as (C.34) but with k in (C.34) now being replaced by $-2m_c$. Again, (C.33) thus readily integrates to

$$\beta(r) = \frac{\hat{c}r}{2m_c} + \tilde{c}\sqrt{r^2 - 2m_c} \tag{C.46}$$

if $m_c \neq 0$, and to

$$\beta(r) = \frac{\hat{c}}{2r} + \tilde{c}r \tag{C.47}$$

if $m_c = 0$. The differential equations (C.25) reduce to just one differential equation as the boundary metric is one-dimensional

$$D_A D_A \Omega = \mathring{h}_{AA}(\hat{c} + 2m_c\Omega) \tag{C.48}$$

with $A = 1$. In a coordinate system $x^1 = \psi$ in which $\mathring{h}_{11}$ equals 1 the solutions are

$$\Omega = \begin{cases} \frac{\hat{c}}{2}\psi^2 + a\psi + b, & m_c = 0; \\ ae^{\sqrt{2m_c}\psi} + be^{-\sqrt{2m_c}\psi} - \frac{\hat{c}}{2m_c}, & m_c > 0; \\ a\sin(\sqrt{-2m_c}\psi) + b\cos(\sqrt{-2m_c}\psi) - \frac{\hat{c}}{2m_c}, & m_c < 0, \end{cases} \tag{C.49}$$

with constants $a, b \in \mathbb{R}$.

Horowitz–Myers

We consider the Horowitz–Myers metrics

$$ds^2 = \frac{1}{f(r)}dr^2 + f(r)d\psi^2 + r^2\Big(-dt^2 + (d\theta^1)^2 + (d\theta^2)^2 + ... + (d\theta^{n-2})^2\Big) \tag{C.50}$$

with

$$f(r) = r^2 - \frac{2m_c}{r^{n-2}}\,, \tag{C.51}$$

and $n \geq 2$. The metric on constant time slices reads

$$g_{ij}dx^i dx^j = \frac{1}{f(r)}dr^2 + f(r)d\psi^2 + r^2\Big((d\theta^1)^2 + (d\theta^2)^2 + ... + (d\theta^{n-2})^2\Big)\,. \tag{C.52}$$

The indices i, j run from 1 to n. The only non-vanishing Christoffel symbols (up to symmetries) for (C.52) are

$$\Gamma^r{}_{rr} = -\frac{\partial_r f}{2f}\,, \quad \Gamma^r{}_{\psi\psi} = -\frac{f\partial_r f}{2}\,, \quad \Gamma^r{}_{\theta^I\theta^I} = -rf\,, \quad \Gamma^\psi{}_{\psi r} = \frac{\partial_r f}{2f}\,, \quad \Gamma^{\theta^I}{}_{\theta^I r} = \frac{1}{r}\,. \tag{C.53a}$$

Next,

$$D_iD_jV(r,\psi,\theta^1,...\theta^{n-2}) = \partial_i\partial_jV(r,\psi,\theta^1,...\theta^{n-2}) - \Gamma^k{}_{ij}\partial_kV(r,\psi,\theta^1,...\theta^{n-2})\,. \quad \text{(C.54)}$$

yields

$$D_rD_rV = \partial_r\partial_rV + \frac{1}{2f}\partial_rf\partial_rV\,, \qquad D_rD_\psi V = \partial_r\partial_\psi V - \frac{1}{2}\frac{\partial_r f}{f}\partial_\psi V\,, \quad \text{(C.55a)}$$

$$D_rD_{\theta^I}V = \partial_r\partial_{\theta^I}V - \frac{1}{r}\partial_{\theta^I}V\,, \qquad D_\psi D_\psi V = \partial_\psi\partial_\psi V + \frac{1}{2}f\partial_rf\partial_rV\,, \quad \text{(C.55b)}$$

$$D_\psi D_{\theta^I}V = \partial_\psi\partial_{\theta^I}V\,, \qquad D_{\theta^I}D_{\theta^J}V = \partial_{\theta^I}\partial_{\theta^J}V + rf\partial_rV\delta_{IJ}\,, \quad \text{(C.55c)}$$

where I, J run from from 1 to $n-2$. The only non-vanishing components of the Riemann tensor

$$R_{ijk}{}^l = \partial_j\Gamma^l{}_{ik} - \partial_i\Gamma^l{}_{jk} + \left(\Gamma^m{}_{ik}\Gamma^l{}_{mj} - \Gamma^m{}_{jk}\Gamma^l{}_{mi}\right) \quad \text{(C.56)}$$

read (up to the ones obtained from antisymmetry in the first index pair)

$$R_{r\psi r}{}^\psi = -\frac{\partial_r\partial_rf}{2f}\,, \quad R_{r\psi\psi}{}^r = -\frac{f\partial_r\partial_rf}{2}\,, \quad R_{r\theta^I r}{}^{\theta^I} = -\frac{\partial_rf}{2fr}\,, \quad R_{r\theta^I\theta^I}{}^r = \frac{r\partial_rf}{2}\,, \quad \text{(C.57a)}$$

$$R_{\psi\theta^I\psi}{}^{\theta^I} = -\frac{f\partial_rf}{2r}\,, \quad R_{\psi\theta^I\theta^I}{}^\psi = \frac{r\partial_rf}{2}\,, \quad R_{\theta^I\theta^J\theta^I}{}^{\theta^J} = -f \qquad \text{with } I \neq J\,. \quad \text{(C.57b)}$$

From this we obtain that the only non-vanishing components of the Ricci-tensor

$$R_{ij} = R_{ikj}{}^k \quad \text{(C.58)}$$

read

$$R_{rr} = -\frac{\partial_r\partial_rf}{2f} - \frac{(n-2)}{2}\frac{\partial_rf}{rf}\,, \qquad R_{\psi\psi} = -\frac{1}{2}f\partial_r\partial_rf - \frac{(n-2)}{2}\frac{f\partial_rf}{r}\,, \quad \text{(C.59a)}$$

$$R_{\theta^I\theta^I} = -(n-3)f - r\partial_rf\,. \quad \text{(C.59b)}$$

This leads to

$$R = -n(n-1)\,. \quad \text{(C.59c)}$$

The KID equations,

$$A_{ij} := D_iD_jV - V\left(R_{ij} - \frac{R}{n-1}g_{ij}\right) = D_iD_jV - V(R_{ij} + ng_{ij}) = 0\,, \quad \text{(C.59d)}$$

thus become

$$A_{rr} = \partial_r\partial_r V + \frac{1}{2f}\partial_r f\partial_r V - V\Big(-\frac{\partial_r\partial_r f}{2f} - \frac{(n-2)}{2}\frac{\partial_r f}{rf} + \frac{n}{f}\Big) = 0\,, \tag{C.60a}$$

$$A_{r\psi} = A_{\psi r} = \partial_r\partial_\psi V - \frac{1}{2}\frac{\partial_r f}{f}\partial_\psi V = 0\,, \tag{C.60b}$$

$$A_{r\theta^I} = A_{\theta^I r} = \partial_r\partial_{\theta^I} V - \frac{1}{r}\partial_{\theta^I} V = 0\,, \tag{C.60c}$$

$$A_{\psi\psi} = \partial_\psi\partial_\psi V + \frac{1}{2}f\partial_r f\partial_r V - V\Big(-\frac{1}{2}f\partial_r\partial_r f - \frac{(n-2)}{2}\frac{f\partial_r f}{r} + nf\Big) = 0\,, \tag{C.60d}$$

$$A_{\psi\theta^I} = \partial_\psi\partial_{\theta^I} V = 0\,, \tag{C.60e}$$

$$A_{\theta^I\theta^J} = \partial_{\theta^I}\partial_{\theta^J} V + \delta_{IJ}\Big(rf\partial_r V - V\big(-(n-3)f - r\partial_r f + nr^2\big)\Big) = 0\,. \tag{C.60f}$$

Solving (C.60e) and (C.60f) with $I \neq J$ we obtain

$$V(r,\psi,\theta^1,\ldots\theta^{n-2}) = \alpha(r,\psi) + \alpha_1(r,\theta^1) + \alpha_2(r,\theta^2) + \ldots + \alpha_{n-2}(r,\theta^{n-2})\,. \tag{C.61}$$

Plugging this into the equation (C.60c) we get that

$$\alpha_I(r,\theta^I) = \beta_I(r) + r\hat{\gamma}_I(\theta^I)\,. \tag{C.62}$$

Solving (C.60b) yields

$$\alpha(r,\psi) = \tilde{\beta}(r) + \sqrt{f(r)}\hat{\gamma}(\psi)\,. \tag{C.63}$$

Setting $\beta(r) = \tilde{\beta}(r) + \sum_{I=1}^{n-2}\beta_I(r)$ we have

$$V(r,\psi,\theta^1,\ldots\theta^{n-2}) = \beta(r) + \sqrt{f(r)}\hat{\gamma}(\psi) + r\sum_{I=1}^{n-2}\hat{\gamma}_I(\theta^I)\,, \tag{C.64}$$

with the last term omitted when $n = 2$. From (C.60f) we obtain (by pairwise substraction)

$$\partial_{\theta^I}\partial_{\theta^I} V = \partial_{\theta^J}\partial_{\theta^J} V \tag{C.65}$$

for any I, J which is equivalent to

$$\partial_I\partial_I\hat{\gamma}_I(\theta^I) = \partial_J\partial_J\gamma_J(\theta^J)\,. \tag{C.66}$$

such that (the θ^I-independent integration constant can be absorbed into $\beta(r)$)

$$V(r,\psi,\theta^1,\ldots\theta^{n-2}) = \beta(r) + \sqrt{f(r)}\hat{\gamma}(\psi) + rc_I\theta^I + r\frac{\hat{c}}{2}|\theta|^2\,. \tag{C.67}$$

We turn now our attention to the equation

$$A_{\psi\psi} - f(r)^2 A_{rr} = 0 = \partial_\psi \partial_\psi V - f^2 \partial_r \partial_r V$$
$$= \frac{1}{4}\sqrt{f(r)}\Big(\hat{\gamma}(\psi)\Big((\partial_r f)^2 - 2f\partial_r\partial_r f\Big) - 4f^{\frac{3}{2}}\partial_r\partial_r\beta + 4\partial_\psi\partial_\psi\hat{\gamma}\Big)\,, \quad \text{(C.68)}$$

from which we find

$$\hat{\gamma}(\psi)\Big((\partial_r f)^2 - 2f\partial_r\partial_r f\Big) + 4\partial_\psi\partial_\psi\hat{\gamma} = 4f^{\frac{3}{2}}\partial_r\partial_r\beta\,. \quad \text{(C.69)}$$

For the function $f(r) = r^2 - \frac{2m_c}{r^{n-2}}$ we have

$$\Big((\partial_r f)^2 - 2f\partial_r\partial_r f\Big) = 4nm_c r^{2-2n}((-1+n)r^n - (-2+n)m_c)\,. \quad \text{(C.70)}$$

If $m_c = 0$ the spatial parts of the toroidal Kottler and the Horowitz–Myers metrics coincide, and this case has already been solved in section C.0.1. In the case $m_c \neq 0$ and $n \neq 2$ we see from (C.70) that $\hat{\gamma}(\psi)$ has to be a constant. This constant is irrelevant as it can be absorbed by a redefinition of $\beta(r)$, which is why we set it to zero in the following. Equation (C.69) then reduces to

$$\partial_r^2\beta = 0\,. \quad \text{(C.71)}$$

Hence, we have $\beta(r) = r\tilde{c}_1 + \tilde{c}_2$ which yields

$$V(r,\psi,\theta^1,\ldots,\theta^{n-2}) = r\tilde{c}_1 + \tilde{c}_2 + rc_I\theta^I + r\frac{\hat{c}}{2}|\theta|^2\,. \quad \text{(C.72)}$$

Plugging this into the equation (C.60a), $A_{rr} = 0$, together with the explicit form of $f(r)$ we obtain

$$A_{rr} = -\frac{(r^n + (-2+n)m_c)}{r^2(r^n - 2m_c)}\tilde{c}_2 = 0\,, \quad \text{(C.73)}$$

from which follows that $\tilde{c}_2 = 0$. The differential equation (C.60d) $A_{\psi\psi} = 0$ is then automatically fulfilled. Plugging all of this into (C.60f) $A_{\theta^I\theta^I} = 0$ yields

$$A_{\theta^I\theta^I} = r\hat{c} = 0\,, \quad \text{(C.74)}$$

from which follows that $\hat{c} = 0$. Hence, we have

$$\boxed{V(r,\psi,\theta^1,...,\theta^{n-2}) = r\tilde{c}_1 + r\sum_{I=1}^{n-2}\Big(c_I\theta^I\Big)\,.} \quad \text{(C.75)}$$

D. Transformation behavior of the mass aspect tensor

This appendix is from [2] (co-authored with Piotr Chruściel and Erwann Delay)

Consider a metric of the following Fefferman-Graham form

$$g = x^{-2}(dx^2 + h_{AB}dx^A dx^B)\,, \tag{D.1}$$

where the coordinate functions h_{AB} depend upon both x and the local coordinates x^A on the boundary $\{x = 0\}$. Here, the index A runs from $1, ...n-1$. In the following we will consider $n \geq 3$. Let us further write a Taylor expansion

$$h_{AB} = (1 - kx^2/4)^2 \mathring{h}_{AB}(x^C) + x^n \mu_{AB}(x^C) + o(x^n)\,, \tag{D.2}$$

where k is a constant. Here, the scalar curvature of $\mathring{h}_{AB}$ is given by

$$R(\mathring{h}) = k(n-1)(n-2)\,. \tag{D.3}$$

Let $\phi = \phi(x^C)$ be a function on the boundary, set

$$\bar{h}_{AB}|_{x=0} = \phi^2 h_{AB}\,, \tag{D.4}$$

thus (D.1) takes the form

$$g = x^{-2}(dx^2 + (\phi^{-2}\bar{h}_{AB} + O(x))dx^A dx^B)\,. \tag{D.5}$$

We wish to rewrite this as

$$g = y^{-2}(dy^2 + \bar{h}_{AB}d\bar{x}^A d\bar{x}^B)\,. \tag{D.6}$$

with

$$\bar{h}_{AB} = (1 - \bar{k}y^2/4)^2 \phi^2(\bar{x}^C)\mathring{h}_{AB}(\bar{x}^C) + y^n \bar{\mu}_{AB}(\bar{x}^C) + o(y^n)\,, \tag{D.7}$$

where $\bar{k} \in \{0, \pm 1\}$.

$$\bar{R}(\phi^2 \mathring{h}) = \bar{k}(n-1)(n-2)\,. \tag{D.8}$$

By matching powers in Taylor expansions, this is equivalent to finding a function y with a Taylor expansion

$$y = \phi x\Big(1 + \phi_1 x + \phi_2 x^2 + \phi_3 x^3 + ...\Big) \tag{D.9a}$$

and new boundary coordinates $\bar{x}^A$ with Taylor expansions

$$\bar{x}^A = x^A + \phi_1^A x + \phi_2^A x^2 + \phi_3^A x^3 + \phi_4^A x^4 ... \tag{D.9b}$$

In order to determine y as a function of the original coordinates, we note that

$$g^{yy} \equiv g(dy, dy) = y^2 \qquad \Longleftrightarrow \qquad |d(\log y)|_g^2 = 1\,. \tag{D.10}$$

This equation says that the integral curves of $d(\log y)$ are affinely parameterized geodesics. The solutions can be found by shooting geodesics orthogonally, in the metric $x^2 g$, to the conformal boundary, with suitable boundary conditions determined by the function ϕ. Hence smooth solutions always exist, which justifies the existence of the expansion (D.9a). Further, we see that the equation for y can be solved independently of the equation for the $\bar{x}^A$'s. Next, the equation

$$0 = g(dy, d\bar{x}^A) \tag{D.11}$$

says that the coordinates $\bar{x}^A$ are constant along the integral curves of dy. So, when a smooth function y is known, one obtains smooth functions $\bar{x}^A$ by solving (D.11) along the integral curves of dy, which again justifies the expansion (D.9b), and provides a prescription for finding the expansion functions ψ_n^A.

We find that

$$\phi_1 = 0\,, \qquad \phi_2 = -\frac{\mathscr{D}_A\phi\mathscr{D}^A\phi}{4\phi^2}\,, \qquad \phi_3 = 0\,, \tag{D.12a}$$

and

$$\phi_1^A = 0\,, \qquad \phi_2^A = -\frac{1}{2}\frac{\mathscr{D}^A\phi}{\phi}\,, \qquad \phi_3^A = 0\,, \tag{D.12b}$$

where $\mathscr{D}$ is the covariant derivative of the metric $\mathring{h}$ and the indices A are raised with $\mathring{h}^{AB}$. With this it holds that

$$g = x^{-2}(dx^2 + (h_{AB} + O(x^2))dx^A dx^B) = y^{-2}(dy^2 + (\bar{h}_{AB} + O(y)^2)d\bar{x}^A d\bar{x}^B) \tag{D.13}$$

However, for general $\mathring{h}_{AB}$ it is not possible to bring the $y^2 d\bar{x}^A d\bar{x}^B$ term into the form (D.7) by changing coordinates as (D.9) after the conformal transformation. Indeed, one finds that the terms of order y^0 in the coordinate-transformed metric read

$$-k\frac{\mathring{h}_{AB}}{2} + \mathscr{D}_A\mathscr{D}_B\log\phi - (\mathscr{D}_A\log\phi)(\mathscr{D}_B\log\phi) + \frac{1}{2}(\mathscr{D}^C\log\phi)(\mathscr{D}_C\log\phi)\mathring{h}_{AB}\,. \tag{D.14}$$

It follows that for (D.7) to hold true the following expression must vanish

$$\frac{\phi^2}{2}(-\bar{k}\phi^2+k)\mathring{h}_{AB}-\phi\mathscr{D}_A\mathscr{D}_B\phi+2(\mathscr{D}_A\phi)(\mathscr{D}_B\phi)-\frac{1}{2}(\mathscr{D}^C\phi)(\mathscr{D}_C\phi)\mathring{h}_{AB}=0\,. \tag{D.15}$$

The trace of (D.15) is equivalent to the transformation of the Ricci scalar under conformal transformations, which was already discussed in subsection 2.1.1,

$$\bar{R}=\phi^{-2}\Big(R-2(n-2)\mathscr{D}^A\mathscr{D}_A\log\phi-(n-3)(n-2)(\mathscr{D}^A\log\phi)(\mathscr{D}_A\log\phi)\Big)\,. \tag{D.16}$$

where we have used the explicit expressions for the Ricci scalars (D.3) and (D.8).

Relation to coordinates in the main text

The coordinates x, x^A in (D.1) are related to the coordinates in the main text r, x^A, section 4.6, as

$$r=\frac{1}{x}-\frac{kx}{4}\,, \tag{D.17a}$$

$$x=\frac{2}{r+\sqrt{r^2+k}}=\frac{1}{r}-\frac{k}{4r^3}+\frac{k^2}{8r^5}+O(r^{-7}) \tag{D.17b}$$

Under this change of coordinates the line element

$$g=x^{-2}(dx^2+\Big((1-kx^2/4)^2\mathring{h}_{AB}(x^C)+x^n\mu_{AB}(x^C)+o(x^n)\Big)dx^Adx^B) \tag{D.18}$$

changes as

$$g=\frac{dr^2}{r^2+k}+r^2\Big(\mathring{h}_{AB}(x^c)+r^{-n}\mu_{AB}(x^C)+o(r^{-n})\Big)dx^Adx^B\,. \tag{D.19a}$$

Using the relations (D.17) we have

$$\bar{x}^A=x^A-\frac{1}{2}\frac{\mathscr{D}^A\phi}{\phi}x^2+O(x^4) \tag{D.20}$$

which, using

$$\psi:=\phi^{-1}\,,$$

translates to

$$\bar{x}^A=x^A+\frac{\mathscr{D}^A\psi}{2\psi r^2}+O(r^{-4})\,, \tag{D.21}$$

while the expansion in y

$$y = \phi x\left(1 - \frac{\mathscr{D}^A\phi\mathscr{D}_A\phi}{4\phi^2}x^2 + \mathcal{O}(x^4)\right) \tag{D.22}$$

leads to an expansion in $\bar{r}$

$$\bar{r} = \psi r\left(1 + \frac{\left(\mathscr{D}^A\psi\mathscr{D}_A\psi + k\psi^2 - \bar{k}\right)}{4\psi^2 r^2} + O(r^{-4})\right). \tag{D.23}$$

Using (D.16) we can also write

$$\bar{r} = \psi r\left(1 + \frac{\left(-\mathscr{D}^A\mathscr{D}_A\log\psi + (n-2)\mathscr{D}^A\log\psi\mathscr{D}_A\log\psi\right)}{2(n-1)r^2} + O(r^{-4})\right). \tag{D.24}$$

$n = 3$

For $n = 3$, the boundary metric is two-dimensional. Thus we have the relation that

$$R_{AB} = \frac{R}{2}\mathring{h}_{AB} = k\mathring{h}_{AB}\,, \qquad \bar{R}_{AB} = \frac{\bar{R}}{2}\phi^2\mathring{h}_{AB} = \bar{k}\phi^2\mathring{h}_{AB}\,. \tag{D.25}$$

Reconsidering (D.15) and using the expression for the Ricci tensor (D.25) we get

$$\bar{R}_{AB} = R_{AB} - 2\mathscr{D}_A\mathscr{D}_B\log\phi + 2\mathscr{D}_A\log\phi\mathscr{D}_B\log\phi - \mathring{h}_{AB}\mathscr{D}^C\log\phi\mathscr{D}_C\log\phi\,. \tag{D.26}$$

This coincides with the transformation behavior of the Ricci tensor in two dimensions if and only if

$$\mathring{h}_{AB}\left(\mathscr{D}^C\mathscr{D}_C\log\phi - \mathscr{D}^C\log\phi\mathscr{D}_C\log\phi\right) = 2(\mathscr{D}_A\mathscr{D}_B\log\phi - \mathscr{D}_A\log\phi\mathscr{D}_B\log\phi)\,. \tag{D.27}$$

Using (D.15) the $y^2 d\bar{x}^A d\bar{x}^B$ term can be brought into the correct form. For $n = 3$ we find that the new mass aspect tensor $\bar{\mu}_{AB}$ takes the form

$$\bar{\mu}_{AB} = \frac{\mu_{AB}}{\phi} = \psi\mu_{AB}\,, \tag{D.28}$$

where $\psi = \phi^{-1}$, which is the variable sometimes used in the main text. From

$$\mathring{h}^{AB}\mu_{AB} = \phi^3\bar{h}_{AB}|_{x=0}\,\bar{\mu}_{AB}\,, \qquad \sqrt{\det\mathring{h}} = \phi^{-2}\sqrt{\det\bar{h}}|_{x=0}\,, \qquad \bar{x}^A = x^A|_{x=0} \tag{D.29}$$

we conclude that

$$\int \mathring{h}^{AB}\mu_{AB}\sqrt{\det \mathring{h}}\,dx^1dx^2 = \int \left(\phi\bar{h}^{AB}\bar{\mu}_{AB}\sqrt{\det \bar{h}}\right)|_{\bar{x}=0}\,d\bar{x}^1d\bar{x}^2\,, \tag{D.30}$$

as well as

$$\int \left(\bar{h}^{AB}\bar{\mu}_{AB}\sqrt{\det \bar{h}}\right)|_{\bar{x}=0}\,d\bar{x}^1d\bar{x}^2 = \int \phi^{-1}\mathring{h}^{AB}\mu_{AB}\sqrt{\det \mathring{h}}\,dx^1dx^2\,. \tag{D.31}$$

$n = 4$

We consider now the transformation formulae for the higher-order terms in the expansion of the metric. These are irrelevant for the mass aspect tensor when $n = 3$ but become relevant in higher dimensions. Because the powers of x in the expansion of y and $\bar{x}^A$ jump by two, and so do the powers in the expansion of the metric up to the mass-aspect level x^{n-2}, when $n \geq 4$ the terms of order x in the physical metric remain zero after the change of coordinates. The terms of order x^2 change in a non-trivial way, which is relevant for the mass aspect function in space dimension $n = 4$, and which we determine now.

The explicit form of the coefficients ϕ_1, ϕ_2, ϕ_3 and $\phi_1^A, \phi_2^A, \phi_3^A$ in (D.12) holds true for arbitrary dimensions $n \geq 3$. However, to determine the transformation behaviour of the mass aspect in $n = 4$ we need to determine further coefficients. We have

$$\phi_4^A = -\frac{\bar{k}}{8}\phi\mathscr{D}^A\phi + \frac{1}{8\phi^2}\mathscr{D}^B\phi\mathscr{D}^C\phi\mathscr{D}_C\mathscr{D}_B x^A\,, \tag{D.32a}$$

$$\phi_4 = -\frac{\bar{k}}{16}\mathscr{D}_C\phi\mathscr{D}^C\phi + \frac{1}{16\phi^4}(\mathscr{D}_C\phi\mathscr{D}^C\phi)^2\,, \tag{D.32b}$$

where x^A in the first equation (D.32a) is treated as a scalar for every A. In dimension $n = 4$ the coefficients ϕ_5^A vanish

$$\phi_5^A = 0\,, \qquad \phi_5 = 0\,. \tag{D.33}$$

This leads to

$$\begin{aligned}\phi^2\bar{\mu}_{AB} = \mu_{AB} &+ \frac{1}{16}\mathring{h}_{AB}\left(k^2 - \bar{k}^2\phi^4\right) - \frac{\bar{k}}{4}\phi\mathscr{D}_A\mathring{D}_B\phi - \frac{3}{8}\bar{k}\mathring{h}_{AB}\mathscr{D}^C\phi\mathscr{D}_C\phi + \frac{3}{4}\bar{k}\mathscr{D}_A\phi\mathscr{D}_B\phi\\
&- \frac{1}{4\phi^2}\mathscr{D}^C\mathscr{D}_A\phi\mathscr{D}_C\mathscr{D}_B\phi + \frac{3}{2\phi^3}\mathscr{D}^C\mathscr{D}_{(A}\phi\mathscr{D}_{B)}\phi\mathscr{D}_C\phi - \frac{1}{4\phi^3}\mathring{h}_{AB}\mathscr{D}^C\phi\mathscr{D}_D\mathscr{D}_C\phi\mathscr{D}^D\phi\\
&- \frac{1}{2\phi^3}\mathscr{D}_A\mathscr{D}_B\phi\mathscr{D}^C\phi\mathscr{D}_C\phi - \frac{3}{4\phi^4}\mathscr{D}_A\phi\mathscr{D}_B\phi\mathscr{D}^C\phi\mathscr{D}_C\phi + \frac{3}{16\phi^4}(\mathscr{D}^C\phi\mathscr{D}_C\phi)^2\mathring{h}_{AB}\\
&- \frac{1}{4\phi^2}R_{ACDB}\mathscr{D}^C\phi\mathscr{D}^D\phi\,.\end{aligned} \tag{D.34}$$

This is best computed using coordinates in which the metric is diagonal, which can always be done locally in dimension three [110]. Here and elsewhere, the symmetrization is defined as $M_{(AB)} = \frac{1}{2}(M_{AB} + M_{BA})$. Contracting (D.34) with $\mathring{h}^{AB}$ we obtain

$$\begin{aligned}\phi^2\bar{\mu}_{AB}\mathring{h}^{AB} - \mu_A{}^A = \frac{3}{16}(k^2 - \bar{k}^2\phi^4) - \frac{\bar{k}}{4}\phi\mathscr{D}^A\mathscr{D}_A\phi - \frac{3}{8}\bar{k}(\mathscr{D}^A\phi\mathscr{D}_A\phi) - \frac{1}{4\phi^2}(\mathscr{D}^A\mathscr{D}^B\phi)(\mathscr{D}_A\mathscr{D}_B\phi)\\ + \frac{3}{4\phi^3}\mathscr{D}^A\phi\mathscr{D}^B\phi\mathscr{D}_A\mathscr{D}_B\phi - \frac{1}{2\phi^3}(\mathscr{D}^A\mathscr{D}_A\phi)(\mathscr{D}^B\phi\mathscr{D}_B\phi) - \frac{3}{16\phi^4}(\mathscr{D}^A\phi\mathscr{D}_A\phi)^2\\ + \frac{1}{4\phi^2}R_{AB}\mathscr{D}^A\phi\mathscr{D}^B\phi\,.\end{aligned} \tag{D.35}$$

Using the transformation behaviour of the Ricci scalar (D.16),

$$\bar{R} = \phi^{-2}\left(R - \frac{4}{\phi}\mathscr{D}^A\mathscr{D}_A\phi + \frac{2}{\phi^2}\mathscr{D}^A\phi\mathscr{D}_A\phi\right), \tag{D.36}$$

and the explicit expression of the Ricci scalars (D.3) and (D.8),

$$R = 6k\,, \qquad \bar{R} = 6\bar{k}\,, \tag{D.37}$$

for $n = 4$ we find that

$$\bar{k} = \frac{3k\phi^2 + (\mathscr{D}^A\phi\mathscr{D}_A\phi) - 2\phi\mathscr{D}^A\mathscr{D}_A\phi}{3\phi^4}\,, \tag{D.38}$$

which yields

$$\begin{aligned}\phi^2\bar{\mu}_{AB}\mathring{h}^{AB} - \mu_A{}^A = &-\frac{1}{3\phi^4}(\mathscr{D}^A\phi\mathscr{D}_A\phi)^2 - \frac{1}{4\phi^3}(\mathscr{D}^A\phi\mathscr{D}_A\phi)(\mathscr{D}^B\mathscr{D}_B\phi) + \frac{(\mathscr{D}^A\mathscr{D}_A\phi)^2}{12\phi^2}\\ &- \frac{1}{4\phi^2}(\mathscr{D}^A\mathscr{D}^B\phi)(\mathscr{D}_A\mathscr{D}_B\phi) + \frac{3}{4\phi^3}\mathscr{D}^A\phi\mathscr{D}^B\phi\mathscr{D}_A\mathscr{D}_B\phi\\ &+ \frac{1}{4\phi^2}(R_{AB} - 2k\mathring{h}_{AB})\mathscr{D}^A\phi\mathscr{D}^B\phi\,.\end{aligned} \tag{D.39}$$

Making the change of variable

$$\phi = \exp(u) \tag{D.40}$$

(so that u here corresponds to $+\omega/2$ in (4.68)), Equation (D.39) becomes

$$\begin{aligned}\exp(2u)\bar{\mu}_{AB}\mathring{h}^{AB} - \mu_A{}^A = &-\frac{1}{12}(\mathscr{D}^A u\mathscr{D}_A u)(\mathscr{D}^B\mathscr{D}_B u) + \frac{1}{12}(\mathscr{D}^A\mathscr{D}_A u)(\mathscr{D}^B\mathscr{D}_B u)\\ &- \frac{1}{4}(\mathscr{D}^A\mathscr{D}^B u)(\mathscr{D}_A\mathscr{D}_B u) + \frac{1}{4}(\mathscr{D}^A\mathscr{D}^B u)(\mathscr{D}_A u\mathscr{D}_B u)\\ &+ \frac{1}{4}(R_{AB} - 2k\mathring{h}_{AB})\mathscr{D}^A u\mathscr{D}^B u\,.\end{aligned} \tag{D.41}$$

Using

$$\sqrt{\det \mathring{h}} = \phi^{-3}\sqrt{\det \bar{h}}|_{x=0}\,, \quad \bar{x}^A = x^A|_{x=0}\,, \tag{D.42}$$

and (D.41) we find that

$$\int \left(\bar{\mu}_{AB}\bar{h}^{AB}\sqrt{\det \bar{h}}\right)|_{x=0}\, d\bar{x}^1 d\bar{x}^2 d\bar{x}^3 = \int e^{-u}\left(\mu^A{}_A + C(x^A)\right)\sqrt{\det \mathring{h}}\, dx^1 dx^2 dx^3 \tag{D.43}$$

with

$$C(x^A) = \frac{1}{6}(\mathscr{D}_A\mathscr{D}_B\mathscr{D}^A u)(\mathscr{D}^B u) + \frac{1}{12}\left(R_{AB} - \frac{R}{2}\mathring{h}_{AB}\right)\mathscr{D}^A u \mathscr{D}^B u\,. \tag{D.44}$$

Bibliography

[1] S. Detournay, W. Merbis, G. S. Ng, and R. Wutte, "Warped Flatland," *JHEP* **11** (2020) 061, arXiv:2001.00020 [hep-th].

[2] P. T. Chruściel, E. Delay, and R. Wutte, "Hyperbolic energy and Maskit gluings," arXiv:2112.00095 [math.DG].

[3] D. Grumiller, M. M. Sheikh-Jabbari, C. Troessaert, and R. Wutte, "Interpolating Between Asymptotic and Near Horizon Symmetries," arXiv:1911.04503 [hep-th].

[4] H. Gonzalez, D. Grumiller, W. Merbis, and R. Wutte, "New entropy formula for Kerr black holes," *EPJ Web Conf.* **168** (2018) 01009, arXiv:1709.09667 [hep-th].

[5] M. Ammon, D. Grumiller, S. Prohazka, M. Riegler, and R. Wutte, "Higher-Spin Flat Space Cosmologies with Soft Hair," *JHEP* **05** (2017) 031, arXiv:1703.02594 [hep-th].

[6] R. M. Wald, *General Relativity*. Chicago Univ. Pr., Chicago, USA, 1984.

[7] C. W. Misner, K. S. Thorne, and J. A. Wheeler, *Gravitation*. W. H. Freeman, San Francisco, 1973.

[8] https://www.nobelprize.org/prizes/physics/2020, 2020.

[9] J. M. Maldacena, "The Large N limit of superconformal field theories and supergravity," *Int.J.Theor.Phys.* **38** (1999) 1113–1133, arXiv:hep-th/9711200 [hep-th].

[10] G. 't Hooft, "Dimensional reduction in quantum gravity," *Conf. Proc. C* **930308** (1993) 284–296, arXiv:gr-qc/9310026.

[11] L. Susskind, "The World as a hologram," *J. Math. Phys.* **36** (1995) 6377–6396, arXiv:hep-th/9409089.

[12] A. Strominger and C. Vafa, "Microscopic origin of the Bekenstein-Hawking entropy," *Phys. Lett.* **B379** (1996) 99–104, arXiv:hep-th/9601029 [hep-th].

[13] A. Strominger, "Black hole entropy from near horizon microstates," *JHEP* **02** (1998) 009, arXiv:hep-th/9712251 [hep-th].

[14] M. Cvetic and F. Larsen, "Statistical entropy of four-dimensional rotating black holes from near-horizon geometry," *Phys. Rev. Lett.* **82** (1999) 484–487, arXiv:hep-th/9805146.

[15] M. Guica, T. Hartman, W. Song, and A. Strominger, "The Kerr/CFT Correspondence," *Phys. Rev.* **D80** (2009) 124008, arXiv:0809.4266 [hep-th].

[16] S. Detournay, T. Hartman, and D. M. Hofman, "Warped Conformal Field Theory," *Phys. Rev. D* **86** (2012) 124018, arXiv:1210.0539 [hep-th].

[17] G. Barnich, "Entropy of three-dimensional asymptotically flat cosmological solutions," *JHEP* **10** (2012) 095, arXiv:1208.4371 [hep-th].

[18] A. Bagchi, S. Detournay, R. Fareghbal, and J. Simon, "Holography of 3d Flat Cosmological Horizons," *Phys. Rev. Lett.* **110** (2013) 141302, arXiv:1208.4372 [hep-th].

[19] H. A. Gonzalez, D. Tempo, and R. Troncoso, "Field theories with anisotropic scaling in 2D, solitons and the microscopic entropy of asymptotically Lifshitz black holes," *JHEP* **11** (2011) 066, arXiv:1107.3647 [hep-th].

[20] G. T. Horowitz and R. C. Myers, "The AdS / CFT correspondence and a new positive energy conjecture for general relativity," *Phys. Rev. D* **59** (1998) 026005, arXiv:hep-th/9808079.

[21] J. D. Brown and M. Henneaux, "Central Charges in the Canonical Realization of Asymptotic Symmetries: An Example from Three-Dimensional Gravity," *Commun.Math.Phys.* **104** (1986) 207–226.

[22] K. A. Moussa, G. Clement, H. Guennoune, and C. Leygnac, "Three-dimensional Chern-Simons black holes," *Phys. Rev.* **D78** (2008) 064065, arXiv:0807.4241 [gr-qc].

[23] P. T. Chruściel and E. Delay, "Exotic hyperbolic gluings," *J. Diff. Geom.* **108** no. 2, (2018) 243–293, arXiv:1511.07858 [math.DG].

[24] P. T. Chruściel, C. R. Ölz, and S. J. Szybka, "Space-time diagrammatics," *Phys. Rev.* **D86** (2012) 124041, arXiv:1211.1718 [gr-qc].

[25] F. Schöller, *Symmetries and Asymptotically Flat Space*. PhD thesis, Vienna, Tech. U., 2020. arXiv:2003.07243 [hep-th].

[26] P. Chruściel, *Geometry of Black Holes*. International Series of Monographs on Physics. Oxford University Press, 8, 2020.

[27] P. T. Chruściel, "Anti-gravity à la Carlotto-Schoen," arXiv:1611.01808 [math.DG].

[28] R. Beig and P. T. Chruściel, "Killing initial data," *Class. Quant. Grav.* **14** (1997) A83–A92, arXiv:gr-qc/9604040.

[29] A. Ishibashi and R. M. Wald, "Dynamics in nonglobally hyperbolic static space-times. 3. Anti-de Sitter space-time," *Class. Quant. Grav.* **21** (2004) 2981–3014, arXiv:hep-th/0402184.

[30] J. A. Wolf, *Spaces of Constant Curvature*. AMS Chelsea Publishing, American Mathematical Society, Providence, Rhode Island, Edition 6, Dec, 2010.

[31] T. Regge and C. Teitelboim, "Role of surface integrals in the Hamiltonian formulation of general relativity," *Ann. Phys.* **88** (1974) 286.

[32] E. Witten, "Three-Dimensional Gravity Revisited," arXiv:0706.3359 [hep-th].

[33] C. Fefferman and C. R. Graham, "Conformal invariants," in *Elie Cartan et les Mathématiques d'aujourd'hui*. Asterisque, 1985.

[34] M. Banados, "Three-dimensional quantum geometry and black holes," *AIP Conf. Proc.* **484** no. 1, (1999) 147–169, arXiv:hep-th/9901148.

[35] M. Bañados, M. Henneaux, C. Teitelboim, and J. Zanelli, "Geometry of the (2+1) black hole," *Phys. Rev.* **D48** (1993) 1506–1525, arXiv:gr-qc/9302012 [gr-qc]. [Erratum: Phys. Rev.D88,069902(2013)].

[36] S. Deser and R. Jackiw, "Three-dimensional cosmological gravity: Dynamics of constant curvature," *Annals of Physics* **153** no. 2, (1984) 405–416. https://www.sciencedirect.com/science/article/pii/0003491684900253.

[37] O. Miskovic and J. Zanelli, "On the negative spectrum of the 2+1 black hole," *Phys. Rev. D* **79** (2009) 105011, arXiv:0904.0475 [hep-th].

[38] G. Barnich, A. Gomberoff, and H. A. Gonzalez, "The Flat limit of three dimensional asymptotically anti-de Sitter spacetimes," *Phys.Rev.* **D86** (2012) 024020, arXiv:1204.3288 [gr-qc].

[39] G. Compère and A. Fiorucci, "Advanced Lectures on General Relativity," arXiv:1801.07064 [hep-th].

[40] D. Ida, "No black hole theorem in three-dimensional gravity," *Phys. Rev. Lett.* **85** (2000) 3758–3760, arXiv:gr-qc/0005129.

[41] M. Bañados, C. Teitelboim, and J. Zanelli, "The Black hole in three-dimensional space-time," *Phys. Rev. Lett.* **69** (1992) 1849–1851, arXiv:hep-th/9204099 [hep-th].

[42] S. Hawking and G. Ellis, *The Large Scale Structure of Space-Time*. Cambridge University Press, 1973.

[43] K. Hinterbichler, "Theoretical Aspects of Massive Gravity," *Rev. Mod. Phys.* **84** (2012) 671–710, arXiv:1105.3735 [hep-th].

[44] S. Deser, R. Jackiw, and S. Templeton, "Topologically Massive Gauge Theories," *Annals Phys.* **140** (1982) 372–411.

[45] D. Anninos and T. Hartman, "Holography at an Extremal De Sitter Horizon," *JHEP* **03** (2010) 096, arXiv:0910.4587 [hep-th].

[46] I. Bengtsson and P. Sandin, "Anti de Sitter space, squashed and stretched," *Class. Quant. Grav.* **23** (2006) 971–986, arXiv:gr-qc/0509076.

[47] D. Anninos, "Sailing from Warped AdS_3 to Warped dS_3 in Topologically Massive Gravity," arXiv:0906.1819 [hep-th].

[48] L. Cornalba and M. S. Costa, "A New cosmological scenario in string theory," *Phys.Rev.* **D66** (2002) 066001, arXiv:hep-th/0203031 [hep-th].

[49] J. L. Cardy, "Operator content of two-dimensional conformally invariant theories," *Nucl. Phys.* **B270** (1986) 186–204.

[50] G. Barnich and B. Oblak, "Holographic positive energy theorems in three-dimensional gravity," *Class. Quant. Grav.* **31** (2014) 152001, arXiv:1403.3835 [hep-th].

[51] E. Shaghoulian, "A Cardy formula for holographic hyperscaling-violating theories," *JHEP* **11** (2015) 081, arXiv:1504.02094 [hep-th].

[52] D. M. Hofman and A. Strominger, "Chiral Scale and Conformal Invariance in 2D Quantum Field Theory," *Phys. Rev. Lett.* **107** (2011) 161601, arXiv:1107.2917 [hep-th].

[53] A. B. Zamolodchikov, "Irreversibility of the Flux of the Renormalization Group in a 2D Field Theory," *JETP Lett.* **43** (1986) 730–732.

[54] J. Polchinski, "Scale and Conformal Invariance in Quantum Field Theory," *Nucl. Phys.* **B303** (1988) 226–236.

[55] M. Bertin, S. Ertl, H. Ghorbani, D. Grumiller, N. Johansson, and D. Vassilevich, "Lobachevsky holography in conformal Chern-Simons gravity," *JHEP* **06** (2013) 015, arXiv:1212.3335 [hep-th].

[56] H. Barzegar, P. T. Chruściel, M. Hörzinger, M. Maliborski, and L. Nguyen, "Remarks on the energy of asymptotically Horowitz-Myers metrics," *Phys. Rev. D* **101** no. 2, (2020) 024007, arXiv:1907.04019 [gr-qc].

[57] D. Birmingham, "Topological black holes in Anti-de Sitter space," *Class. Quant. Grav.* **16** (1999) 1197–1205, arXiv:hep-th/9808032.

[58] F. Kottler, "Über die physikalischen Grundlagen der Einsteinschen Gravitationstheorie," *Annalen der Physik,* **56** (1918) 401–462.

[59] C. P. Boyer, K. Galicki, and J. Kollar, "Einstein metrics on spheres," arXiv:math/0309408.

[60] R. Mazzeo and M. Taylor, "Curvature and uniformization," *Israel Jour. Math.* **130** (2002) 323–346. http://dx.doi.org/10.1007/BF02764082.

[61] M. Walker, "Block diagrams and the extension of timelike two-surfaces," *J. Math. Phys.* **11** (1970) 2280.

[62] E. Woolgar, "The rigid Horowitz-Myers conjecture," *JHEP* **03** (2017) 104, arXiv:1602.06197 [math.DG].

[63] P. T. Chruściel and E. Delay, "The hyperbolic positive energy theorem," arXiv:1901.05263 [math.DG].

[64] P. T. Chruściel and G. J. Galloway, "Positive mass theorems for asymptotically hyperbolic Riemannian manifolds with boundary," *Class. Quant. Grav.* **38** no. 23, (2021) 237001, arXiv:2107.05603 [gr-qc].

[65] X. Wang, "Mass for asymptotically hyperbolic manifolds," *Jour. Diff. Geom.* **57** (2001) 273–299.

[66] P. Chruściel and M. Herzlich, "The mass of asymptotically hyperbolic Riemannian manifolds," *Pacific Jour. Math.* **212** (2003) 231–264. arXiv:math/0110035 [math.DG].

[67] H. Barzegar, P. T. Chruściel, M. Hörzinger, M. Maliborski, and L. Nguyen, "Remarks on the energy of asymptotically Horowitz-Myers metrics," *Phys. Rev. D* **101** no. 2, (2020) 024007, arXiv:1907.04019 [gr-qc].

[68] H. Pedersen, "Eguchi-Hanson metrics with cosmological constant," *Classical Quantum Gravity* **2** no. 4, (1985) 579–587. http://stacks.iop.org/0264-9381/2/579.

[69] D. Lee and A. Neves, "The Penrose inequality for asymptotically locally hyperbolic spaces with nonpositive mass," *Commun. Math. Phys.* **339** (2015) 327–352. http://dx.doi.org/10.1007/s00220-015-2421-x.

[70] P. T. Chruściel, "Quo Vadis, Mathematical General Relativity?," arXiv:2112.02126 [gr-qc].

[71] G. L. Bunting and A. K. M. Masood-ul Alam, "Nonexistence of multiple black holes in asymptotically Euclidean static vacuum space-time," *General Relativity and Gravitation* **19** (1987) 147–154.

[72] P. T. Chruściel and J. Lopes Costa, "On uniqueness of stationary vacuum black holes," *Asterisque* **321** (2008) 195–265, arXiv:0806.0016 [gr-qc].

[73] M. Khuri, F. Marques, and R. Schoen, "A compactness theorem for the Yamabe problem," *Journal of Differential Geometry* **81** no. 1, (2009) 143 – 196. https://doi.org/10.4310/jdg/1228400630.

[74] R. Schoen and S. T. Yau, "Proof of the positive mass theorem. II," *Communications in Mathematical Physics* **79** no. 2, (1981) 231 – 260. https://doi.org/.

[75] N. R. Constable and R. C. Myers, "Spin two glueballs, positive energy theorems and the AdS / CFT correspondence," *JHEP* **10** (1999) 037, arXiv:hep-th/9908175.

[76] M. T. Anderson, "Boundary regularity, uniqueness and non-uniqueness for ah einstein metrics on 4-manifolds," *Advances in Mathematics* **179** no. 2, (2003) 205–249.

[77] G. J. Galloway, S. Surya, and E. Woolgar, "On the geometry and mass of static, asymptotically AdS space-times, and the uniqueness of the AdS soliton," *Commun. Math. Phys.* **241** (2003) 1–25, arXiv:hep-th/0204081.

[78] S. de Haro, S. N. Solodukhin, and K. Skenderis, "Holographic reconstruction of spacetime and renormalization in the AdS/CFT correspondence," *Commun. Math. Phys.* **217** (2001) 595–622, hep-th/0002230.

[79] M. Herzlich, "Mass formulae for asymptotically hyperbolic manifolds," in *AdS/CFT correspondence: Einstein metrics and their conformal boundaries*, vol. 8 of *IRMA Lect. Math. Theor. Phys.*, pp. 103–121. Eur. Math. Soc., Zürich, 2005. https://doi.org/10.4171/013-1/5.

[80] R. Clarkson and R. B. Mann, "Soliton solutions to the Einstein equations in five dimensions," *Phys. Rev. Lett.* **96** (2006) 051104, arXiv:hep-th/0508109.

[81] J. Chen and X. Zhang, "Metrics of Eguchi–Hanson types with the negative constant scalar curvature," *J. Geom. Phys.* **161** (2021) 104010, arXiv:2007.15964 [math.DG].

[82] D. Dold, "Global dynamics of asymptotically locally AdS spacetimes with negative mass," *Class. Quant. Grav.* **35** no. 9, (2018) 095012, arXiv:1711.06700 [gr-qc].

[83] J. Isenberg, J. M. Lee, and I. S. Allen, "Asymptotic gluing of asymptotically hyperbolic solutions to the Einstein constraint equations," *Annales Henri Poincare* **11** (2010) 881, arXiv:0910.1875 [math.DG].

[84] R. Mazzeo and F. Pacard, "Maskit combinations of Poincare-Einstein metrics," arXiv:math/0211099.

[85] P. T. Chruściel and G. Nagy, "The Mass of space - like hypersurfaces in asymptotically anti-de Sitter space-times," *Adv. Theor. Math. Phys.* **5** (2002) 697–754, arXiv:gr-qc/0110014.

[86] L. Abbott and S. Deser, "Stability of gravity with a cosmological constant," *Nucl. Phys.* **B195** (1982) 76–96.

[87] P. T. Chruściel and W. Simon, "Towards the classification of static vacuum space-times with negative cosmological constant," *J. Math. Phys.* **42** (2001) 1779–1817, arXiv:gr-qc/0004032.

[88] P. T. Chruściel and E. Delay, "Gluing constructions for asymptotically hyperbolic manifolds with constant scalar curvature," arXiv:0711.1557 [gr-qc].

[89] S. Aminneborg, I. Bengtsson, S. Holst, and P. Peldan, "Making anti-de Sitter black holes," *Class. Quant. Grav.* **13** (1996) 2707–2714, arXiv:gr-qc/9604005.

[90] S. Holst and P. Peldan, "Black holes and causal structure in anti-de Sitter isometric space-times," *Class. Quant. Grav.* **14** (1997) 3433–3452, arXiv:gr-qc/9705067.

[91] M. Dahl and A. Sakovich, "A density theorem for asymptotically hyperbolic initial data," *Pure Appl. Math. Quart.* **17** no. 5, (2021) 1669–1710, arXiv:1502.07487 [math.DG].

[92] M. Herzlich, "Computing asymptotic invariants with the Ricci tensor on asymptotically flat and asymptotically hyperbolic manifolds," *Ann. Henri Poincaré* **17** (2016) 3605–3617. http://dx.doi.org/10.1007/s00023-016-0494-5. arXiv:1503.00508 [math.DG].

[93] H. Barzegar, P. Chruściel, and M. Hörzinger, "Energy in higher-dimensional spacetimes," *Phys. Rev. D* **96** (2017) 124002, 25 pp., arXiv:1708.03122 [gr-qc]. https://link.aps.org/doi/10.1103/PhysRevD.96.124002. arXiv:1708.03122 [gr-qc].

[94] R. Bryant https://mathoverflow.net/questions/396848/einstein-metrics-on-connected-sums/397631#397631, 2021.

[95] P. T. Chruściel, E. Delay, and P. Klinger, "Nonsingular spacetimes with a negative cosmological constant: Stationary solutions with matter fields," *Phys. Rev. D* **95** no. 10, (2017) 104039, arXiv:1701.03718 [gr-qc].

[96] M. T. Anderson, P. T. Chruściel, and E. Delay, "Nontrivial, static, geodesically complete space-times with a negative cosmological constant. 2. n >= 5," vol. 8, pp. 165–204. 2005. arXiv:gr-qc/0401081.

[97] M. T. Anderson, P. T. Chruściel, and E. Delay, "Nontrivial, static, geodesically complete, vacuum space-times with a negative cosmological constant," *JHEP* **10** (2002) 063, arXiv:gr-qc/0211006.

[98] P. T. Chruściel, E. Delay, and P. Klinger, "Non-singular spacetimes with a negative cosmological constant: IV. Stationary black hole solutions with matter fields," *Class. Quant. Grav.* **35** no. 3, (2018) 035007, arXiv:1708.04947 [gr-qc].

[99] P. T. Chruściel and E. Delay, "Non-singular, vacuum, stationary space-times with a negative cosmological constant," *Annales Henri Poincare* **8** (2007) 219–239, arXiv:gr-qc/0512110.

[100] C. Guillarmou, S. Moroianu, and F. Rochon, "Renormalized volume on the Teichmüller space of punctured surfaces," *Ann. Sc. Norm. Super. Pisa Cl. Sci. (5)* **17** no. 1, (2017) 323–384.

[101] S. Wolpert, "The hyperbolic metric and the geometry of the universal curve," *Jour. Diff. Geom.* **31** (1990) 417–472. http://projecteuclid.org/euclid.jdg/1214444322.

[102] K. Chou and T.-H. Wan, "Correction to: "Asymptotic radial symmetry for solutions of $\Delta u + e^u = 0$ in a punctured disc" [Pacific J. Math. **163** (1994), no. 2, 269–276; MR1262297 (95a:35038)]," *Pacific J. Math.* **171** (1995) 589–590. http://projecteuclid.org/euclid.pjm/1102368934.

[103] D. Gilbarg and N. Trudinger, *Elliptic Partial Differential Equations of Second Order*. Springer, Berlin, 1983.

[104] M. Rupflin, P. Topping, and M. Zhu, "Asymptotics of the Teichmüller harmonic map flow," *Adv. Math.* **244** (2013) 874–893. https://doi.org/10.1016/j.aim.2013.05.021.

[105] R. Melrose and X. Zhu, "Boundary behaviour of Weil-Petersson and fibre metrics for Riemann moduli spaces," *Int. Math. Res. Not. IMRN* (2019) 5012–5065. https://doi.org/10.1093/imrn/rnx264.

[106] D. Anninos, W. Li, M. Padi, W. Song, and A. Strominger, "Warped AdS_3 Black Holes," *JHEP* **03** (2009) 130, arXiv:0807.3040 [hep-th].

[107] T. Sugawa, "Estimates of hyperbolic metric with applications to Teichmüller spaces," *Kyungpook Math. J.* **42** (2002) 51–60.

[108] J. Hempel, *3–manifolds*. Princeton University Press, Princeton, 1976. Annals of Mathematics Studies No 86.

[109] Y. Tashiro, "Complete Riemannian manifolds and some vector fields," *Trans. Amer. Math. Soc.* **117** (1965) 251–275. https://doi.org/10.2307/1994206.

[110] D. DeTurck and D. Yang, "Existence of elastic deformations with prescribed principal strains and triply orthogonal systems," *Duke Math. Jour.* **51** (1984) 243–260. https://doi.org/10.1215/S0012-7094-84-05114-7.